Design, Development and Evaluation of Quasi-Passive Wearable Assistive Devices

By

Erik Paul Lamers

Dissertation

Submitted to the Faculty of the

Graduate School of Vanderbilt University

in partial fulfillment of the requirements

for the degree of

DOCTOR OF PHILOSOPHY

in

Mechanical Engineering

September 30, 2020

Nashville, Tennessee

Approved:

Karl Zelik

Michael Goldfarb

Kevin Galloway

Aaron Yang

Gerasimos Bastas

Acknowledgements

I would like to thank Dr. Karl Zelik for being the best advisor and mentor that I could have wished for. Your support, guidance, and sense of humor, were crucial in making this experience great.

To all my friends at Vanderbilt, and especially those in CREATe, I would like to thank you for making these some of the most enjoyable years of my life.

Finally, I want to thank my friends and family for being endlessly supportive.

TABLE OF CONTENTS

Page

ACKNOWLEDGMENTS ii

LIST OF TABLES vii

LIST OF FIGURES viii

Chapter

1 Introduction 2

1.1 Wearable Assistive Devices 2

1.2 Low Back Pain and Injury Risks 3

1.3 Prosthetic Limitations and Gait Challenges for Individuals with Limb Loss . 4

2 Feasibility of a Biomechanically-Assistive Garment to Reduce Low Back Loading during Leaning and Lifting 5

2.1 Abstract 5

2.2 Introduction 5

2.3 Methods 9

2.3.1 Prototype Design & Function 9

2.3.2 Experimental Testing 11

2.3.3 Data Collection 12

2.3.4 Data Processing 12

2.3.5 Data Analysis 13

2.3.6 Model-Based Estimates of Reduction in Disc Loading 14

2.4 Results 14

2.4.1 Leaning Task 14

2.4.2 Lifting Task 16

2.4.3 Model-Based Estimates of Disc Loading 17

2.4.4 Discussion . . . 20
2.4.5 Conclusion . . . 24
3 Passive Elastic Exosuit Reduces Back Muscle Fatigue . . . 25
3.1 Introduction . . . 25
3.2 Methods . . . 27
3.2.1 Summary . . . 27
3.2.2 Instrumentation & Prototype . . . 28
3.2.3 Test Apparatus/Setup . . . 30
3.2.4 Study Design . . . 32
3.2.5 Subject Testing . . . 32
3.2.5.1 Day 1 - Measurement Validation . . . 32
3.2.5.2 Day 2 - Exosuit Evaluation . . . 34
3.2.6 sEMG Fatigue Analysis . . . 36
3.3 Results . . . 37
3.3.1 Day 1 - Measurement Validation . . . 37
3.3.2 Day 2 - Exosuit Evaluation (Subject-Specific) . . . 38
3.3.3 Day 2 - Exosuit Evaluation (Inter-Subject) . . . 43
3.4 Discussion . . . 45
3.4.1 Effects of Exosuit on Lumbar Muscle Fatigue . . . 46
3.4.2 Fatigue Effects across Subjects . . . 47
3.4.3 Fatigue Effects across Muscles . . . 48
3.4.4 Insights from Group-Level Analysis . . . 49
3.4.5 Effects of Latissimus Dorsi . . . 50
3.5 Conclusion . . . 53
4 Subject-Specific Responses to an Adaptive Ankle Prosthesis During Incline Walking . . . 55
4.1 Introduction . . . 56

4.2 Methods . . . 58
4.2.1 Participants and Intervention . . . 58
4.2.2 Procedure . . . 60
4.2.3 Data Analysis . . . 61
4.2.4 Outcome Metrics . . . 62
4.3 Results . . . 63
4.4 Discussion . . . 68
4.5 Conclusion . . . 72
5 Design, Modeling and Demonstration of a New Dual-Mode Back-Assist Exosuit 73
5.1 Introduction . . . 74
5.2 Design Approach Overview . . . 77
5.3 Modeling . . . 78
5.3.1 Model Development . . . 81
5.3.2 Model Parameter Exploration . . . 82
5.3.3 Key Model Findings . . . 83
5.4 Design . . . 87
5.4.1 Design Criteria . . . 87
5.4.2 Softgoods Design . . . 88
5.4.3 Extension Mechanism Design . . . 88
5.5 Case Study Demonstration . . . 91
5.5.1 Exosuit Assistance Demonstration . . . 92
5.5.2 Exosuit Non-Interference Demonstration . . . 93
5.5.3 Case Study Results . . . 93
5.6 Discussion . . . 95
5.6.1 Summary . . . 95
5.6.2 Applications of an Extensible Exosuit . . . 96
5.6.3 Alternative and Future Designs . . . 97

5.6.4 Additional Model Insights 99
5.6.5 Scope of Work and Limitations 102
5.7 Conclusion 103
6 Future Work and Conclusions 104
6.1 Conclusion 104
6.2 Future Work 104
A Chapter 3 Appendix 135
A.1 Subject-Specific Fatigue Results 135
B Chapter 4 Appendix 139
C Chapter 5 Appendix 150
C.0.1 Extended Results from Model Parameter Sweep Exploration 151
C.0.2 Model Parameter Selection 153
C.0.3 Examples of Alternative Extensible Exosuit Designs 154
C.0.4 Butt Friction and Dissipative Butt Work 157
C.0.5 Table of Evidence for Low-Back Exosuits 165

LIST OF TABLES

Table Page

2.1 Subject-specific low-back EMG responses with assistance 19
2.2 Subject task performance metrics during leaning and lifting 20

3.1 Individual subject metrics for Day 2 intervention session 36
3.2 Change in MDF slope for individual muscles across all subjects for Cases I, II and III 42
3.3 Subject-specific exosuit assistance magnitude 44

4.1 Prosthesis user information 67
4.2 Subject-specific prosthesis set-point angles 68

5.1 Anthropometric measurements used to scale the model to a 50^{th} percentile male 85

C.1 Subject survey responses after common movement tasks with extensible exosuit in disengaged mode 150
C.2 Table of evidence for effect of low-back exosuits on muscle activity, strain and fatigue 165

LIST OF FIGURES

Figure Page

2.1 Low-back muscle model 7
2.2 Biomechanically-assistive garment prototype 10
2.3 Biomechanically-assistive garment prototype model 11
2.4 Low-back EMG during leaning and lifting 15
2.5 Low-back EMG during leaning with vs. without assistance 16
2.6 Low-back EMG during lifting with vs. without assistance 17
2.7 Theoretical benefits from altering moment arm of device 18

3.1 Subject experimental setup (Day 2) 30
3.2 Experimental setup for leaning 35
3.3 Representative (N=1) muscle-level, median frequencies (Day 2) 40
3.4 Subject-specific, muscle-level response to exosuit 41
3.5 Group-level response to exosuit 44
3.6 Individual muscle responses to exosuit vs. muscle fatigue rate 45
3.7 Latissimus dorsi (LD) and lumbar muscle interaction 51

4.1 Premarket microprocessor-controlled prosthetic ankle 60
4.2 Prosthetic-side sagittal ankle angle 64
4.3 Anterior/posterior position of the prosthetic-side center-of-pressure 65
4.4 Prosthetic-side sagittal knee angle 66
4.5 Prosthetic-side sagittal knee moment 67

5.1 Conceptual depiction of the extensible exosuit 77
5.2 Static model of the exosuit-human system 80
5.3 Extensible exosuit moment arm (r_T) contour plot 86

5.4 Extensible exosuit k_R contour plot 87
5.5 Extensible exosuit prototype schematic 90
5.6 Photos of the extensible exosuit prototype 91
5.7 Mechanics of extensible vs. form-fitting exosuit from case study 95

A.1 Subject 1, individual muscle MDF vs. time 136
A.2 Subject 2, individual muscle MDF vs. time 136
A.3 Subject 3, individual muscle MDF vs. time 137
A.4 Subject 4, individual muscle MDF vs. time 137
A.5 Subject 5, individual muscle MDF vs. time 138
A.6 Subject 6, individual muscle MDF vs. time 138

B.1 Prosthetic-side sagittal center of pressure (CoP) 140
B.2 Prosthetic-side sagittal ankle angle 140
B.3 Prosthetic-side sagittal ankle moment 141
B.4 Prosthetic-side distal shank power 141
B.5 Prosthetic-side sagittal knee angle 142
B.6 Prosthetic-side sagittal knee moment 142
B.7 Prosthetic-side sagittal knee power 143
B.8 Prosthetic-side sagittal hip angle 143
B.9 Prosthetic-side sagittal hip moment 144
B.10 Prosthetic-side sagittal hip power 144
B.11 Intact-side sagittal center of pressure (CoP) 145
B.12 Intact-side sagittal ankle angle 145
B.13 Intact-side sagittal ankle moment 146
B.14 Intact-side distal shank power 146
B.15 Intact-side sagittal knee angle 147
B.16 Intact-side sagittal knee moment 147

B.17 Intact-side sagittal knee power . . . 148
B.18 Intact-side sagittal hip angle . . . 148
B.19 Intact-side sagittal hip moment . . . 149
B.20 Intact-side sagittal hip power . . . 149

C.1 Extensible exosuit moment arm (r_T), full parameter exploration . . . 151
C.2 Extensible exosuit k_R, full parameter exploration . . . 152
C.3 Extensible exosuit moment arm (r_T) for extended y_2 range . . . 153
C.4 Proof-of-concept extensible exosuit with extension mechanism on the back or waist . . . 155
C.5 Alternative extensible exosuit design with an extension mechanism on the buttocks . . . 156
C.6 Alternative extensible exosuit design uses two extension mechanisms . . . 157
C.7 Exosuit with elastic element over the buttocks . . . 161
C.8 Exosuit with inelastic element over the buttocks, and elastic element along the back and waist . . . 162
C.9 Exosuit with inelastic element over the buttocks, and elastic element along the thighs . . . 163

Chapter 1

Introduction

1.1 Wearable Assistive Devices

Wearable assistive devices, such as exoskeletons and prostheses, can assist human movement to achieve a variety of goals such as: alleviating musculoskeletal disorders and pain, compensating for a missing limb, improving performance, or reducing muscular effort and fatigue [156, 47, 48, 140]. Wearable assistive devices are distinct from traditional assistive devices (e.g. wheel chairs) because they are intended to be **worn** by the user, and distinct from wearable devices (e.g. smart watches) because they are designed to mechanically **assist** the user. In recent years, wearable assistive devices have seen significant growth in funding, research and commercial/industrial/military use [48]. Wearable assistive devices may be categorized as active (e.g. powered exoskeleton with motors), passive (e.g. exoskeleton with springs) or quasi-passive device (e.g. exoskeleton with springs and a low-power clutch). Powered wearable assistive devices have the greatest capacity to restore function [142]; however, these devices are the heaviest, most costly, most complex, and most difficult to control. Passive and/or quasi-passive wearable assistive devices can partially restore or augment body function, with less added weight (i.e. no large motors and batteries), less cost and less complexity. [111, 142]. Quasi-passive wearable assistive devices are particularly appealing because they leverage passive mechanical elements (e.g. springs and dampers) with simple control strategies (e.g. powered or passive clutching mechanisms to enable, disable or tune the device [144, 39, 37, 126]) to provide selective assistance when it is needed by the user.

In my dissertation I focus on (i) the modeling, design and testing of a novel quasi-passive exosuit to help reduce low-back muscle activity, fatigue and musculoskeletal

load (which is a key risk factor underlying back pain and injury risk) during leaning and lifting and (ii) on understanding how a quasi-passive ankle prosthesis affects sloped walking for individuals with transtibial amputation.

1.2 Low Back Pain and Injury Risks

The primary focus of my research is wearable assistive devices that provide an assistive torque to the user, to reduce muscle effort, fatigue, and musculoskeletal loading in order to alleviate biomechanical risks factors associated with low back injury and pain. Low back pain is experienced by an estimated 60-85% of adults within their lifetime and is the leading cause of limited physical activity [71, 9, 53], the second leading cause of missed work in the U.S. [131], and a significant economic burden [76]. Many biomechanics studies have shown that high (overloading) and/or repetitive (overuse) forces on the biological tissues of the spine (e.g. muscles, ligaments, vertebrae and intervertebral discs) are a major risk factor of back pain [80, 32, 5, 123]. The forces on these biological tissues are primarily due to muscles that span the spine and create torques (e.g. during lifting) over small biological moment arms ($\sim$6cm) [19]. From a biomechanics perspective, wearable assistive devices (e.g. exoskeletons) apply joint torques which can reduce loading on biological tissues [89], which is hypothesized to reduce the risk of low back injury and pain [89]. The majority of wearable assistive devices for the low back have an exoskeleton design that rely on rigid components (which are often bulky) and as a result, often limit user mobility and device acceptance [12, 13, 26]. In my research I explored a novel, textile-based exosuit for the low-back to overcome these limitations of existing exoskeletons. Exosuits, similar to exoskeletons can provide torque assistance to the users, but are distinct from exoskeletons because they mainly use soft components rather than rigid components [91]. My scientific contributions include biomechanical modeling, device design (patent-pending) and human subject experimentation with this novel exosuit.

1.3 Prosthetic Limitations and Gait Challenges for Individuals with Limb Loss

Another focus of my research is exploring the benefits of an adaptive prosthetic ankle for individuals with lower-limb amputation. As of 2005, lower-limb loss affected over 1 million people in the United States, 60% of this population have major limb loss (i.e. amputation above the knee, below the knee, or at the foot) [165]. The majority of available prosthetic feet have a fixed ankle set-point, which can limit prosthetic ankle range of motion during daily activities like walking [40]. Limited prosthetic ankle range of motion may have detrimental effects such as, reduced walking speed, prosthetic-side single-support time and reduced toe clearance [141, 143, 35]. Returning passive ankle range of motion to individuals with lower limb amputation is possible with adaptive prostheses such as the Össur Propriofoot. Previous studies have suggested that adaptive prostheses can result in group-level changes in; kinetics and kinematics [51], limb symmetry [7], and metabolic cost [33]. However, prosthesis users are a highly heterogeneous population, and group-level responses may not reflect the responses and preferences of individuals [25, 127]. In this work I performed a subject-specific investigation with a new commercially available adaptive prosthetic ankle, to explore how individuals respond to the prosthetic ankle and to what extent these individual responses are reflected in the group-level findings.

Chapter 2

Feasibility of a Biomechanically-Assistive Garment to Reduce Low Back Loading during Leaning and Lifting

2.1 Abstract

The purpose of this study was to design and fabricate a biomechanically-assistive garment which was sufficiently lightweight and low-profile to be worn underneath, or as, clothing, and then to perform human subject testing to assess the ability of the garment to offload the low back muscles during leaning and lifting. We designed a prototype garment which acts in parallel with the low back extensor muscles to reduce forces borne by the lumbar musculature. We then tested 8 healthy subjects while they performed common leaning and lifting tasks with and without the garment. We recorded muscle activity, body kinematics, and assistive forces. The biomechanically-assistive garment offloaded the low back muscles, reducing erector spinae muscle activity by an average of 23-43% during leaning tasks, and 14-16% during lifting tasks. Experimental findings in this study support the feasibility of using biomechanically-assistive garments to reduce low back muscle loading, which may help reduce injury risks or fatigue due to high or repetitive forces. Biomechanically-assistive garments may have broad societal appeal as a lightweight, unobtrusive and cost-effective means to mitigate low back loading in daily life.

2.2 Introduction

Low back pain is a disabling condition experienced by an estimated 60-85% of adults within their lifetime [9, 53, 71]. Low back pain is the leading cause of limited physical activity [9], the second leading cause of missed work in the U.S. [131], and a significant

economic burden. It is estimated to cost >$100 billion per year in the U.S. due to medical expenses and lost worker productivity [76, 96]. The etiology of low back pain is multifactorial, but major risk factors include high (overloading) and/or repetitive (overuse) forces on lumbar tissues (muscles, ligaments, vertebrae and intervertebral discs). Such forces can occur during common daily activities such as leaning and lifting [19, 124, 102], in both occupational and non-occupational settings. Low back pain is particularly common among individuals who perform heavy lifting [80, 32, 29, 46, 68]. Static bending and twisting postures, and to a lesser extent prolonged static work postures (e.g., leaning), have also been implicated as potential risk factors for low back pain [18]. Elevated or even moderate loads applied repetitively to the lumbar spine can increase the risk of low back pain [80, 32, 29, 97, 71], weaken or damage the vertebrae [24, 65, 5] and cause intervertebral disc degeneration or herniation [59]. Similarly, elevated and repetitive loading of passive (e.g., ligament) or active (muscle) tissues can cause fatigue, discomfort or damage, such as strains [123, 120, 38, 4]. Reducing loading on lumbar tissues during daily activities could help lower the risk of back injury and resultant pain, or benefit other outcomes related to muscle effort and fatigue.

During tasks such as lifting and leaning, back extensor muscles and ligaments apply the majority of the compression force experienced by the lumbar spine. The lumbar spine experiences a flexion moment during forward leaning due to the weight of the upper-body (F_{HAT}, **Figure 2.1**) and any additional external (e.g., carried) weight (F_W) which act at moment arms (r_{HAT} and r_W) about a given spinal disc (**Figure 2.1**). To prevent the upper-body from falling forward, this flexion (clockwise) moment must be counter-balanced by an extension (counter-clockwise) moment. This extension moment is provided by back extensor muscles (e.g., erector spinae muscles), and passive tissues (e.g., interspinous ligaments, **Figure 2.1**, b). These muscles and ligaments act at much smaller moment arms than the upper-body center-of-mass and external weight [106, 19]; and therefore produce much larger forces in order to generate the required extension

moment [95]. Muscles and ligaments apply forces roughly parallel to the lumbar spine. As a result, they also apply substantial compression forces to the lumbar spine when they are loaded [19] (**Figure 2.1**). It has been shown that extensor muscles and ligaments are responsible for the majority of the compression force experienced by the lumbar spine during tasks such as forward leaning [29, 6, 113]. Reducing these muscle and/or ligament forces may therefore also reduce forces on the spine.

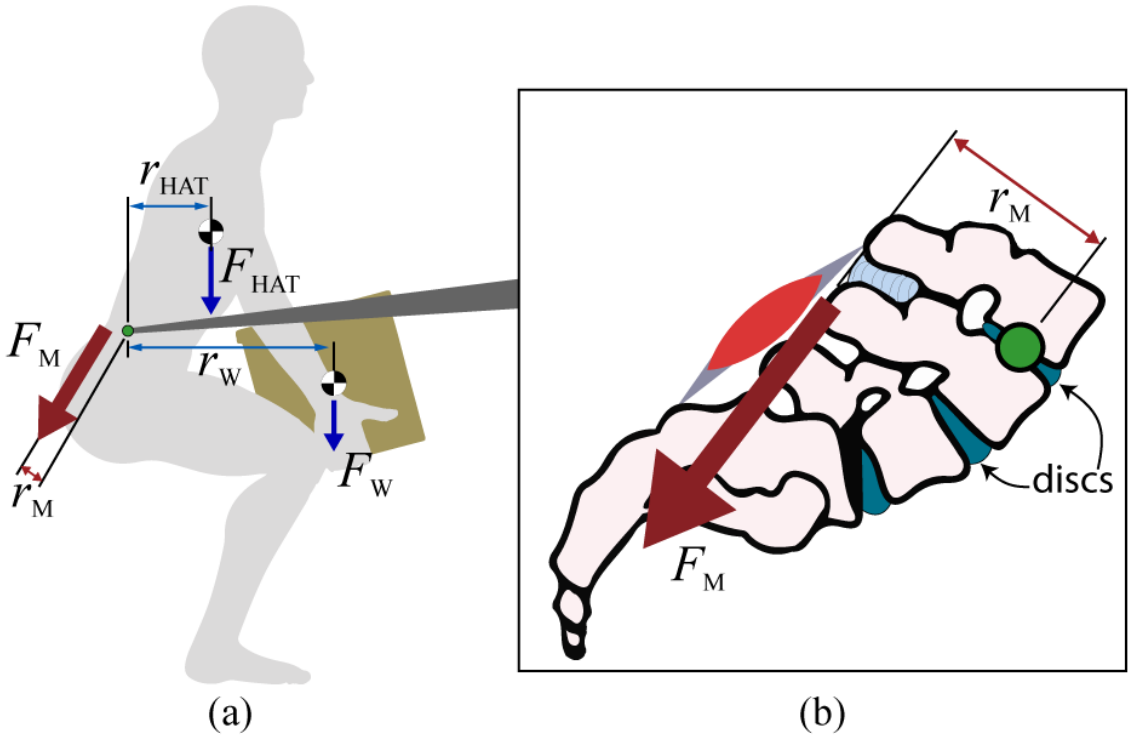

Figure 2.1: (a) During tasks such as lifting or leaning, the lumbar (low back) extension moment is the result of large muscle and ligament forces (F_M) acting at short moment arms (r_M) about the spine. This extension moment counterbalances flexion moments from the weight of the head-arms-trunk (F_{HAT}) and carried weight (F_W), which act at larger moment arms (r_{HAT} and r_W). (b) The large muscle and ligament forces constitute the majority of loading experienced by the intervertebral discs. Excessive and/or repetitive loading can lead to degeneration or injury of the lumbar tissues (muscles, ligaments, vertebrae, and intervertebral discs).

Wearable assistive devices (e.g., exoskeletons, orthoses) provide potential means for reducing lumbar tissue loading, which may then reduce the risk of force-induced low back injury and associated pain. Various wearable assistive devices have recently been

developed, which assist via actuators (e.g., [66, 104, 150, 166]) and/or springs (e.g., [22, 92, 134, 136, 146]). The devices apply forces to the body in order to provide an assistive extensor moment about the lumbar spine; this offloads the lumbar extensor muscles. Because these devices are worn outside the body they operate with a larger moment arm (often >20 cm [3, 146]) than muscles (6-8 cm [98, 106]) and ligaments (1-5 cm [19]). Therefore, these devices can provide equivalent extensor moments with smaller force magnitudes, resulting in reduced lumbar spine compression forces [3, 19]. Experimental studies indicate that wearable assistive devices can reduce extensor muscle loads by, on average, 9-54% as evidenced indirectly by reductions in muscle activity [1, 22, 92, 146, 163].

The majority of these wearable devices have relatively bulky form-factors, which make them less practical for at-home daily use, or use in other business, social or clinical settings. Often these devices are designed with components that protrude from the lower back to lengthen the extensor moment arm; however, these components can interfere with common daily activities (e.g., sitting, stair ascent/descent, navigating home or work environments). Furthermore, users are generally required to wear these exoskeletal devices conspicuously on top of their clothing, which can be undesirable. An appealing alternative to these exoskeletal devices may be to adapt form-fitting clothing itself by embedding passive (spring-like), quasi-passive (clutchable spring-like), or active (actuated) structures to assist the low back musculature. We propose that a garment embedded with load-bearing structures may provide similar offloading benefits as exoskeletons but without the burden of bulky components. The key distinguishing feature of our proposed garment-like device is that it could be worn underneath or integrated into clothing; whereas current powered and passive assistive devices are worn on top of clothing. However, it is currently unclear to what degree such a form-fitting garment could offload lumbar tissues. Therefore, the purpose of this initial study was: (i) to design and fabricate a biomechanically-assistive garment which was sufficiently

lightweight and low-profile to be worn underneath (or as) clothing and then (ii) to perform human subject testing to assess the ability of the garment to offload the low back during leaning and lifting.

2.3 Methods

2.3.1 Prototype Design & Function

We designed and fabricated a passive (unactuated) biomechanically-assistive garment prototype that provides an extension moment about the user's lumbar spine during forward leaning and lifting [160]. The prototype is composed of an upper-body interface (shirt), lower-body interface (shorts), and elastic bands which run along the back, coupling the upper and lower-body interfaces (**Figure 2.2**). The lower-body interface was comprised of thigh sleeves with a high friction elastomer interior and a sturdy fabric exterior, which served as an anchoring point for the elastic bands. The upper and lower interfaces distribute forces across the surface area of the shoulders and thighs, respectively, allowing them to support substantial loading. The elastic bands (6.3 cm x 0.45 cm x 29 cm, 800 N/m stiffness) were connected to clasps on the shoulders allowing the slack length in the bands to be adjusted. The total weight of the prototype, without testing-related instrumentation, was 2 kg.

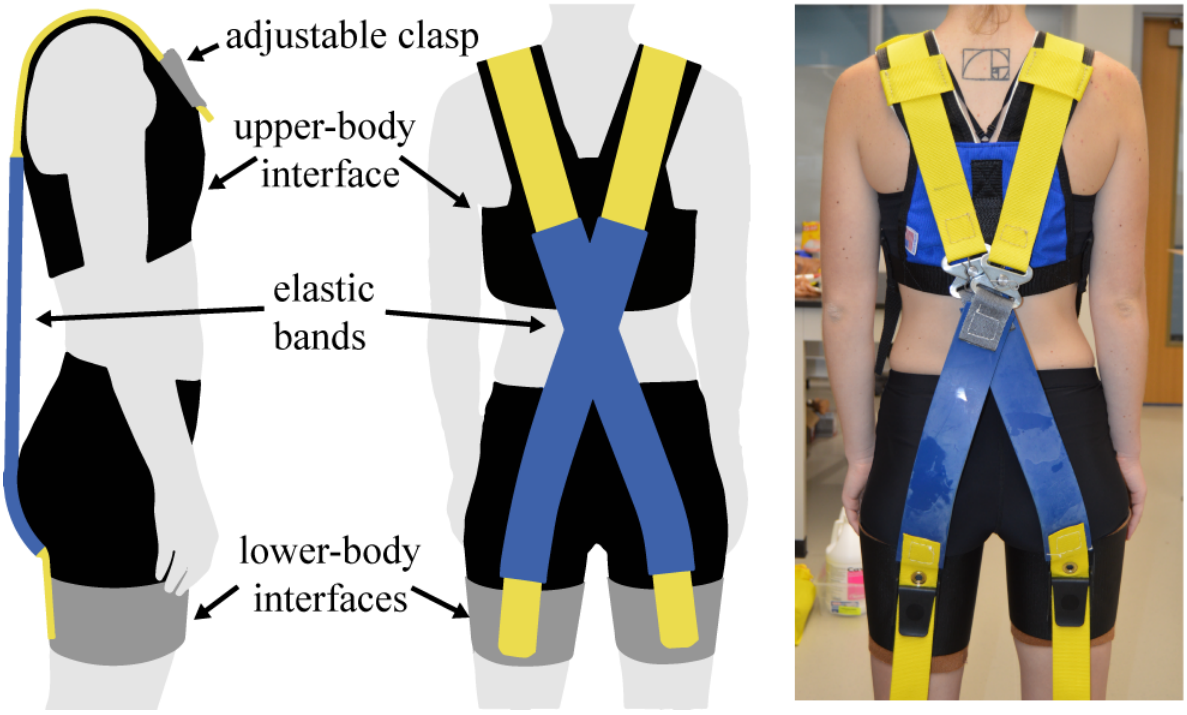

Figure 2.2: Biomechanically-assistive garment prototype. The prototype distributes forces over the shoulders and thighs via the upper- and lower-body interfaces. Elastic bands connect these two interfaces and act in parallel with muscles and ligaments to support the lumbar extension moment. Slack length of the elastic bands was set via adjustable clasps.

As the user leans forward via lumbar flexion and/or hip flexion, the elastic bands stretch, applying tension forces that act roughly parallel to the lumbar extensor muscles and ligaments, and thus generate an extension moment about the lumbar spine (**Figure 2.3**). Because the elastic bands act at a larger moment arm (>9 cm) than biological tissues (1-8 cm), the biomechanically-assistive garment provides a mechanical advantage over these tissues (**Figure 2.3**). As a result, the elastic bands can provide equivalent extension moments at lower force magnitudes, thus reducing compression force on the lumbar spine [1].

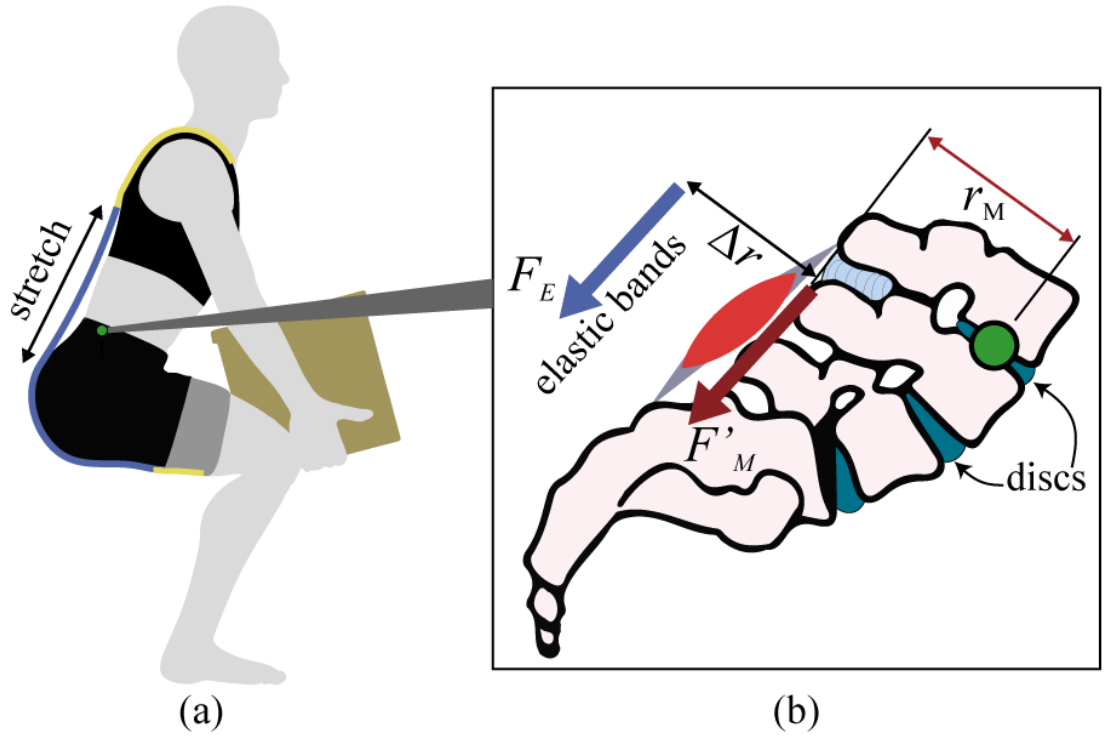

Figure 2.3: (a) The biomechanically-assistive garment stretches during lifting and leaning. (b) Forces borne by the elastic bands are expected to offload the extensor muscles, and to reduce intervertebral disc loading by increasing the extensor moment arm (Δr). Analytically, from the moment balance equation, $F_E + F\prime_M < F_M$ from **Figure 2.1**

2.3.2 Experimental Testing

Eight healthy subjects (7 male, 1 female, 74 ± 8.7 kg, 1.8 ± 0.05m, 23 ± 3 yrs.) performed a series of leaning and lifting tasks with vs. without the prototype, while we recorded body kinematics, elastic band force and electromyography (EMG) data. The subjects, with no history of low back injury or pain in the past 6 months, provided informed, written consent prior to participating in this study. For each leaning task, subjects leaned forward for 30 seconds to pre-determined angles (30°, 60°, 90° from vertical) while holding a 4.5 kg weight (diameter: 20 cm, thickness: 3 cm) to their sternum. This weight approximated the additional flexion moment about the lumbar spine resulting from holding arms outstretched (e.g., a surgeon manipulating tools). A plumb line

was used as a visual reference to assist subjects in reaching each pre-determined angle. For each lifting task, the subjects lifted a weight (12.7 kg and 24 kg) from the floor up to a standing posture (using squat lifting form) for 10 cycles, paced at 30 beats per minute (via metronome). Subjects performed lifting and leaning tasks without (control) and then while wearing the prototype. Before each task was performed with the prototype, the slack length of the elastic bands were manually adjusted such that peak elastic band forces were $>$20% of bodyweight during the task.

2.3.3 Data Collection

Body kinematics, EMG and elastic band forces were measured. Kinematics of the pelvis, trunk, and of the kettle-bell weight, were measured at 100 Hz with an optical motion capture system (Vicon). To track pelvic motion, retroreflective markers were placed bilaterally on the following landmarks: anterior superior iliac spine, iliac crest, posterior superior iliac spine, and greater trochanter. To track trunk motion, retroreflective markers were placed on the 7th cervical vertebrae, and bilaterally on the acromion and clavicle. The motion of the kettle-bell weight was tracked using a cluster of 4 markers on the handle. EMG of the bilateral lumbar erector spinae muscles (30 mm bilateral to L3 spinal processes) were recorded at 2000 Hz using wireless sensors (Delsys). The erector spinae muscles were chosen because they generate the majority of the extensor moment during sagittal plane manual handling tasks [98, 113], and provide an estimate of general back muscle activity [19]. Tension forces in each elastic band were measured at 2000 Hz using two uniaxial load cells (Futek). All data were collected synchronously.

2.3.4 Data Processing

Motion data were low-pass filtered at 6 Hz, and load cell data at 15 Hz (each via 4th order dual-pass Butterworth filter). EMG signals were de-meaned, high-pass filtered at

30 Hz, rectified, and then low-pass filtered at 10 Hz, using 3rd order, dual-pass Butterworth filters [161]. EMG envelopes were then normalized to the maximum filtered EMG value observed across all trials (max observed activation).

2.3.5 Data Analysis

Mean normalized EMG was computed as the primary outcome metric for leaning and lifting tasks, and was used as an indicator of muscle loading. Mean EMG for leaning tasks was calculated by first averaging left and right lumbar erector spinae EMG, and then averaging the result over the duration of static leaning (**Figure 2.4** a). A vector projected from the L_5S_1 junction to the mid-point between the suprasternal notch and 7_{th} cervical vertebrae was used to measure trunk angle. Subject-specific leaning trials were excluded from analysis if the maximum measured elastic band force was $<$20% of subject bodyweight (suggesting that the prototype may have shifted during the trial). Lifting tasks were divided into cycles. Each cycle was normalized to 1000 data points (due to differing cycle lengths), and then averaged. Mean EMG for lifting tasks was calculated by first averaging left and right erector spinae EMG, and then averaging the result over the lifting cycle duration (**Figure 2.4** a). Peak EMG during the lifting cycle was also quantified, and was used as an indicator of peak loading, assuming a proportional relationship between EMG activity and muscle force. Average lifting cycle durations were calculated and compared for each subject across conditions with vs. without the prototype to ensure that cycle durations were consistent. Subject-specific lifting trials were excluded if the maximum elastic band force was $<$20% of subject body-weight, if maximum or minimum trunk angles varied by $>10°$, or if displacement of the weight varied by >5 cm with vs. without the prototype. Intersubject means and standard deviations were calculated and paired t-tests were performed to evaluate differences in outcome metrics with vs. without the prototype (=0.05).

2.3.6 Model-Based Estimates of Reduction in Disc Loading

To gain an insight into the effects of the biomechanically-assistive garment on intervertebral disc compression force, we implemented a simple, analytical model of the lumbar spine during static leaning (similar to [3, 135]). The model assumes a static leaning posture, achieved with hip flexion and no lumbar flexion, at a fixed angle from the vertical (θ = 45°). This results in a constant flexion moment about the L_5S_1 intervertebral disc (105 Nm) due to the weight of the HAT estimated using anthroprometrics of a 50_{th} percentile male [88] (**Figure 2.1**). For case I, the extension moment was assumed to be generated entirely by an extensor muscle force (F_M) acting with a 7 cm moment arm (r_M) [106]. Disc compression force (F_{disc}, acting axially along the spine) in case I was computed as the sum of the muscle force and the force due to the weight of the HAT ($F_{disc,I} = F_M + F_{HAT}\cos\theta$). In case II, we introduced another source of extension moment, due to forces in the elastic bands of the biomechanically-assistive garment (F_E, **Figure 2.3**) acting at a larger moment arm than the muscles ($r_M + \Delta r$). We then updated the disc compression force calculation ($F_{disc,II} = F\prime_M + F_{HAT}\cos\theta + F_E$). Next, we varied Δr from 0 to 20 cm, and F_E from 0 to 380 N, and calculated the updated disc compression force. Reduction in disc compression, vs. case I (with no external assistance), was then computed as ($100 \times \frac{F_{disc,II} - F_{disc,I}}{F_{disc,I}}$) and used to create a contour plot.

2.4 Results

2.4.1 Leaning Task

When wearing the prototype, mean EMG was reduced by 23% ± 13% (p=0.011), 27% ± 10% (p=0.006) and 43% ± 33% (p=0.001) for the 30°, 60°and 90°leaning tasks, respectively (**Figure 2.5**). All subjects exhibited a reduction in EMG for all leaning angles, although the magnitude of reduction varied significantly from subject to subject (reduction range: 1-88%, **Table 2.1**). Elastic band forces were 23% ± 3%, 26% ± 3%, and 30%

± 5% bodyweight for the 30°, 60°and 90°leaning tasks respectively. Mean leaning angles with vs. without the prototype were not significantly different for the 30°(p=0.071), 60°(p=0.847) or 90°(p=0.121) tasks (**Table 2.2**). One subject was excluded from the analysis of the 30°and 60°conditions because measured elastic band forces were <20% of their bodyweight.

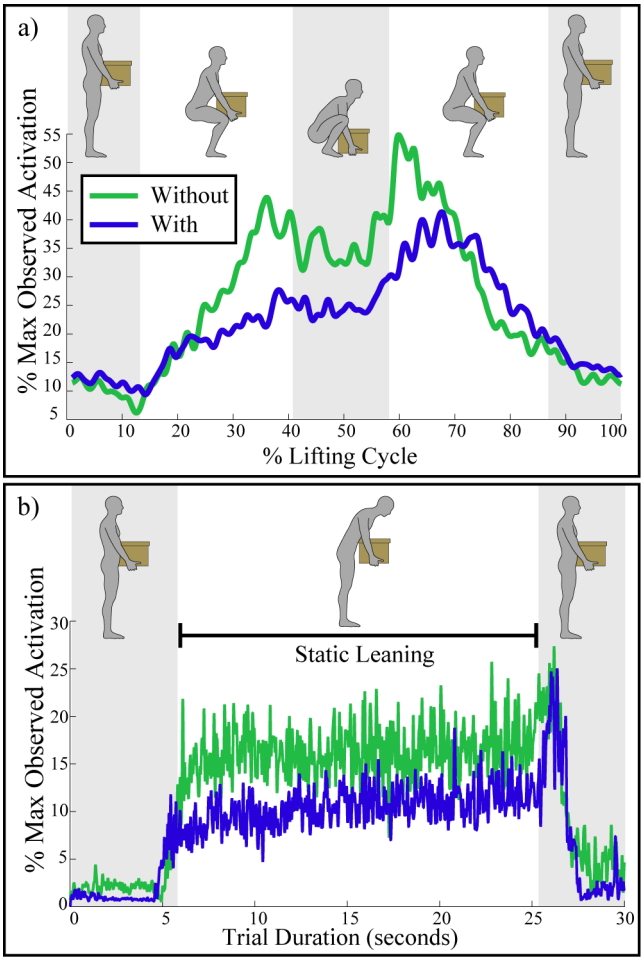

Figure 2.4: Mean normalized EMG for a representative subject. (a) EMG for lifting task with vs. without the biomechanically-assistive garment prototype. Trials were parsed into cycles; a cycle began with the subject standing upright, next the subject squatted down, and then stood back upright to complete the cycle. (b) EMG for leaning task with vs. without the prototype. Mean EMG was calculated over the middle of the trial, during which the subject was leaning statically.

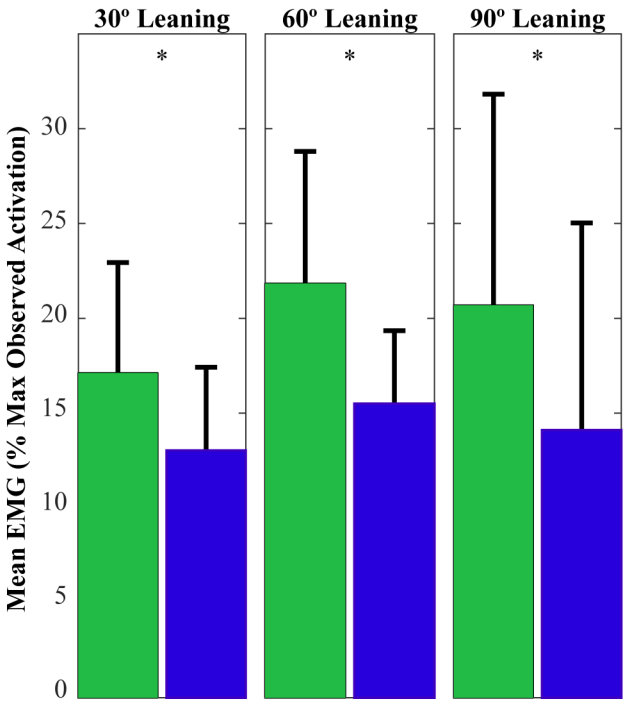

Figure 2.5: Mean EMG of the erector spinae muscles was reduced during leaning when wearing the biomechanically-assistive garment prototype (dark blue) vs. not wearing it (green). Reductions were statistically significant for all leaning angles tested ($p<0.05$, denoted with asterisks). Intersubject means and standard deviations are depicted.

2.4.2 Lifting Task

When wearing the prototype, mean EMG was reduced by 14% ± 9% (p=0.015) and 16% ± 8% (p=0.004) for the 12.7 kg and 24 kg lifting tasks, respectively. Peak EMG was reduced by 19% ± 13% (p=0.025) and 23% ± 9% (p=0.004) for the 12.7 kg and 24 kg lifting tasks, respectively (**Figure 2.6**). All subjects exhibited EMG reductions while using the prototype to lift the kettle-bell weights (reduction range: 2-30%, **Table 2.1**). Peak elastic band forces were 27% ± 4% and 27% ± 5% bodyweight for the 12.7 kg and 24 kg lifting tasks, respectively. On average across subjects, maximum trunk angles (12.7 kg: p=0.156, 24 kg: p=0.224), mean cycle duration times (12.7 kg: p=0.625, 24 kg: p=0.413) and kettle-bell displacements (12.7 kg: p=0.546, 24 kg: p=0.111) were not significantly different with vs. without the prototype (**Table 2.2**). Two subjects were excluded from the analysis of

the lifting tasks because there was > 10 of difference in max/min trunk angles and > 5 cm difference in kettle-bell displacement when comparing task performance with vs. without the prototype.

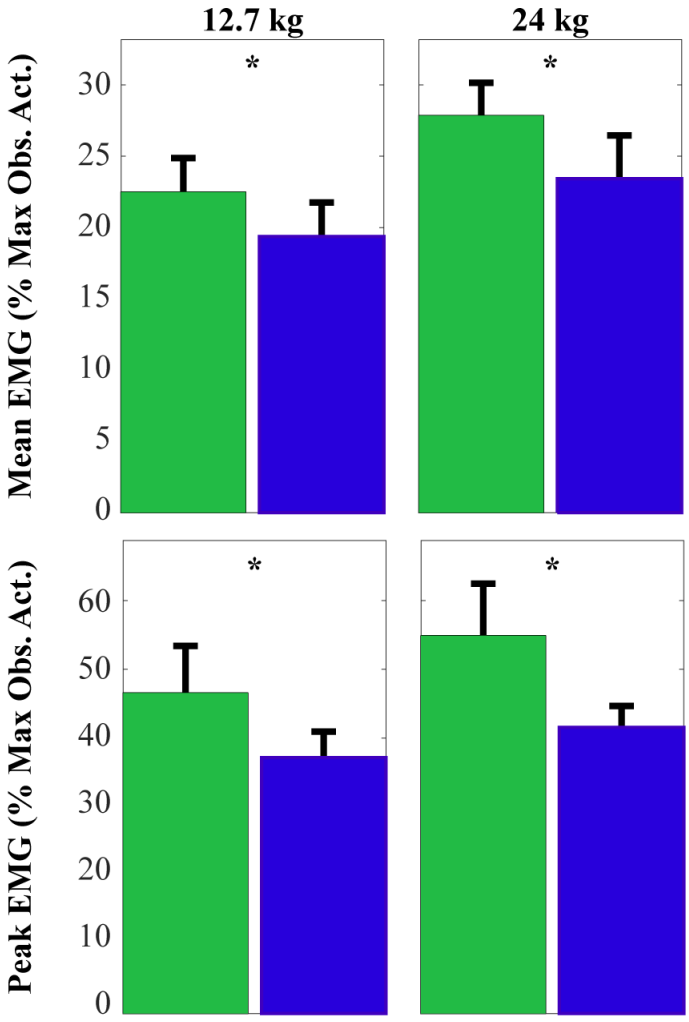

Figure 2.6: Mean and peak EMG of the erector spinae muscles were reduced during lifting when wearing the biomechanically-assistive garment (dark blue) vs. when not wearing it (green). All reductions were statistically significant ($p<0.05$, denoted with asterisks). Intersubject means and standard deviations are depicted

2.4.3 Model-Based Estimates of Disc Loading

Model predictions, based on a simple moment balance, indicate that offloading the low back muscles with a biomechanically-assistive garment is expected to reduce inter-

vertebral disc compression forces (**Figure 2.7**). The magnitude of disc force reduction is expected to increase with both increasing elastic band force (F_E) and increasing moment arm (Δr).

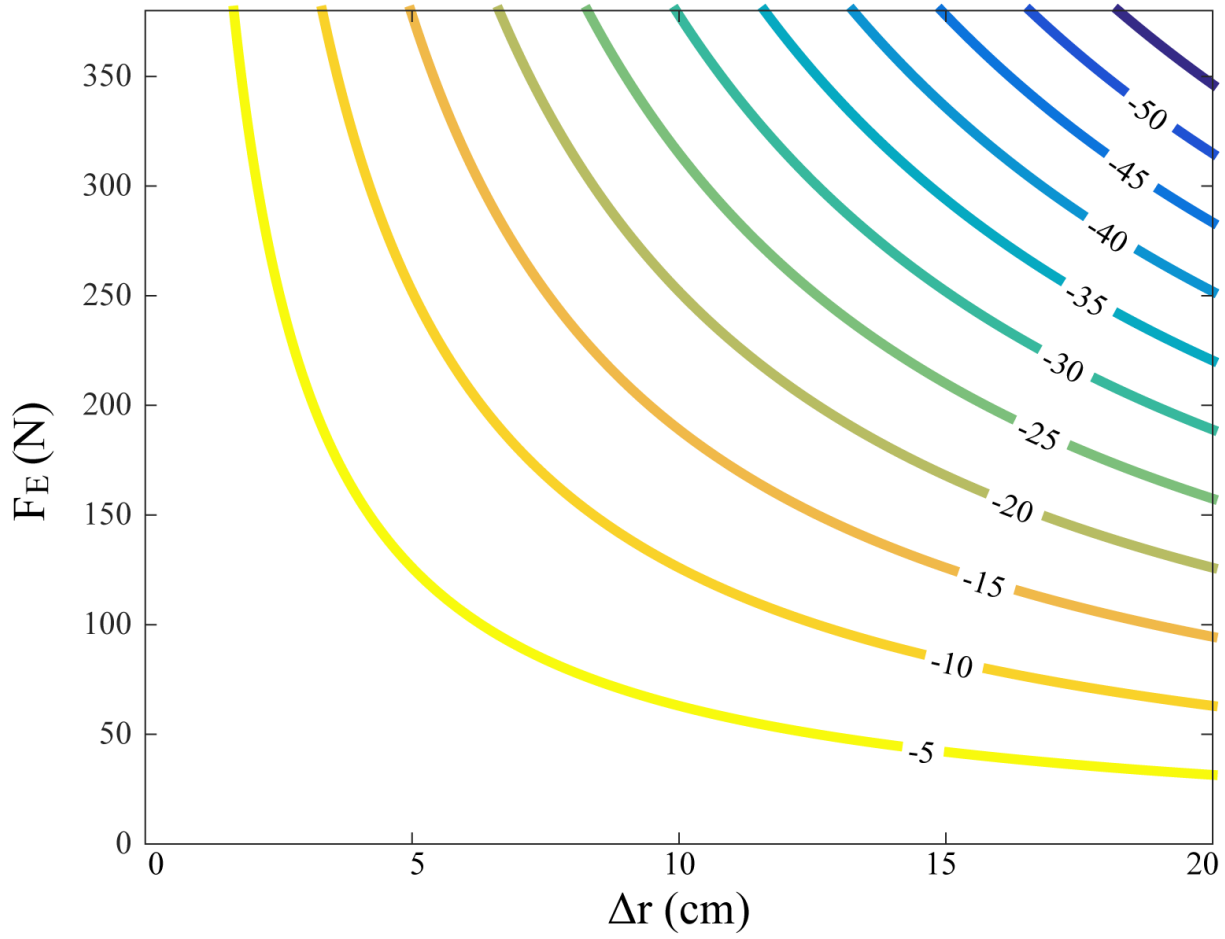

Figure 2.7: Theoretical reduction in lumbar disc compression force when wearing a biomechanically-assistive garment. Disc force reduction increases as a function of increasing elastic cable force (F_E) and increasing moment arm (Δr).

Table 2.1: Subject-Specific Responses. Changes in subject-specific EMG, while wearing the biomechanically-assistive garment prototype, relative to not wearing it (control). N/A indicates subject-specific tasks that were excluded.

		Trials				
		30°	**60°**	**90°**	**12.7 kg**	**24 kg**
Subject	**1**	-26%	-18%	-88%	-11%	-16%
	2	-3%	-41%	-23%	N/A	N/A
	3	-35%	-14%	-18%	-15%	-14%
	4	-30%	-35%	-82%	N/A	N/A
	5	-9%	-29%	-26%	-13%	-22%
	6	-35%	-22%	-1%	-2%	-19%
	7	-27%	-33%	-33%	-30%	-22%
	8	N/A	N/A	-72%	-10%	-2%

Table 2.2: Task Performance Metrics. Kinematic metrics and cycle time durations were comparable (i.e., not significantly different) when performing each task with vs. without the biomechanically-assistive garment.

	Lean 30°	**Lean 60°**	**Lean 90°**
	Trunk Angle	Trunk Angle	Trunk Angle
Without	28 ± 6°	54 ± 6°	91 ± 6°
With	31 ± 7°	55 ± 10°	89 ± 8°
	Lifting 12.7 kg		
	Trunk Angle	Cycle Time	Weight Displacement
Without	54 ± 11°	3.99 ± 0.01 s	54.2 ± 2.8 cm
With	53 ± 11°	3.99 ± 0.01 s	53.6 ± 2.5 cm
	Lifting 24 kg		
	Trunk Angle	Cycle Time	Weight Displacement
Without	50 ± 7°	3.99 ± 0.02 s	53.8 ± 2.9 cm
With	53 ± 11°	4.00 ± 0.01 s	53.0 ± 3.1 cm

2.4.4 Discussion

Here we introduce a new design concept for a biomechanically-assistive garment, and demonstrate its potential to mitigate forces experienced by the low back muscles and discs. We found that our biomechanically-assistive garment prototype offloaded the lumbar extensor muscles during both static leaning and dynamic lifting, as evidenced by reductions in EMG. The magnitudes of mean EMG reductions presented in this study (intersubject means ranging 14-43%) were comparable to reductions shown from previous exoskeletal devices with larger form-factors (9-54%, [1, 22, 92, 146, 163]). Furthermore, the biomechanically-assistive garment demonstrated the ability to reduce both mean and peak EMG, which may affect risk of injuries due to repetitive (overuse)

or high (overloading) forces. Model-based estimates indicate that the garment could also offload the intervertebral discs because the garment acts with a mechanical advantage over the extensor muscles. Overall, preliminary evidence strongly supports the feasibility of using low–profile, biomechanically-assistive garments to offload lumbar extensor muscles, which may help to reduce force-induced injury risks and/or fatigue during leaning and lifting tasks.

All subjects exhibited reduced lumbar erector spinae muscle activity when wearing the prototype; however, the magnitude of EMG reduction was subject and task-specific (**Table 2.1**). Four of the eight subjects (subjects 1, 3, 4, and 7) exhibited reductions $\geq 10\%$ for all leaning and lifting trials completed, suggesting that a subset of the population could derive broad and substantial benefits (in terms of offloading muscles) from a biomechanically-assistive garment. The four remaining subjects (subjects 2, 5, 6 and 8) exhibited reductions $\geq 10\%$ for most tasks they completed, but $< 10\%$ for other tasks. These results may reflect subject-specific adaptations (e.g., altered kinematics or muscle co-contractions), or variability in EMG recordings, or in how we pretensioned the prototype for each person and task. Overall these reductions suggest that the prototype consistently reduced loading of the lumbar extensor muscles.

The degree to which a biomechanically-assistive garment (and other similar wearable assistive devices) can reduce disc compression forces depends on the mechanical advantage (increased moment arm, Δr) it provides relative to the extensor muscles, and on the force the device applies to the user (F_E). There are practical limits for F_E and Δr: F_E is primarily limited by the amount of force that can be safely and comfortably applied to a person, whereas r is limited by the desired form-factor and tolerable size of the device; both of which may vary for a given individual, task and/or setting. Using the parameters of the prototype tested in this experiment ($F_E =$ 200-300 N and $\Delta r =$ 1-4 cm), reductions in disc loading of 5-10% would be expected. If a biomechanically-assistive garment were used on a daily basis or for extended periods of time, then relatively small reductions

could provide cumulative offloading of the spine. Alternatively, modestly increasing the moment arm, via a permanent protruding structure (e.g., [3]) or an extensible mechanism, could serve to further offload the discs. In support of this, Abdoli-Eramaki et al. estimated that a similar device acting in parallel to the lumbar spine with $\Delta r = 15$ cm would reduce disc loading by 23-29% [3].

There were several limitations to this study. A relatively small sample (N=8) and subset of tasks were tested in this initial feasibility experiment; however, this was sufficient to demonstrate proof-of-concept for the biomechanically-assistive garment. This study only addressed short-term effects on the activity of isolated lumbar extensor muscles. It would be of value in future studies to measure additional back extensor muscles as well as quantify abdominal co-contraction (which can contribute to lumbar tissue loading [61, 98], estimate compressive and shear loading on the lumbar spine (e.g., using optimization or EMG-assisted modeling techniques similar to previous work [16, 61, 95, 98]), and to explore longer-term effects. In this work, muscle activity was normalized to the maximum observed activation across all trials. Relative changes in EMG were then interpreted to assess the feasibility of the biomechanically-assistive garments to offload the low back; however, there is limited ability to draw conclusions about clinical significance at this time. Further studies are needed. If future testing is performed on a population with a history, or elevated risk, of back pain, then it would also be beneficial to collect self-reported pain metrics or to track injuries over time; though the latter would require a larger longitudinal study. The moment balance model used to estimate relative changes in disc compression forces assumed anatomical simplicity and did not explicitly model muscle co-contraction, passive tissues or other segmental dynamics. Nevertheless, this model provides an order-of-magnitude approximation of expected force reduction and insight regarding the sensitivity of disc compression force to device design parameters. Though these approximations would benefit from further or more direct (invasive) validation, conclusions in this study do not depend on model force predictions being highly

accurate. The prototype tested in this study required us to manually adjust elastic band tension for each person and task. Future prototypes may integrate quasi-passive clutching capabilities (to engage/disengage the elastic elements) and wearable sensors in order to more precisely control the magnitude and timing of assistance. Alternatively, further assistance and versatility might be provided using a portable actuator unit, similar to robotic exosuit hardware that has been developed to assist walking [10, 155]. Finally, we note that for all physical interventions, the act of redistributing forces (in this case, applying forces to the shoulders and thighs to offload the spine) may have unexpected or unintended consequences in terms of altering loading elsewhere in the body. These concomitant biomechanical effects warrant investigation in future studies.

Biomechanically-assistive garments may have broad societal appeal as a lightweight, unobtrusive and cost-effective means of reducing low back loading, which could affect the risk of low back injury and pain in daily life. The ability to non-invasively alter lumbar loading and muscular effort may also have applications for reducing fatigue (which is distinct from, but can be associated with discomfort or low back pain [120]) or aiding in patient recovery post-injury. These garments provide a unique means to mitigate low back loading by adapting clothing, which is ubiquitous and already worn every day. These garments are expected to be cost-effective because they can leverage existing soft goods manufacturing methods and infrastructure. Moving forward, biomechanically-assistive garments could also be instrumented with wearable sensors and smart algorithms to control quasi-passive structures (e.g., elastic bands that can be clutched or unclutched to selectively provide assistance during certain tasks). One future possibility would be for this instrumented clothing to also provide users with actionable biofeedback about their low back loading (similar to how pedometers track and report steps per day), and to alert users to high loading or predicted injury risks.

2.4.5 Conclusion

We found that a passive, biomechanically-assistive garment was able to offload low back muscles during leaning and lifting. These findings support the feasibility of using biomechanically-assistive garments to reduce low back injury and resultant pain due to high (overloading) and/or repetitive (overuse) forces on lumbar musculature.

Chapter 3

Passive Elastic Exosuit Reduces Back Muscle Fatigue

We investigated the extent to which an un-motorized, low-profile, elastic exosuit reduced the rate of fatigue for six lumbar extensor muscles during leaning. Six healthy subjects participated in an A-B-A (withdrawal design) study protocol, which involved leaning at 45 degrees for up to 90 seconds without exosuit assistance (A1), then with assistance (B), then again without assistance (A2). The exosuit provided approximately 12-16 Nm of lumbar extension torque. We measured lumbar muscle activity (via surface electromyography) and assessed fatigue rate via median frequency slope. We found that five of the six subjects showed consistent reductions in fatigue rate (ranging from 26-87%) for a subset of lumbar muscles (ranging from one to all six lumbar muscles measured). These findings objectively demonstrate the ability of a low-profile elastic exosuit to reduce back muscle fatigue during leaning, which may improve endurance for various occupations.

3.1 Introduction

Prolonged leaning and repeated lifting often lead to fatigue of the low back muscles, specifically the muscles that extend the lumbar spine. Muscles undergo undesired functional changes as they fatigue (e.g., tremoring [28] and/or sensorimotor deficits [132]), which can result in discomfort, soreness, exhaustion or the inability to produce a desired force [41, 43]. Lumbar muscle fatigue can have detrimental effects on task performance and can negatively impact a person's productivity, satisfaction or safety (e.g., for populations that frequently perform tasks that are demanding on the low back, such as nurses [72, 129], construction workers [85], automotive assembly workers [117], and

workers in manual material handling environments [79]). Lumbar muscle fatigue can be reduced during leaning or lifting using external aids and wearable assistive devices [22, 90]. However, most devices are limited by practical factors such as affordability, form factor, and their ability to integrate into current workflows without interfering [12, 34, 82, 90, 164]. To address these practical factors, we previously introduced a new elastic exosuit that combines the low-profile benefits of daily clothing with the physical assistance benefits of an exoskeleton [82, 84] . This wearable device can fit underneath typical daily clothing and uses elastic elements to apply assistive forces in parallel with the lumbar extensor muscles to reduce the effort required by these muscles. In more recent prototypes, passive or motorized clutching has been incorporated so that the wearer can engage/disengage assistance on demand [84]. In the current work, we use a force-instrumented prototype, which will hereafter be referred to as the exosuit. We previously demonstrated that an early prototype of the exosuit reduced the mean muscle activity of lumbar extensor muscles by 23-43% during leaning and 14-16% during lifting (N=8,[82]). These reductions, along with subjective feedback from prior study participants, suggest that the exosuit may also reduce lumbar muscle fatigue. However, lumbar muscle fatigue was not evaluated in the prior study because it required a different experimental protocol. Moreover, in Lamers et al. [82], only two lumbar extensor muscles were monitored; however, several muscles contribute to lumbar extension [19]. It is currently unknown to what degree the exosuit can reduce the rate of lumbar muscle fatigue. Furthermore, it is unknown whether these effects are consistent between subjects, or whether these changes in fatigue occur uniformly across multiple back extensor muscles. The purpose of this study was to evaluate whether the exosuit reduced the fatigue rate of six lumbar extensor muscles during a leaning task, relative to a control condition (i.e., no exosuit assistance). Since we did not know a priori whether individual users would adopt similar muscle activation patterns when receiving exosuit assistance, we approached this study primarily from a subject-specific perspective (i.e., using single-subject study design and

analysis methods). Secondarily, we compiled and reported group-averaged results as a supplementary analysis.

3.2 Methods

3.2.1 Summary

Twelve subjects (seven male, five female) participated in the Day 1 data collection (detailed in 3.2.5.1). The purpose of Day 1 was measurement validation; to ensure we could objectively measure changes in the rate of lumbar muscle fatigue in individual subjects, using common surface electromyography (sEMG) techniques [45]. Subjects did not wear the exosuit during Day 1, rather subjects performed leaning tasks with heavier vs. lighter hand-held weights to induce higher vs. lower rates of lumbar muscle fatigue, using an A-B-A protocol. First, subjects performed the task while holding a 16 kg mass (i.e., more fatiguing condition – A1), then holding an 11 kg mass (less fatiguing condition - B), then holding the 16 kg mass again (A2). These masses were chosen to induce a contraction magnitude of at least 20% MVC, which is considered the minimum contraction level to elicit fatigue that can be detected with sEMG [29, 108]. Furthermore, study participants confirmed that they experienced noticeably more back muscle fatigue when holding the 16 kg vs. 11 kg mass, as expected. Six of twelve subjects exhibited a discernible decrease in fatigue rate (based on median frequency slope of sEMG) for a subset of lumbar muscles while holding the lighter mass (11 kg). To come to this conclusion, we visually inspected individual subject results and judged that six of the twelve subjects exhibited reduced median frequency slopes for the 11 kg vs. 16 kg conditions. Thus, for these subjects we had high confidence that we could objectively measure changes in their back muscle fatigue rates. Next, these six subjects (four male, two female, 23.5 ± 1.4 yr., 69.6 ± 7.7 kg., 1.8 ± 0.1 m) participated in the exosuit evaluation session (Day 2, detailed in subsubsection 3.2.5.2). The purpose of Day 2 was to assess

whether the exosuit reduced the fatigue rate for one or more of the six recorded lumbar muscles. Subjects performed leaning without (A1), then with (B), then again without (A2) assistance from the exosuit, in each case while holding the same 16 kg mass. We then assessed differences in muscle fatigue rate via median frequency slope of sEMG. All subjects reported no history of low back pain in the past six months and gave written consent prior to testing. The experimental protocol was approved by the Vanderbilt University Institutional Review Board, and these methods were carried out in accordance with the IRB-approved protocol.

3.2.2 Instrumentation & Prototype

On Day 1, we placed six sEMG sensors (Delsys Inc., Natick MA, USA) bilaterally over lumbar extensor muscles: right and left lumbar multifidus (RLM and LLM respectively) at L5 level, right and left iliocostalis lumborum (RIL and LIL respectively) at L2 level and the right and left longissimus thoracis (RLT and LLT respectively) at L1 level (**Figure 3.1**, a, b and c) ([45]). Two additional sEMG sensors were placed bilaterally over the latissimus dorsi (LD) muscles (**Figure 3.1**, e). A goniometer (Biometrics Ltd., UK) was placed across the lumbar region (sacrum to 12th thoracic vertebrae) to measure the sagittal (flexion/extension) angle of the lumbar spine (**Figure 3.1**, d). Day 2 involved the same instrumentation as Day 1, but with the addition of four sEMG sensors placed bilaterally over abdominal muscles (rectus abdominis and external oblique, **Figure 3.1**, f and g) to provide insight on potential co-contraction of these muscles [115]. All skin surfaces were abraded with alcohol wipes prior to EMG placement in accordance with SENIAM guidelines [69]. Additionally, plastic guards were placed over each sEMG sensor on the low back (**Figure 3.1**) to minimize motion artifacts due to the movement of the exosuit bands. Abdoli et al. [1] used similar methods to reduce motion artifact when testing their personal lift assist device. On Day 2, subjects wore an instrumented exosuit prototype that applied an extension torque about the lumbar spine during the intervention

trial (trial B in the A-B-A protocol). The prototype, described in detail in previous work [84], couples a trunk harness to two thigh sleeves with an elastic element (**Figure 3.1**, h, i, j, and **Figure 3.2**, h, i, g). The magnitude of assistive torque provided by the exosuit was adjusted manually and measured using an in-series load cell (**Figure 3.1**, k). The tension for each user was set between 150-200 N (the range in tension was due to practical challenges such as exosuit fit). For each subject this resulted in approximately 12-16 Nm of constant torque assistance (assuming a moment arm of 0.08 m between the L5-S1 joint and the exosuit elastic element line of action ([82]) throughout the intervention trial. Load cell, sEMG and goniometer data were collected synchronously at 2000 Hz.

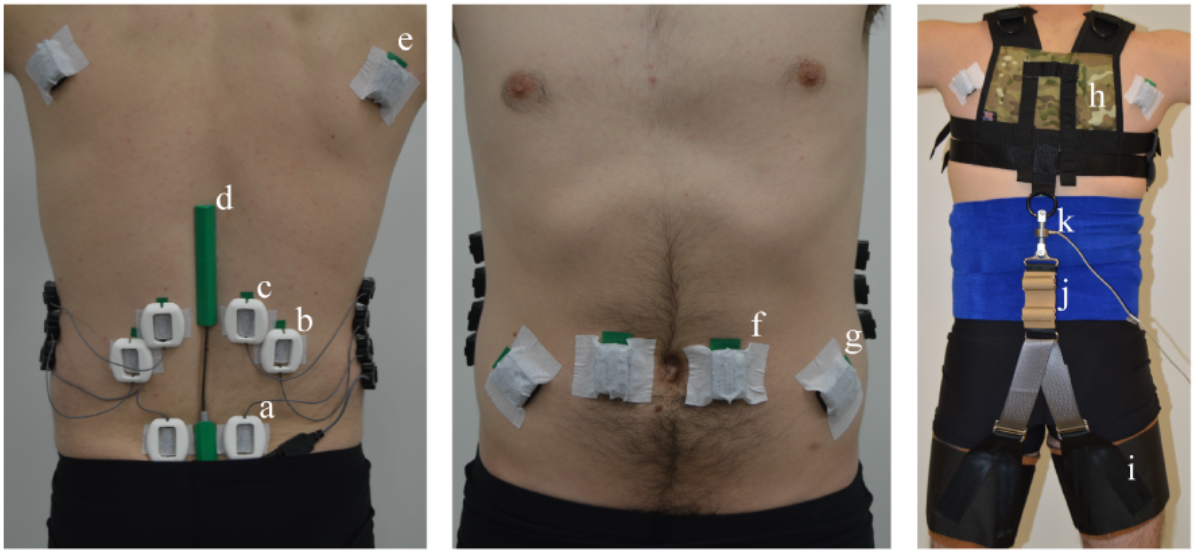

Figure 3.1: sEMG sensors were placed bilaterally over the multifidus muscles (2 cm lateral to the L5 vertebrae, a), the iliocostalis lumborum muscles (4 cm lateral to the L2 vertebrae, b), the longissimus thoracis muscles (2 cm lateral to the L1 vertebrae, c), the latissimus dorsi muscles (scapular level e), the rectus abdominis muscles (2 cm lateral to the umbilicus, f), and the external obliques (8 cm lateral to the umbilicus, g). Each sEMG sensor on the low back was covered with a protective cover to minimize motion artifacts caused by the exosuit moving above the skin and sensors. A digital goniometer (d) was adhered to the skin, spanning from the L5 to the L1/T12 vertebrae. A compression wrap (right) was wrapped around the torso to protect sEMG electrodes and prevent wires from snagging. The exosuit prototype was comprised of a trunk harness (h) and left/right thigh sleeves (i), which were coupled along the back-side of the subject via an elastic element (j). A uniaxial load cell (k) measured forces in-series with the elastic element.

3.2.3 Test Apparatus/Setup

In order to enable valid comparisons between trials, we developed a protocol to ensure that subjects had the same posture (both full-body and local lumbar angle) for each trial, because lumbar muscle fatigue is sensitive to changes in these postures [103, 119]. To ensure subjects adopted the same full-body posture during each trial we developed and used a custom scaffold (**Figure 3.2**) that is similar in function to the postural constraint device in Roy et al. [120]. The scaffold has rigid foot, knee and pelvis constraints

that set the position of the lower-body segments (**Figure 3.2**, a, b and c). A compliant trunk constraint (thin, taut string spanning the width of the user) then provides the subject with light tactile feedback on the upper back to help them maintain a consistent trunk angle (**Figure 3.2** d). Note that the string does not provide enough reaction force for the subject to induce non-negligible load on their lumbar muscles when they pushed against it. To ensure subjects adopted the same lumbar spine angle in each trial, we asked subjects to maintain their lumbar angle within ± 2° (which we determined in pilot tests to be a controllable lumbar angle range) of their preferred lumbar angle (established prior to trial A1) using real-time visual feedback. Visual feedback of the lumbar angle (from the goniometer) was displayed on a computer monitor in front of the subject (**Figure 3.2**, f).

To prevent subjects from compensating with their LD muscles while leaning, we used real-time visual feedback to minimize LD muscle activity. While the primary function of the LD muscle is to adduct, extend and medially rotate the shoulder joint [77], it also generates an extension moment about the lumbar spine [21]. In pilot tests, we observed that some subjects would greatly increase their LD activity partway through a leaning trial. This increased activity occurred inconsistently, and affected the activity of the six lumbar muscles we sought to study. As a result, this LD behavior confounds our ability to objectively assess lumbar muscle fatigue across trials (e.g., if a subject employed this sporadic strategy for one trial, but not the other trial) and to apply established muscle fatigue analysis methods based on linear regression. To avoid this confound, subjects had real-time visual feedback of both the left and right LD sEMG signals (simultaneously with the lumbar angle feedback), and were asked to minimize LD activity during each trial. See Discussion for more on this topic.

3.2.4 Study Design

During both Day 1 and Day 2 testing sessions we used an A-B-A protocol (withdrawal design) in which we established a baseline fatigue rate (first control – A1), introduced an intervention (B) that we expected to reduce the fatigue rate, and then removed the intervention (second control – A2) to examine if the fatigue rate returned back to the initial baseline rate. We compared the rates of individual muscle fatigue (within and between subjects) for three cases:

Case I: First control trial (A1) vs. intervention trial (B)

Case II: Second control trial (A2) vs. intervention trial (B)

Case III: First control trial (A1) vs. second control trial (A2)

Cases I and II informed whether the intervention (Day 1: lighter held mass, Day 2: exosuit assistance) reduced muscle fatigue relative to the control trials. Case III assessed whether fatigue rates returned to the baseline level, which would strengthen the inference that the observed change was caused by the intervention, rather than chance, task acclimation or natural variability [11]

3.2.5 Subject Testing

3.2.5.1 Day 1 - Measurement Validation

Subjects first performed maximum voluntary contractions (MVC) of their lumbar muscles in a back extension machine, by extending their trunk (aligned parallel with the ground) against manual resistance applied by the test administrator. Subjects then performed MVCs for their LD muscles by pulling down on an anchored rope with their left and then right arm (as if attempting a pull-up with one arm). MVC trials were 5 seconds in duration, and were separated by a rest period of at least 1 minute. Next, the foot, knee, pelvis and trunk constraints of the scaffold (**Figure 3.2**) were adjusted for each subject. The trunk constraint was adjusted until the trunk angle was approximately

45 degrees. Subjects then assumed a leaning posture and were instructed to choose a preferred lumbar angle while keeping their back flat. This was to ensure that the preferred lumbar angle was near neutral spine alignment, thus mitigating passive torque contributions from spinal ligaments (observed during large magnitudes of lumbar flexion [105]). A shaded band with ± 2° of the preferred lumbar angle was placed on the real-time visual feedback monitor. During testing, subjects were instructed to keep their lumbar angle within this shaded band. Subjects performed the first leaning trial (A1) with a 16 kg mass, the second trial (B) with an 11 kg mass, and the third trial (A2) with a 16 kg mass. Leaning trials were 90 seconds long, which we determined during pilot testing to be sufficiently long for participants to report considerable back muscle fatigue. Subjects were given at least 15 minutes in between trials to recover [42].

The purpose of the Day 1 session was to perform measurement validation on a subject-specific basis. In other words, Day 1 allowed us to confirm (or refute) that for a given subject we could confidently measure differences in back muscle fatigue rate (via sEMG) when comparing tasks with different physical demands (i.e., holding 16 kg vs. 11 kg). This subject-specific measurement validation was considered a critical inclusion criteria because we needed to confirm that subject sEMG median frequency followed logical trends (i.e., indicating more fatigue with higher weights), in order to ensure the fidelity and interpretability of data from the Day 2 session. Subjects only participated in the Day 2 data collection if during Day 1 they exhibited a reduction in lumbar muscle fatigue rate (as estimated by the median frequency slope of sEMG, detailed below in **Section 3.2.6**) for at least 1 lumbar muscle during the reduced load condition (11 kg, trial B) relative to the higher load conditions (16 kg, trials A1 and A2), and if the remaining lumbar muscles showed small changes (i.e., where the variation between A1 and B or A2 and B was smaller than or similar to variation between A1 and A2). Differences in lumbar muscle fatigue rate were assessed using visual inspection of the sEMG median frequency data and slope.

3.2.5.2 Day 2 - Exosuit Evaluation

Testing performed during the Day 2 session was similar to Day 1, except that for trial B the subjects (**Table 3.1**) were given lumbar torque assistance via the exosuit, rather than a different hand-held weight. Subjects performed the same MVC and setup procedures as detailed in **Section 3.2.5.1**, with the addition of MVC trials for the abdominal muscles (in which subjects flexed their trunk against manual resistance while positioned face up in the back extension machine). Subjects then performed the first leaning trial (A1) without exosuit assistance, the second trial with assistance (B), and the third trial again without assistance (A2). Subjects held the same mass for each trial and rested at least 15 minutes between trials. Subjects had the exosuit donned for the entire Day 2 session, but the elastic element was fully detached during the control trials (A1 and A2) such that the exosuit provided no assistance. Subject 2 (**Table 3.1**) held 20.5 kg, while the remaining subjects held 16 kg (**Figure 3.2**, e). Subject 2 exhibited greater resistance to fatigue during Day 1 testing and was given a heavier mass to ensure measurable levels of fatigue within the prescribed trial duration (90s).

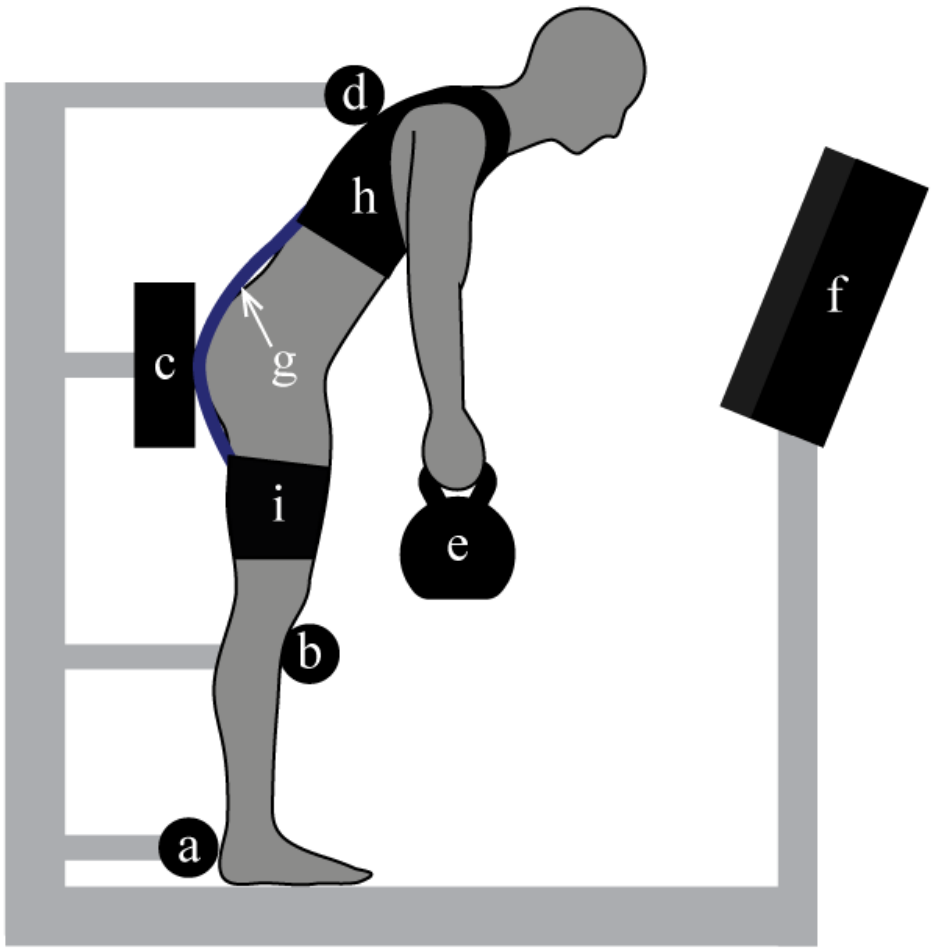

Figure 3.2: During leaning trials, participants stood within the test-apparatus which constrained the position of their feet (a), knees (b), and pelvis (c) with hard stops. A compliant trunk constraint (d) allowed subjects to use tactile feedback on their upper back to maintain a consistent trunk angle, but minimized their ability to load their lumbar muscles by pushing against the constraint. While leaning forward at 45 degrees, and holding a mass (e), subjects were given visual feedback (via lab monitor, f) of their lumber angle and instructed to maintain their preferred lumbar angle (designated prior to trial A1). Subjects were also given visual feedback of their left/right latissimus dorsi muscle activity and were asked to minimize the activity magnitude. During the second trial (trial B) of the Day 2 session, subjects were given lumbar torque assistance via the elastic element (g) which ran along their back-side, connecting the trunk interface (h) to the thigh interfaces (i) of the exosuit.

Table 3.1: Individual subject metrics for Day 2 intervention session

Subject #	Mass (kg)	Height (m)	Age (yrs.)	Gender
1	59.1	1.73	23	F
2	63.6	1.73	24	F
3	68.2	1.68	22	M
4	70.5	1.91	23	M
5	77.3	1.85	26	M
6	79.1	1.8	23	M
Mean ± SD	69.6 ± 7.7	1.8 ± 0.1	23.5 ± 1.4	-

3.2.6 sEMG Fatigue Analysis

Raw sEMG signals were filtered with a fourth-order, zero-lag, bandpass filter (10-500 Hz) [45]. Median frequency (MDF) and the root mean square (RMS) of the filtered sEMG signals were calculated over non-overlapping 1-second epochs for each trial [45, 101] (**Figure 3.3**). Linear regressions were fit to MDF data from each muscle, where the y-intercept of the regression indicated the initial MDF (value at t=0). Fatigue measurement epochs where discarded from the regression analysis if a subject's lumbar angle showed sustained deviation greater than ±2°. We present the slope of the regression fit in terms of the initial MDF value, i.e., in units of % initial MDF per second (hereafter simply referred to as the MDF slope). RMS for each muscle was normalized to the maximum RMS magnitude observed in the MVC trials. In single-subject studies such as this visual inspection is recommended as the primary assessment method whereas as inferential statistics are only intended to supplement visual inspection procedures [49]. Therefore, visual inspection was used to assess the effect of the exosuit on single-subject, muscle-level MDF slope. Specifically, two of the research investigators independently

assessed whether the intervention (trial B) appeared to have an effect on MDF slope relative to the controls (trials A1 and A2). As a key summary metric, they summed the number of individual muscles across all six subjects that showed reduced MDF slope during trial B. To supplement findings from visual inspection, the effect of the exosuit on single-subject, muscle-level MDF slope was also analyzed via analysis of covariance with unequal slopes (aoctool function in MATLAB). Significant main effects (=0.05) from the analysis of covariance, were followed up with a multiple comparison test using a Tukey-Kramer test (multcompare function in MATLAB). For inter-subject analysis, if the data passed a Shapiro-Wilk normality test (swtest function in MATLAB), then repeated measures analysis of variance tests (rmfit function in MATLAB) were performed to assess changes in MDF slope for Cases I-III. Friedman tests (friedman function in MATLAB) were performed if data did not pass the Shapiro-Wilk test. Significant main effects (=0.05) from the repeated measures analysis of variance and Friedman tests were followed up with a multiple comparison test using a Tukey-Kramer test (multcompare function in MATLAB).

3.3 Results

3.3.1 Day 1 - Measurement Validation

Six of the twelve subjects who participated in the Day 1 session showed reductions in MDF slope for a subset of lumbar muscles when holding the lighter weight, and only small changes in MDF slope for the remaining lumbar muscle (based on a visual inspection). These six individuals were invited to participate in Day 2. The six remaining subjects exhibited inconsistent muscle fatigue behaviors (e.g., no clear changes in MDF slope, or a combination of increases and decreases in the MDF slope for different muscles) despite differences in held mass. Consequently, we did not have confidence that we could reliably monitor changes in fatigue for this subset of participants. We therefore

erred on side of excluding them from Day 2 exosuit evaluation. Also of note, sEMG RMS magnitude results on Day 1 were not consistent (i.e., often did not exhibit expected fatigue trends) and sometimes contradicted MDF findings (which has also been observed in previous literature [114]). As a result, the RMS metric was not used in the Day 2 study to evaluate fatigue. This analysis approach is consistent with previous literature [120], in which MDF is typically used as the primary fatigue metric, and RMS is used as a secondary metric or not used at all (especially with lower levels of muscle contraction magnitudes [125])).

3.3.2 Day 2 - Exosuit Evaluation (Subject-Specific)

Visual inspection

Two investigators independently reviewed the sEMG results for 36 muscles (six subjects x 6 lumbar extensor muscles) and determined via visual inspection that between 18 and 21 individual muscles showed reduced MDF slope with the exosuit intervention (trial B) vs without the exosuit intervention (trials A1 and A2).

Supplementary statistics

Case I: First control trial (A1) vs. exosuit intervention (B): Five of six subjects exhibited statistically significant reductions in MDF slope in a subset of muscles (without any significant changes in any other muscles) with the exosuit vs. the first control trial (**Table 3.2**). Of these five, one (subject 1) showed statistically significant reductions for all muscles, and the remaining (subjects 2, 3, 5, 6) showed significant reductions for two to four muscles, and non-significant changes for the remaining muscles. Only one subject (subject 4) showed no significant changes across all muscles. During trial B, subject 5 deviated from the target lumbar posture range (± 2°) at 77 seconds into the trial, thus

the final 13 seconds of this trial were excluded from analysis.

Case II: Second control trial (A2) vs. exosuit intervention (B): The same five subjects exhibited reductions in MDF slope with the exosuit vs. the second control trial (**Table 3.2**), corroborating the results from Case I. One of these five (subject 1) showed significant reductions for all muscles. Four subjects (subjects 2, 3, 5, 6) showed significant reductions for one to four muscles, and non-significant changes for the remaining muscles. Subject 4 showed a significant increase in MDF slope for one muscle, and non-significant changes in the remaining muscles. During trial A2 subject 5 deviated from the target lumbar posture range (± 2°) at 30 seconds into the trial, thus the final 60 seconds of data were excluded from analysis.

Case III: First control trial (A1) vs. second control trial (A2): Four of six subjects showed no significant changes in MDF slope for any muscles when comparing the first vs. second control trial (**Table 3.2**). Subject 1 showed significant reductions for two muscles, whereas subject 4 showed significant increases for two muscles.

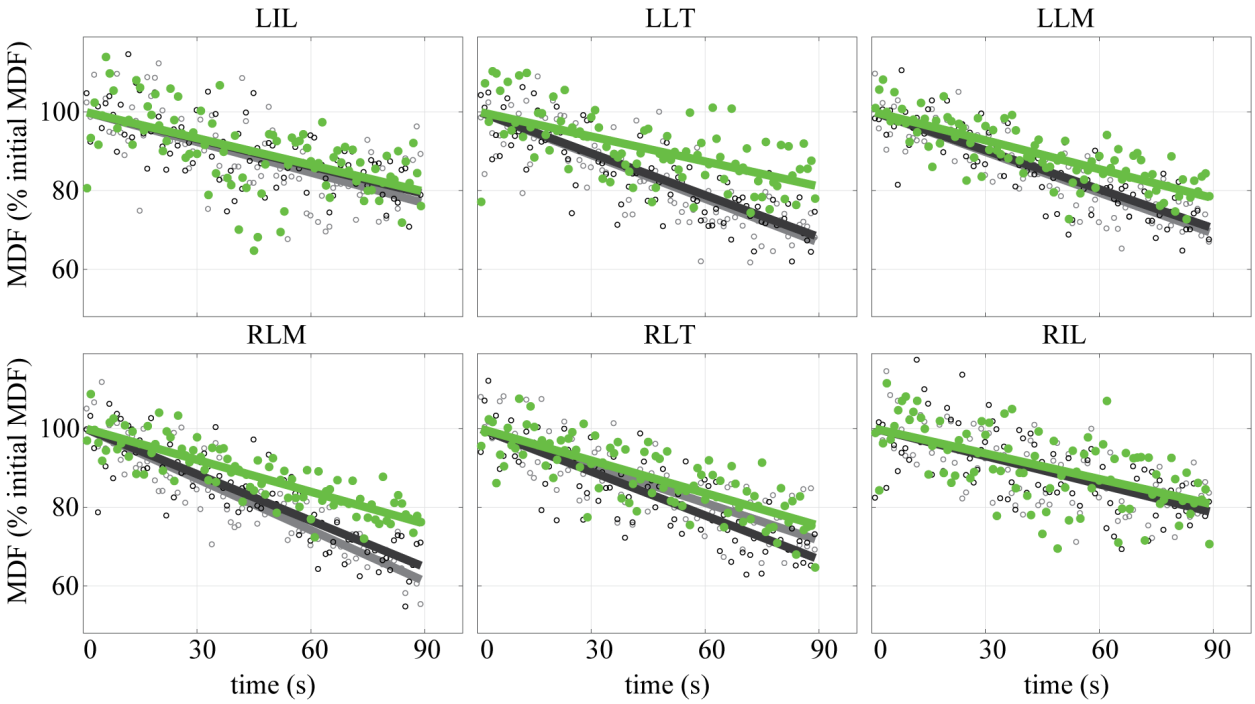

Figure 3.3: Representative (N=1) muscle-level, median frequencies (Day 2). The decrease in median frequency (MDF) over the duration of leaning is fit by linear regression lines. The slope of the regression line (i.e., MDF slope) is commonly used as a measurement of the rate of muscle fatigue [101]. Data are plotted for each muscle and each trial condition; control trial A1 (black line, open black circles), intervention trial B (green line, shaded green circles), control trial A2 (gray line, open gray circles). This figure illustrates MDF slope being significantly reduced for some muscles (LLT, LLM, and RLM) while wearing the exosuit, but not significantly reduced for other muscles (LIL, RLT and RIL). Note that the variability in MDF data points (i.e., each sample point shown) is common and characteristic of this sEMG measurement of fatigue [94, 93]. Depicted is data from Subject 3.

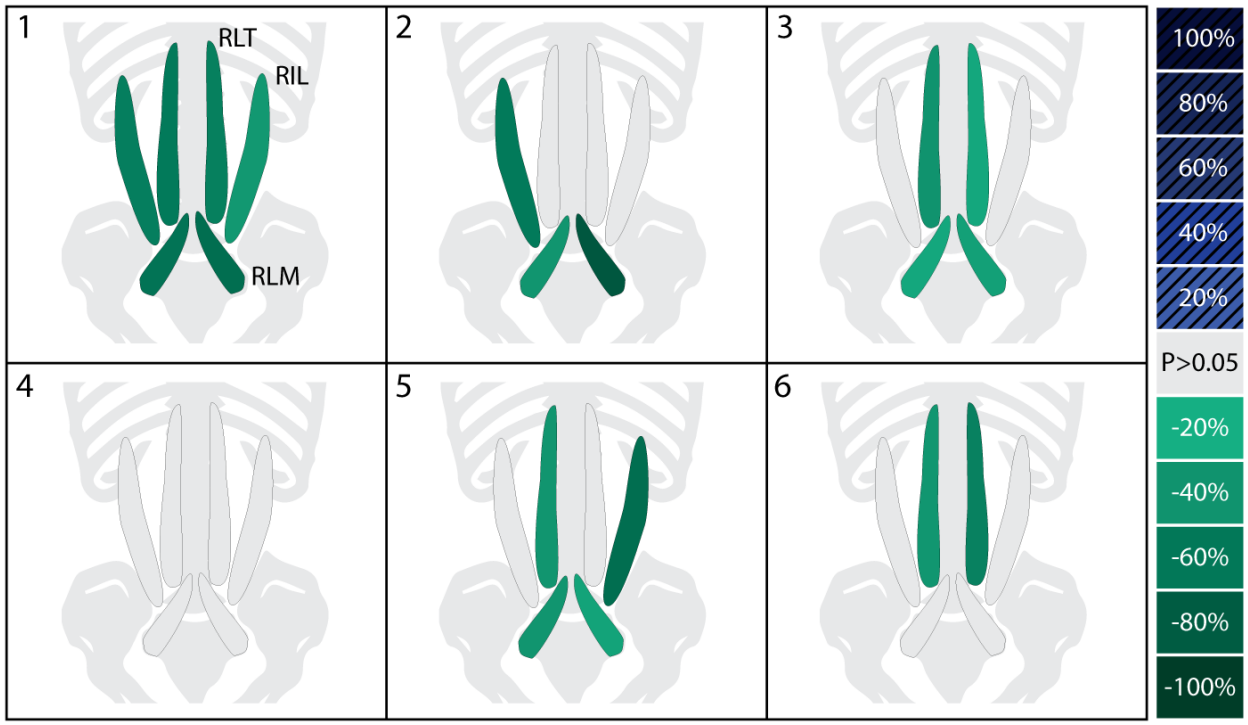

Figure 3.4: Subject-specific, muscle-level response to exosuit. Depicted are the changes in fatigue rate (MDF slope) for individual muscles when receiving exosuit assistance as compared to not receiving assistance (Case I: A1 vs. B). Significant decreases (and increases) in MDF slope with the exosuit are denoted by green (and blue-hatched) shading, where darker shades indicate larger magnitudes of change. Non-significant changes are denoted by light gray shading. The degree to which individual muscles experienced significant reductions in fatigue varied from subject to subject, with some showing significant reductions for all muscles (e.g., subject 1) and others showing significant reductions for a subset (e.g., subject 2). Shading is based on based on the analysis of covariance results, which were very similar to visual inspection. These responses highlight the variability across individual subjects, as well as the variability across the individual muscles of a single subject, demonstrating that there are multiple ways a wearer can adapt to and benefit from the exosuit.

Table 3.2: Change in MDF slope for individual muscles across all subjects for Cases I, II and III. Significant reductions in MDF slope (based on the analysis of covariance) when receiving exosuit assistance are denoted by green shading. Significant increases in MDF slope are denoted by blue shading, and non-significant changes are denoted by light gray shading. Changes are expressed as a percent change in MDF slope from one trial to the next (e.g., Case I, first control vs. intervention) where negative values indicate a reduction in MDF slope when wearing the exosuit relative to the control trials (Case I and Case II). Negative values in Case III indicate a reduction in MDF slope during the second control trial relative to the first control trial.

Case I (first control vs. intervention)						
Subject #	LIL	LLT	LLM	RLM	RLT	RIL
1	-55	-58	-63	-67	-54	-37
2	-58	-33	-39	-83	-20	-33
3	-3	-40	-26	-31	-26	-9
4	-19	-2	16	19	6	-2
5	-26	-39	-39	-29	-30	-67
6	14	-38	-31	-4	-53	-15
Case II (second control vs. intervention)						
Subject #	LIL	LLT	LLM	RLM	RLT	RIL
1	-45	-50	-54	-58	-46	-38
2	-53	-14	-33	-85	-26	-8
3	-13	-43	-29	-38	-13	-10
4	-24	103	21	60	10	-3
5	-48	-67	-60	-60	-34	-87
6	26	-21	4	2	-47	-24
Case III (first control vs. second control)						
Subject #	LIL	LLT	LLM	RLM	RLT	RIL
1	-19	-16	-19	-21	-15	1
2	-10	-22	-10	9	8	-27
3	11	4	4	10	-14	0
4	6	-52	-5	-26	-3	1
5	43	85	52	76	7	166
6	-9	-22	-34	-6	-12	12

3.3.3 Day 2 - Exosuit Evaluation (Inter-Subject)

On average, across the six subjects during Day 2, all lumbar muscles showed mean reductions in MDF slope with the exosuit relative to the first control trial (LIL:-34% LLT:-39% LLM: -38% RLM:-42% RLT: -32% RIL: -30%) and second control trial (LIL:-37% LLT:-43% LLM: -39% RLM:-47% RLT: -29% RIL: -44%). Of these muscles, two (LLT and RLT) showed statistically significant reductions in MDF slope (LLT: -39%, p=0.020, RLT: -32%, p=0.043) with the exosuit versus the first control trial (Case I), and two muscles (RLT, RIL) showed statistically significant reductions in MDF slope (RLT: -29%, p=0.047, RIL: -44%, p=0.004) with the exosuit versus the second control trial (Case II). Across all subjects in Case I, 19 of 36 muscles showed significant reductions in MDF slope. Similarly for Case II, 17 of 36 muscles showed significant reductions in MDF slope while only 1 muscle showed significant increases. Between Cases I and II, significant increases in MDF slope were only observed in subject 4. In Case III, 4 muscles showed significant changes in MDF slope. No abdominal muscles showed significant changes in MDF slope, nor did abdominal activation exceed 5% of the MVC magnitudes, and thus for brevity these results are not depicted.

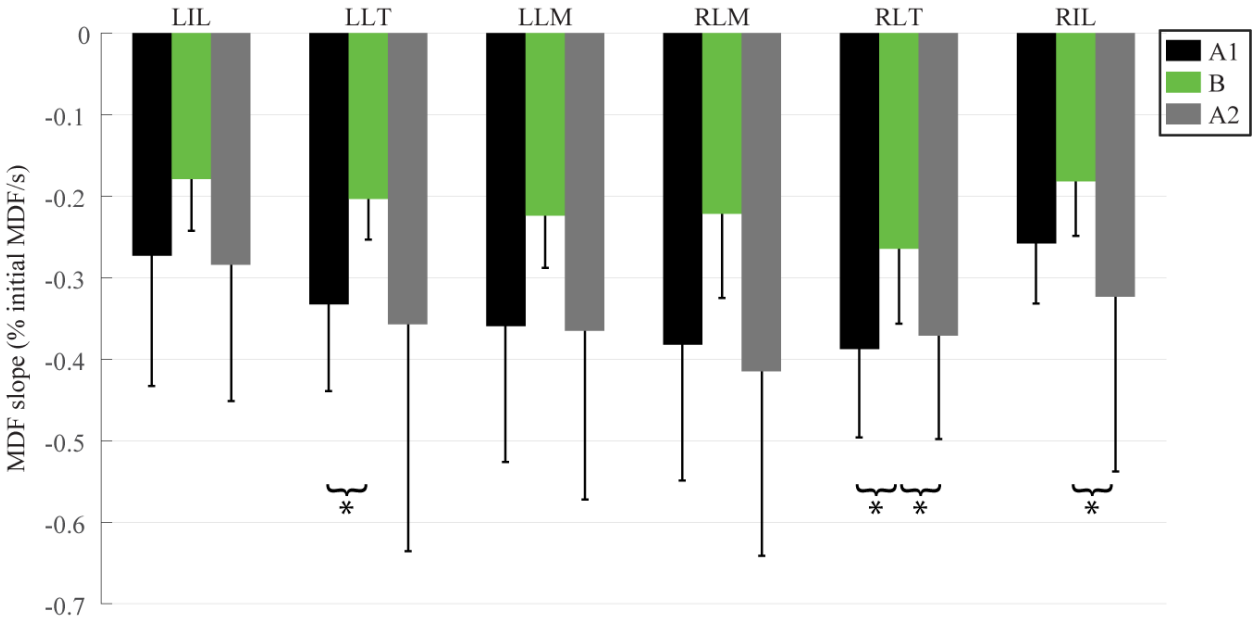

Figure 3.5: Group-level response to exosuit. Median frequency slopes (MDF slopes) are presented as a percentage of the initial median frequency (initial MDF). Reductions in the inter-subject average (N=6) MDF slopes were statistically significant (indicated by asterisks) for LLT and RLT for Case I (A1 vs. B) and RLT and RIL for Case II (B vs. A2).

Subject #	Assistance (N/kg)	N_I	N_{II}
1	3.0	6	6
5	2.7	4	4
6	2.4	2	1
3	2.3	4	3
2	2.3	3	3
4	2.0	0	0

Table 3.3: Subject-specific exosuit assistance magnitude. The magnitude of normalized exosuit assistance (tension in elastic element (N) per body mass (kg)) varied across subjects (ranging 2.0-3.0 N/kg). The number of muscles that showed significant reductions in MDF slope during Case I (NI) and Case II (NII) tended to be higher for subjects who received greater magnitudes of normalized exosuit assistance.

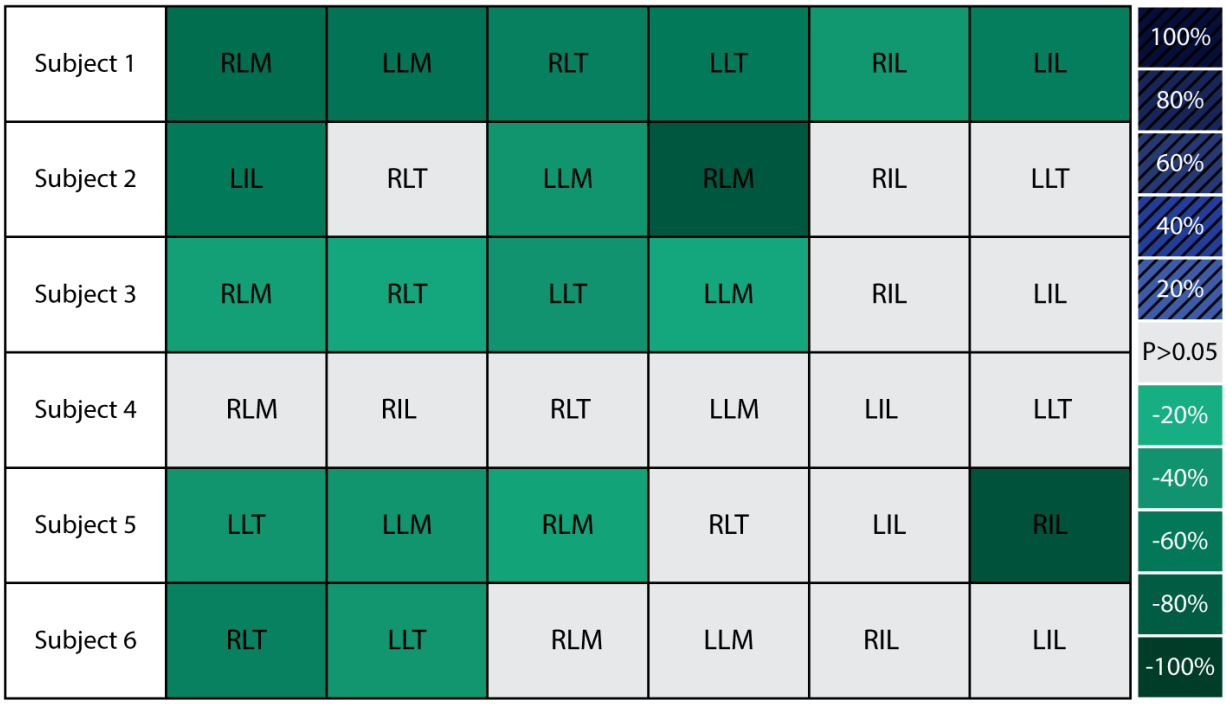

Figure 3.6: Individual muscle responses to exosuit vs. muscle fatigue rate. This shows Case I results (from Table 3.2) reorganized such that muscles are ordered from left to right, where left is the fastest (and right is the slowest) rate of fatigue during control trial A1. Significant decreases (and increases) in MDF slope are denoted by green (and blue) shading, where darker shades indicate larger magnitudes of change. Non-significant changes are denoted by light gray shading. Muscles that fatigued the fastest during control trial A1 tended to show significant reductions with the exosuit intervention, depicted by the higher density of green boxes on the left (and gray boxes on the right).

3.4 Discussion

Summary

We found that the exosuit reduced the lumbar muscle fatigue rate during leaning, with benefits exhibited by five of six subjects. The number of muscles that showed fatigue reductions and the magnitude of these reductions varied between individuals. From visual inspection, it was determined that between 18-21 individual muscles (of the 36 assessed across all subjects) experienced reduced fatigue rate with the exosuit vs. without the exosuit; and this was corroborated by statistical analysis. Based on inferen-

tial statistics, one subject showed significant reductions across all muscles, four showed significant reductions in 1-4 muscles, and one subject showed increases for 1 muscle. Across all subjects, the exosuit significantly reduced the fatigue rates for about half (18 of 36) muscles, consistent with findings from visual inspection. These findings suggest that the exosuit provides a viable option for reducing lumbar muscle fatigue in various occupations and work environments where leaning, bending or stooping is common (e.g., a doctor performing surgery, a material handler, or a worker at an assembly line).

3.4.1 To what degree did the exosuit reduce the rate of lumbar muscle fatigue?

Individual subjects showed significant reductions in MDF slope (i.e., fatigue rate) ranging from 26-87% across the lumbar muscles (relative to control trials, Cases I and II in Table 2), and exhibited consistent benefits for at least 1 and up to 6 lumbar muscles. Previous studies on lumbar muscle fatigue found that reduced MDF slopes corresponded with increased endurance times (i.e., duration that someone can sustain a leaning posture before task failure) [94]. Thus, this exosuit may have practical applications in work environments where leaning is common, such as dentistry [137], surgery [130], nursing [129], construction [85] or material handling, and where excessive lumbar muscle fatigue may necessitate workers to take frequent breaks, or may increase the likelihood of mistakes, injuries or employee turnover. For a practical comparison, we processed sEMG data from Day 1 and computed fatigue rates for the same six subjects. We found that significant reductions in fatigue rate during Day 1, when holding an 11 kg vs. 16 kg mass, ranged from 21-57% across individual muscles; and on average each subject exhibited significant reductions in fatigue rate in 1.4 ± 1.2 muscles. Relative to the Day 2 range (26-87% reductions in fatigue rate) and average number of muscles exhibiting reduced fatigue (3.0 ± 1.9 muscles), this suggests that the exosuit assistance provided an offloading effect that was greater than reducing the mass of a weight held

about 0.3 m in front of the L5/S1 joint by 5 kg. Stated simply, the exosuit made holding a 16 kg mass less fatiguing on the back than holding an 11 kg mass without the exosuit. This magnitude of benefit is consistent with physics-based estimates, i.e., that the 12-16 Nm assistance from the exosuit (150-200 N applied at 0.08 m moment arm) would be expected to offload 4-5 kg from a hand-held mass located 0.3 m anterior to the L5/S1 joint. Prior studies [1] and physics based estimates [82] both indicate that further extending the moment-arm of the device could increase assistance to the user, which may facilitate greater reductions in muscle fatigue; though potentially at the cost of increasing device form-factor (i.e., how much it protrudes from the body).

3.4.2 Were changes in the lumbar muscle fatigue rate consistent between subjects?

Changes in the rate of lumbar muscle fatigue were not consistent between subjects. Subject 1 showed significant reductions across all lumbar muscles, whereas subjects 2, 3, 5 and 6 had significant reductions for a subset of muscles (ranging from 1 to 4 muscles). This inter-subject variability may be partially explained by the difference in body-weight normalized exosuit assistance between subjects (ranging from 2.0-3.0 N/kg, **Table 3.3**). Subjects who received a higher magnitude of assistance (e.g., subjects 1 and 5 who received 2.7-3.0 N/kg) showed significant reductions across more lumbar muscles than those who received a lower magnitude (e.g., subjects 2, 3 and 6 who received 2.3-2.4 N/kg). These trends suggest that increasing exosuit assistance may yield more significant reductions in lumbar muscle fatigue, as one would intuit. This result is consistent with prior back exosuit studies; for example, Frost et al. [54] demonstrated that greater magnitudes of torque assistance (generated by using stiffer springs) yielded greater reductions in back muscle sEMG. Subject 4 received the least assistance (2.0 N/kg, **Table 3.3**), and did not exhibit reductions in muscle fatigue rate. Aside from receiving less assistance, we are unable to identify (from the data we collected) why this individual re-

sponded so differently from the other subjects. We did not observe substantial changes in the antagonistic abdominal muscle activity, which remained small across conditions (i.e., did not exceed 5% MVC), nor did we observe changes in posture; although minor compensatory strategies may have been used which were not captured by our measurements. It is known that people habituate to assistive devices at different rates, and thus differences in learning/adaptation rate may explain some of the inter-subject variability observed in this study; particularly, given the relatively short training/acclimation period. In the future it will be interesting to test subjects after longer (e.g., multi-day or multi-week) training periods, or to test individuals at different time points during the habituation process.

3.4.3 Did changes in the fatigue rate occur uniformly across the lumbar muscles?

Changes in fatigue rate were generally not uniform across lumbar muscles based on findings from both visual inspection and inferential statistics (**Table 3.2**, **Figure 3.4**). For instance, subjects 2, 3 and 6 showed considerable variability across muscles; with significant reductions in some muscles and non-significant changes in others. Even for subjects 1 and 5 who showed significant reductions across 4-6 muscles (**Table 3.2**), the magnitudes of these reductions varied across muscles (from 38-67% in subject 1, and from 26-85% in subject 5). Because many muscles span the lumbar spine, there are countless different muscle activation patterns that can result in the same net lumbar joint torque. This begs the question: how do subjects decide which lumbar muscles to offload/relieve when exosuit assistance is provided? Based on our findings, the lumbar muscles that fatigued the fastest (i.e., had the greatest MDF slope magnitude) during the A1 control trial appeared more likely to have statistically significant reductions when the exosuit intervention was introduced (**Figure 3.6**). This trend suggests that subjects may have chosen to preferentially offload muscles that were fatiguing the fastest during

this leaning task. Previous work shows that the fastest fatiguing lumbar muscles best predict endurance time [93], indicating that they may be a limiting factor for endurance. By preferentially offloading the fastest fatiguing lumbar muscles (as opposed to other, slower fatiguing lumbar muscles), subjects may derive the greatest benefit in terms of increasing their endurance time. The hypothesis that individuals choose to relieve muscles that are fatiguing the fastest, warrants further investigation.

3.4.4 Insights from group-level analysis

On average, all muscles exhibited reductions in fatigue rate when wearing the exosuit vs. both control trials, by between 29% and 47% (**Figure 3.5**). However, these reductions only reached statistical significance for the left and right longissimus thoracis muscles for Case I and the right longissimus thoracis and the right iliocostalis lumborum muscle for Case II (**Figure 3.5**). This result (i.e., a limited number of statistically significant reductions) was not surprising given the small sample size (N=6), meaning that the study was underpowered from a group analysis perspective. However, biomechanical interventions often result in high inter-subject variability in responses [11], which is why we focused on subject-specific findings in this study. Based on the subject-specific results it was clear that individual users received benefits to different lumbar muscles. For instance, subject 2 and subject 6 each benefited from the exosuit, yet showed reductions in fatigue for a different (non-overlapping) subset of lumbar muscles (**Figure 3.4**). This observation is potentially relevant for the development of biomechanical test methods or ergonomic assessment standards for exosuits and exoskeletons. For example, if we had only recorded a subset of the lumbar muscles (e.g., only RLM and LLM) we would have concluded that the exosuit benefitted subject 3, but not subject 6 (**Figure 3.4**). But with a more comprehensive sample of lumbar muscles (e.g., the six monitored in this work) we conclude that the exosuit benefitted both subjects 3 and 6; however, these

subjects happen to derive benefits for a different subset of back extensor muscles. Thus, assuming that synergistic muscles (e.g., lumbar extensor muscles) will behave or adapt similarly to an intervention may generate misleading conclusions. Given the abundance of muscles that can contribute to lumbar extension it generally will not be known a priori which specific muscles will exhibit benefits for each individual, and thus it may not be known which muscles should be monitored. This may bring about challenges related to the standardization of assessment metrics across tasks and devices, and complicate objective comparisons and interpretations between individuals.

3.4.5 Latissimus dorsi (LD) observations

We observed that the LD muscles could significantly affect the activity of the six lumbar muscles. The LD muscles primarily adduct, extend and medially rotate the shoulder joint, but they also contribute to lumbar extension. Previous studies have suggested that the magnitude of lumbar extension torque provided by the LD is generally small (and often negligible) relative to the contributions of other lumbar muscles during tasks such as lifting [21, 98, 99]. However, during pilot testing of the leaning task, we observed that some individuals would greatly increase their LD activity (typically about 60 seconds into the trial, **Figure 3.7**). Concurrently, muscle activity from the six lumbar muscles would noticeably decrease; suggesting that subjects were offloading the six lumbar muscles by activating their LD muscles. Interestingly, this behavior of the LD muscles is somewhat similar to the behavior of the exosuit, because they both apply forces across the entire thoracolumbar spine, they both have a mechanical advantage relative to the underlying lumbar muscles (i.e., larger moment arm about the lumbar spine), and when engaged they can both offload other lumbar extensor muscles. Because of this LD behavior (which was employed inconsistently by subjects) we implemented a real-time visual feedback system (as detailed in Methods) to help minimize LD activity that would oth-

erwise confound our interpretation of muscle fatigue rate based on conventional metrics (i.e., fitting a single linear regression to MDF data).

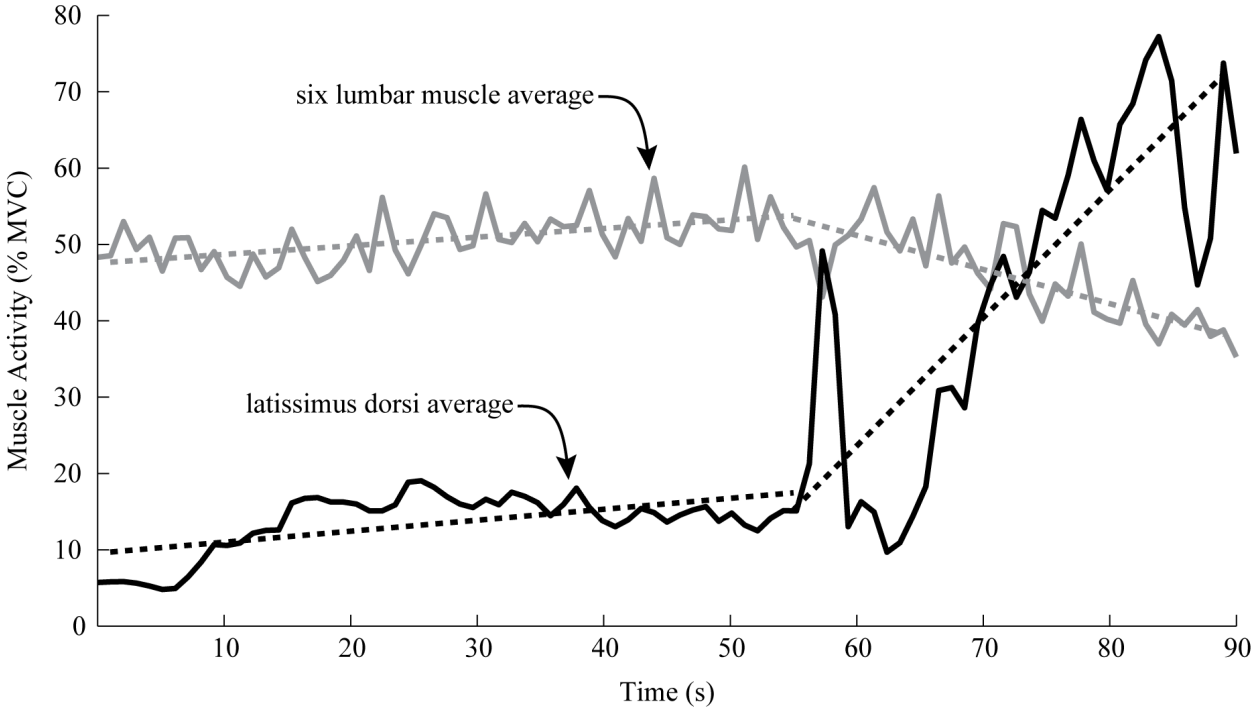

Figure 3.7: Latissimus dorsi (LD) and lumbar muscle interaction. Representative normalized muscle activity (RMS magnitude in %MVC, N=1) of the LD muscle group (black line, mean of left and right LD) and the muscle activity of the lumbar muscles (gray lines, mean of all six recorded lumbar muscles) during a leaning trial (i.e., trial A2). Dashed lines are linear regression fits of each group mean during two distinct phases, i.e., phase 1 (0-60s) where LD amplitude remains low, and phase 2 (60-90s) where the LD amplitude increases substantially. The extension torque applied by the LD muscles about the lumbar spine can become significant (phase 2, increase in dashed-black slope) reducing the effort required by the low back muscles (phase 2, negative slope of dashed-gray line).

Limitations

These findings should be considered and interpreted with a few experimental limitations in mind. The number of subjects tested with the exosuit intervention (N=6) was relatively small, resulting in low-power group-level (inter-subject) results. However, our main goal was to investigate responses at a subject-specific level. Using an A-B-A (withdrawal design) protocol provided convincing evidence that the exosuit assistance

reduced the rate of lumbar muscle fatigue, and that the fatigue rate increased back to the baseline when assistance was removed (**Table 3.2**, **Figure 3.5**). The magnitude of exosuit assistance varied between subjects (2.0-3.0 N/kg, **Table 3.3**). This variability was the result of prototype fit, manual tuning and other practical factors. Although this variability was not intentional, it revealed how the magnitude of fatigue reduction may be related to the magnitude of assistance, which is consistent with intuition and prior literature. We did not include dynamic movements (such as lifting) in this study. For the simple leaning task explored in this work, we needed a highly controlled setup (e.g., custom scaffold and real-time feedback). The protocol would need to be altered to test dynamic movements. Nevertheless, in previous work we showed that this exosuit design can reduce lumbar muscle activity during dynamic movements like lifting, and this matches subjective feedback on perceived exertion while wearing the exosuit [82]. Also prior studies using a somewhat similar back assistive device have demonstrated reductions in back muscle fatigue rate during lifting [90]. Therefore, our expectation is that the type of exosuit tested in this study will also reduce fatigue during other related tasks such as lifting and lowering. We measured sEMG over numerous sites (12, if we include abdominal and LD muscles); however, this still only represents a subset of muscles that contribute to lumbar flexion/extension. On a related note, we did not estimate contributions from passive (e.g., ligament) tissues around the spine; instead we attempted to keep these contributions small and consistent by targeting a neutral lumbar angle and by keeping this angle consistent across trials using biofeedback. Only half of subjects tested during the Day 1 session showed reductions in MDF slope between the two weight conditions (11 kg vs. 16 kg). One potential explanation for this finding is that the 5 kg difference between the two conditions may not have caused a large enough change in muscle activation for some subjects to exhibit changes in MDF slope; reflecting potential limitations in sEMG measurement sensitivity. Inducing greater changes in muscle activation would likely elicit more distinct changes in MDF slope (e.g., 10 kg difference in Farina

et al. [45]). We note that non-parametric statistical tests are generally recommended for single-subject analysis, as detailed in Fisch 2001 [49]. But in this study we used a parametric test (analysis of covariance) for the supplementary statistics. We used a parametric test because the accepted measure of sEMG muscle fatigue is based on linear regression, which is a parametric regression; thus, we could not perform non-parametric statistics without fundamentally altering the accepted measure of muscle fatigue (MDF slope from linear regression). Nevertheless, we have confidence in our findings because they were corroborated by visual inspection (**Figure 3.3**) and because the muscle fatigue rate during A2 returned back to the A1 baseline after the exosuit assistance was removed (**Figure 3.5**, **Table 3.2**). Finally, asking subjects to lean without activating their latissimus dorsi muscles did add an additional constraint, but we found that it was necessary to control latissimus dorsi activity for conventional fatigue metrics to be valid (e.g. linear regression to MDF data). Qualitatively, the sudden increase in latissimus dorsi muscle activity may serve as another practical indicator of lumbar extensor muscle fatigue in some individuals, but at present there is not a generalized framework for assessing muscle fatigue using both MDF slope and latissimus dorsi behavior in combination. We do not believe any of these limitations alter the overall conclusions from this study; the A-B-A protocol provides unambiguous evidence of reduced lumbar muscle fatigue in 5 of the six subjects when wearing the exosuit.

3.5 Conclusion

We found that an un-motorized, low-profile elastic exosuit could significantly reduce the rate of lumbar muscle fatigue during leaning. We observed inter-subject variability in the number of muscles that benefited, which specific muscles benefited, and the degree to which each muscle benefited (percentage reduction in fatigue rate) from wearing the exosuit prototype. These findings suggest that this type of exosuit could be effective for reducing the lumbar fatigue of individuals who perform bouts of leaning,

bending or stooping (e.g., dentists, nurses, assembly line workers, material handlers and construction workers).

Chapter 4

Subject-Specific Responses to an Adaptive Ankle Prosthesis During Incline Walking

Individuals with lower-limb amputation often have difficulty walking on slopes, in part due to limitations of conventional prosthetic feet. Conventional prostheses have fixed ankle set-point angles and cannot fully replicate able-bodied ankle dynamics. Microprocessor-controlled ankles have been developed to help overcome these limitations. The objective of this study was to characterize how the slope adaptation feature of a microprocessor-controlled ankle affected individual prosthesis user gait biomechanics during sloped walking. Previous studies on similar microprocessor-controlled ankles have focused on group-level results (inter-subject mean), but did not report individual subject results. Our study builds upon prior work and provides new insight by presenting subject-specific results and investigating to what extent individual responses agree with the group-level results. We performed gait analysis on seven individuals with unilateral transtibial amputation while they walked on a 7.5 °incline with a recently redesigned microprocessor-controlled ankle that adjusts ankle set-point angle to the slope. We computed gait kinematics and kinetics, and compared how users walked with vs. without this set-point adjustment. The microprocessor-controlled ankle increased minimum toe clearance for all subjects. Despite the microprocessor-controlled ankle behaving similarly for each user, we observed marked differences in individual responses. For instance, two users switched from a forefoot landing pattern with the microprocessor-controlled ankle locked at neutral angle to rearfoot landing when the microprocessor-controlled ankle adapted to the slope, while two maintained a forefoot and three maintained a rearfoot landing pattern across conditions. Changes in knee angle and moment were also subject-specific. Individual user responses were often not well represented by inter-subject mean. Although the prevailing experimental paradigm in

prosthetic gait analysis studies is to focus on group-level analysis, our findings call attention to the high inter-subject variability which may necessitate alternative experimental approaches to assess prosthetic interventions.

4.1 Introduction

Healthy individuals adjust to sloped terrains via characteristic changes in gait kinematics and kinetics [52, 63, 81, 86, 87, 100, 121]. For example, healthy individuals typically dorsiflex their ankle more during stance and generate more positive ankle work when walking uphill than during level ground walking [100]. Individuals with lower-limb amputation, however, are often incapable of making similar adjustments with their prosthetic side [141, 143], due in part to the limitations of conventional prosthetic feet. Most conventional prosthetic feet are passive (cannot generate net-positive work) and have a fixed ankle set-point angle [7, 40], which limits prosthetic ankle articulation during common daily activities like incline walking [141]. Limitations of conventional prosthetic feet can have detrimental effects on individuals with lower-limb amputation. For instance, reduced speed, cadence, prosthetic-side single-support time and knee moment have been attributed to the limited range of motion of conventional prostheses [141, 143]. Other studies have reported reduced toe clearance of the prosthetic side relative to the intact side which may increase trip and fall risk [35]. Prosthesis users have also been observed to exhibit an increased amplitude and duration of muscle activity during sloped walking [141] which may accelerate the rate of fatigue.

Adaptive prosthetic ankles have been developed in recent years in an effort to address limitations of conventional passive prosthetic feet. Various adaptive prostheses are commercially available and have been designed to restore some degree of healthy ankle behavior (e.g., dorsi-/plantar-flexion range-of-motion (Endolite Elan and Fillauer Raize), powered push-off (Ottobock Empower)). Among these adaptive ankles are quasi-passive devices, such as the Össur ProprioFoot, which uses a microprocessor and low-power mo-

tor to adjust the set-point of the ankle angle when the device is unloaded (i.e., during swing phase) to better conform to sloped terrains [78]. For example, during incline walking the ProprioFoot increases the ankle dorsiflexion angle [51], as is observed in healthy ankle behavior [64]. A few previous studies on individuals with unilateral transtibial amputation have investigated the biomechanical effects of the ProprioFoot on sloped terrains. Fradet et al. [51] found that on average the increased dorsiflexion of the ProprioFoot led to increased peak prosthetic-side knee flexion (by 8°) and increased peak knee flexion moment (by 0.2 Nm/kg) in early stance (0-40% gait cycle) during 7.5°incline walking (N=16), compared against the ProprioFoot without the set-point adjustment. Otherwise, they observed minimal changes in prosthetic-side and intact-side kinematics and kinetics during both incline and decline walking. Agrawal et al. [7] found that the ProprioFoot improved inter-limb work symmetry for K2-level [56] prosthesis users during decline walking as compared against a K1 (solid ankle cushioned heel prosthesis) foot (N=10). Statistically significant differences were not found for incline walking, nor for K3-level prosthesis users. Darter et al. [33] found that the ProprioFoot reduced metabolic energy expenditure during decline walking relative to users' daily-use prostheses (N=6). However, metabolic differences were not statistically significant when comparing the ProprioFoot with vs. without the set-point angle adjustment.

Previous adaptive prosthesis studies [7, 33, 51] have primarily analyzed and reported results from a group-level perspective (i.e., computing inter-subject means and standard deviations, paired t-tests and repeated measures analysis of variance); however, group-level behaviors may not reliably reflect the behaviors of individuals within the group [50]. Prosthesis users are well known to be a heterogeneous population, even within a given K-level. It is not uncommon for multiple prosthesis users to adapt in different ways to the same intervention, or for some users to benefit while others do not (e.g., [25]). This variability may be due to inherent differences amongst prosthesis users (e.g., cause, level and type of amputation) and/or clinical adjustments, such as prosthesis alignment,

which can be highly variable. With a large enough sample size, these covariates could be factored into an analysis (e.g., stratification, multivariate models, or logistic regression [116]) to help explain the effects of these covariates on biomechanical outcomes. However, most instrumented gait analysis studies on prosthesis interventions are conducted on small sample sizes (10.2 ± 5.5 subjects [138]). It is not uncommon for the number of covariates (confounding variables) to exceed the number of subjects tested, thus these population-based analyses are generally not adequate to account for covariates in gait analysis studies. In light of these limitations and challenges, the objective of this study was to characterize how individual prosthesis users alter their gait biomechanics during sloped walking with an adaptive ankle prosthesis, versus walking with the same ankle when the adaptive feature was turned off (i.e., ankle fixed in the nominal prosthetist alignment). This comparison allows us to directly evaluate the effects of the ankle adaptation without introducing additional confounds due to differences in size, mass, shape, or stiffness across prostheses. This study provides a unique contribution to the literature, and builds upon prior work, by presenting subject-specific outcomes in order (i) to better elucidate how individuals adapt their gait pattern to an increase in ankle dorsiflexion set-point angle provided by a recently redesigned microprocessor-controlled ankle, and (ii) to investigate to what extent these individual adaptations are reflected by group-level responses.

4.2 Methods

4.2.1 Participants and Intervention

Eight individuals with unilateral transtibial amputation were recruited for this study. However, one prosthesis user was omitted from the analysis because he was not comfortable walking on slopes when the MPA was locked at neutral angle. The seven participants analyzed (6 male, 1 female, height 1.76 ± 0.07 m, mass 89.0 ± 14.1 kg, age

41.4 ± 13.4 yrs.) were either K3- or K4-level ambulators, each at least 6 months post amputation surgery (**Table 4.1**, for participant details). All participants provided written informed consent, according to Vanderbilt Institutional Review Board procedures. Participants were fitted with an adaptive microprocessor-controlled ankle (MPA) by a trained prosthetist, and were educated on the functions of the device. The prosthesis tested in this work was a premarket MPA developed and fabricated by Össur; it is the next generation of the ProprioFoot, which has various software and hardware updates relative to its predecessor (**Figure 4.1**, A). Specifically, this device has an updated foot blade design based on the Pro-Flex LP (Össur), which may affect the stiffness and elastic energy storage/return properties of the prosthesis [31], whereas the previous generation ProprioFoot's foot blade was based on the Vari-Flex LP (Össur). This MPA provided two behaviors not found in conventional prosthetic feet. First, the MPA changed the set-point angle proportionally to the ground slope. It was programmed to dorsiflex the ankle to 75% of the incline slope angle (estimated via onboard sensors). Second, to facilitate toe clearance, the MPA dorsiflexed the ankle during early leg swing, then plantarflexed the ankle later in swing to return to the ankle set-point angle (in preparation for stance phase). After the fitting, prosthesis users wore the MPA for at least two weeks of at-home acclimation before returning for instrumented gait analysis testing.

Figure 4.1: Premarket microprocessor-controlled prosthetic ankle (MPA) developed by Össur (left) and sagittal view of the placement of passive reflective markers on the MPA and socket (right). Foot marker placement was intended to mirror markers on the intact foot (medial epicondyle, medial malleolus, and 1st metatarsal not shown).

4.2.2 Procedure

Prosthesis users performed level (0°) and sloped (incline/decline 7.5°[51]) walking on a treadmill at a fixed speed (0.8 m/s for 6 users, and 0.9 m/s for user 6 who felt more comfortable at this speed), and also stair ascent and descent. Prosthesis users performed walking conditions in the following order: (i) the MPA with the ankle adaptation feature turned on (hereafter referred to as the MPA condition), (ii) the MPA with the adaptation feature turned off and the ankle fixed at a neutral angle (i.e., the alignment set by the prosthetist during fitting, hereafter referred to as the MPA-unadapted condition), and (iii) with their daily-use prosthesis (**Table 4.1**). Prosthesis users wore

their preferred shoes during each testing condition (**Table 4.1**). Prosthesis users were not instructed to adopt any particular gait pattern, and were allowed to adapt as they desired. For brevity, and due to the large number of subject-specific results, we only present findings on the incline walking with the MPA vs. MPA-unadapted conditions in this work. These conditions allow us to isolate the effect of changing the ankle set-point angle on slopes without confounds due to the physical differences between the MPA and daily-use prostheses. Ground reaction force data were collected under each foot at 1000 Hz using a split-belt force-instrumented treadmill (Bertec, Columbus, OH, USA), and lower-body kinematics were recorded at 200 Hz via a synchronized 10-camera motion capture system (Vicon, Oxford, UK). Passive reflective markers were placed bilaterally over the anterior/posterior superior iliac spines, medial/lateral femoral epicondyles and malleoli, calcaneus, 1st and 5th metatarsal, and navicular bone. Clusters of four markers were placed bilaterally on the thigh and shank for segment tracking. Six markers were placed on the prosthetic socket (cluster of four on the body of the socket and two near the medial/lateral femoral epicondyles), and six were placed on the prosthetic-side shoe (estimated location of medial/lateral malleoli, calcaneus, 1st and 5th metatarsal heads and navicular bone, **Figure 4.1**, B).

4.2.3 Data Analysis

Joint angles, moments and powers were calculated over the stride, via inverse dynamics (Visual3D, C-Motion, Germantown, USA). Of note, ankle-foot power was calculated using an inverse dynamics estimate that considers contributions from all sources distal to the shank (or distal to the prosthetic socket for the prosthetic side) to avoid errors resulting from rigid-body assumptions of the ankle-foot [133, 158]. Toe height during swing phase was estimated using a geometric model based on reflective markers placed on the foot, similar to previously published techniques [17]. All data were divided into strides and processed for each participant and condition (yielding a mean of 25 strides

± 9 strides per trial). Note that for the MPA condition, only strides after the foot had adapted to the slope were used in the average. Data were normalized to 100% stride cycle, and then averaged across strides prior to reporting. Prior to analysis, ground reaction force and motion capture data were filtered with a zero-lag 3rd order low-pass Butterworth filter at 15 and 6 Hz, respectively. Inter-subject comparisons between the MPA and MPA-unadapted conditions were performed with a non-parametric Wilcoxon signed-rank test (=0.05).

4.2.4 Outcome Metrics

In this work, we focus on a few select metrics. First, we report prosthetic-side sagittal ankle angle in order to confirm proper MPA function (i.e., that the MPA dorsiflexed to accommodate the sloped terrain, and also dorsiflexed during swing phase to aid toe clearance). Next, we report a few key outcome metrics that capture changes in participant gait biomechanics. These metrics include prosthetic-side (i) minimum toe clearance (MTC) during swing phase, (ii) fore-aft center-of-pressure, which provided an objective means of differentiating a rearfoot vs. forefoot landing pattern, and (iii) sagittal knee angle and moment, which were reported in prior work [51] and may be important towards understanding changes in knee behaviors such as knee joint loading [122]. A few additional results are presented in the main text to assist readers in contextualizing and interpreting results and/or generating their own hypotheses based on the subject-specific results provided. First, we computed inter-subject mean outcomes, similar to prior ProprioFoot studies (e.g., [8, 51]). The inter-subject mean curves provide a reference to visualize if and when individuals adopted gait strategies that are consistent or inconsistent with the group mean. In order to remove the variability in kinetic measurements due to physical differences between subjects, data were non-dimensionalized using base units of mass, gravity and leg length prior to computing the inter-subject averages [110]. Second, we included data from the participants' daily-use prosthesis, which provides a reference for

how each individual walks in daily life. Third, six healthy controls (4 female, 2 male, height 1.78 m ± 0.1 m, mass 69 kg ± 10.6 kg, age 21 years ± 1.8 years were tested with the same protocol. To help account for differences in size and weight, control data were non-dimensionalized. We then computed kinematic and kinetic outcome measure means and standard deviations. Finally, we re-dimensionalized these mean control outcomes using the mean mass and leg length of the analyzed unilateral transtibial amputation group.

4.3 Results

For all individuals, the MPA adjusted to the incline slope and provided dorsiflexion during swing phase (**Figure 4.2**), as expected. The MPA increased dorsiflexion by 6.6° ± 1.5° relative to the MPA-unadapted. During leg swing, the MPA provided 4.5° ± 0.5° of additional dorsiflexion at 80% of the gait cycle (**Figure 4.2**). This resulted in an increase in minimum toe clearance (MTC) for all participants (mean 2.0 cm ± 0.4 cm more clearance, p=0.0156) relative to the MPA-unadapted. Participants exhibited two distinct incline walking strategies on their prosthetic side: (i) rearfoot landing, which was qualitatively similar to the behavior of the healthy controls and is characterized by a posterior-to-anterior (i.e., heel-to-toe) progression of the center-of-pressure (CoP, presented in the reference frame of the foot) and (ii) forefoot landing, which is characterized by an anterior bias of the CoP during the first 40% of the gait cycle. Rearfoot vs. forefoot landing were characterized using the CoP, and confirmed visually using video footage of the trial. However, the landing pattern used for a given condition (MPA vs. MPA-unadapted) was highly user-specific. Three users adopted a rearfoot landing pattern on the MPA-unadapted and maintained that pattern on the MPA. Out of the four users who adopted a forefoot pattern on the MPA-unadapted, two transitioned to a rearfoot pattern on the MPA while two maintained the forefoot pattern (**Figure 4.3**). Prosthetic-side knee angle and moment trends were also user-specific. For three users, stance-phase knee-flexion was decreased with the MPA vs. MPA-unadapted (**Figure 4.4**).

Three users showed the opposite trend, i.e., greater stance-phase knee-flexion with the MPA vs. MPA-unadapted, while one user exhibited minimal changes to knee angle between the conditions. Six of seven users showed increased prosthetic-side knee-extension moments with the MPA relative to the MPA-unadapted (**Figure 4.5**). The remaining user showed a reduction in prosthetic-side knee-extension moment with the MPA relative to the MPA-unadapted. There were also various other differences between users in terms of peak knee moment magnitude and time-varying waveform over the stride (**Figure 4.5**).

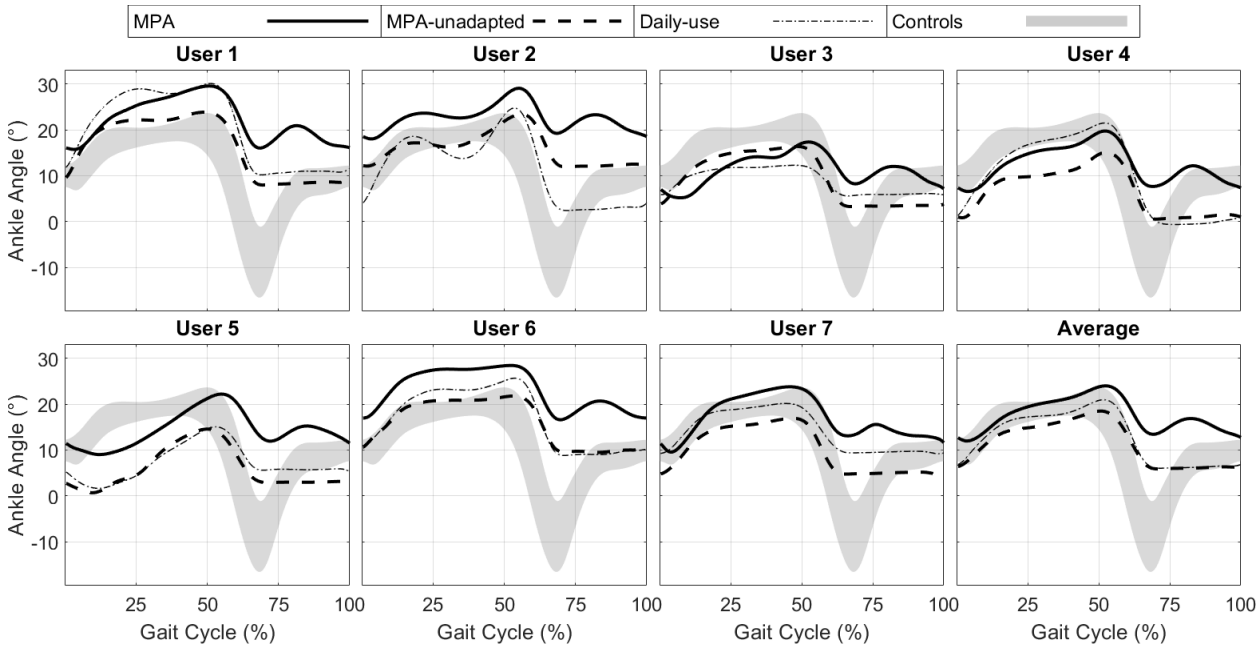

Figure 4.2: Prosthetic-side sagittal ankle angle for each prosthesis user as well as the seven-subject average during incline walking for the MPA (solid), MPA-unadapted (dashed), and daily-use prosthesis (dash-dot) conditions. Positive values indicate dorsiflexion. Shaded gray region represents control mean ± one standard deviation. Ankle angle is defined as the angle between the shank and the foot and was calculated via motion capture markers on the foot and shank segments.

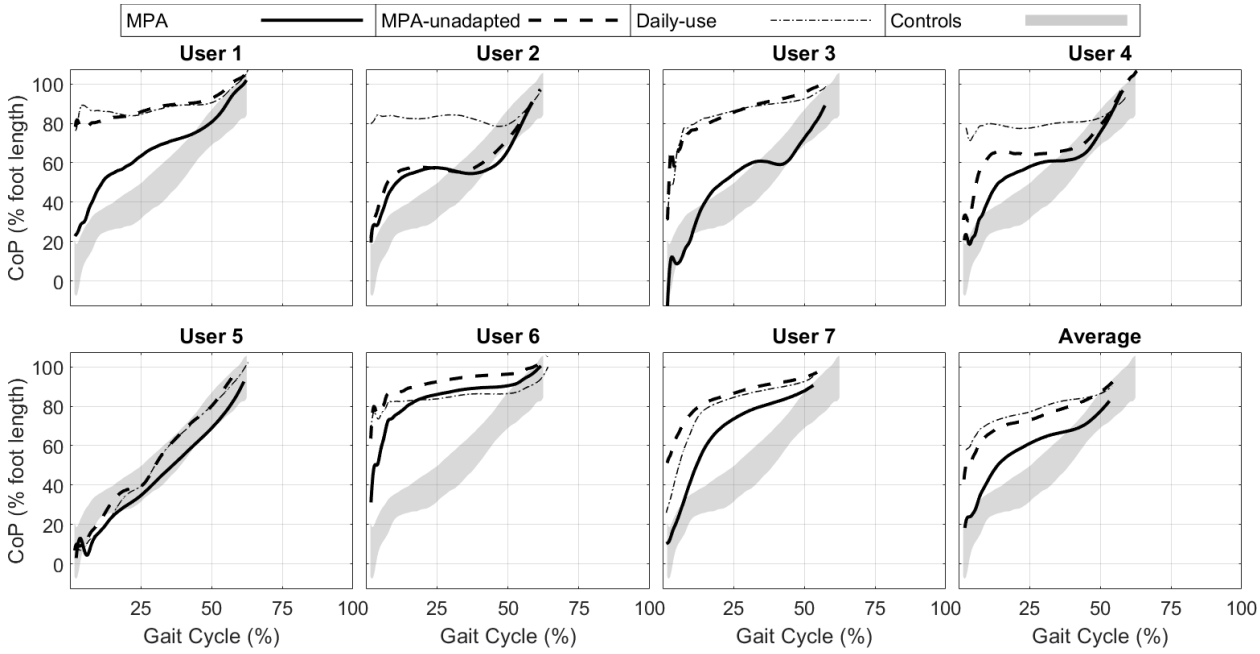

Figure 4.3: Anterior/posterior position of the prosthetic-side center-of-pressure (CoP) in the foot reference frame (where 0% and 100% correspond to the rearfoot and forefoot, respectively) during incline walking for each prosthesis user as well as the seven-subject average for the MPA (solid), MPA-unadapted (dashed), and daily-use (dash-dot) conditions. CoP provides a means of visualizing whether users adopted a rearfoot landing pattern (similar to control subjects, shaded gray) vs. a forefoot landing pattern (larger CoP value in early stance indicates CoP is under forefoot). CoP measurements were truncated for vertical ground reaction forces less than 30 N to minimize noise for plotting purposes. Users 1 and 3 transitioned from a forefoot landing pattern with the MPA-unadapted to a rearfoot pattern with the MPA, whereas users 2, 4 and 5 exhibited a rearfoot landing pattern for both conditions. Users 6 and 7 exhibited forefoot landing for both conditions. Shaded gray region represents control mean ± one standard deviation.

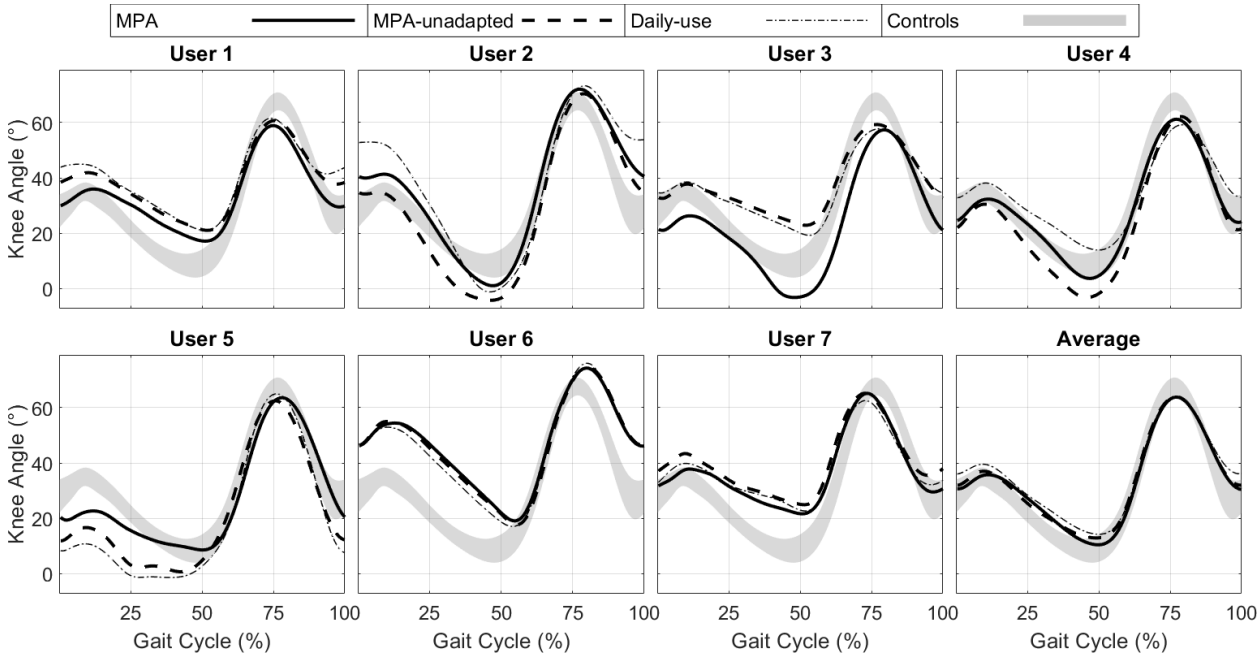

Figure 4.4: Prosthetic-side sagittal knee angle for each prosthesis user, as well as the seven-subject average during incline walking with the MPA (solid), MPA-unadapted (dashed), and daily-use (dash-dot) conditions. Positive values indicate knee flexion. Six of seven users exhibited changes >5 in their maximum knee flexion in early stance (10–15% of gait cycle); however, these changes were not consistent among subjects. A subset of users (1, 3 and 7) exhibited reduced knee flexion with the MPA vs. MPA-unadapted, whereas another subset (2, 4, 5) exhibited increased knee flexion. Shaded gray region represents control mean ± one standard deviation.

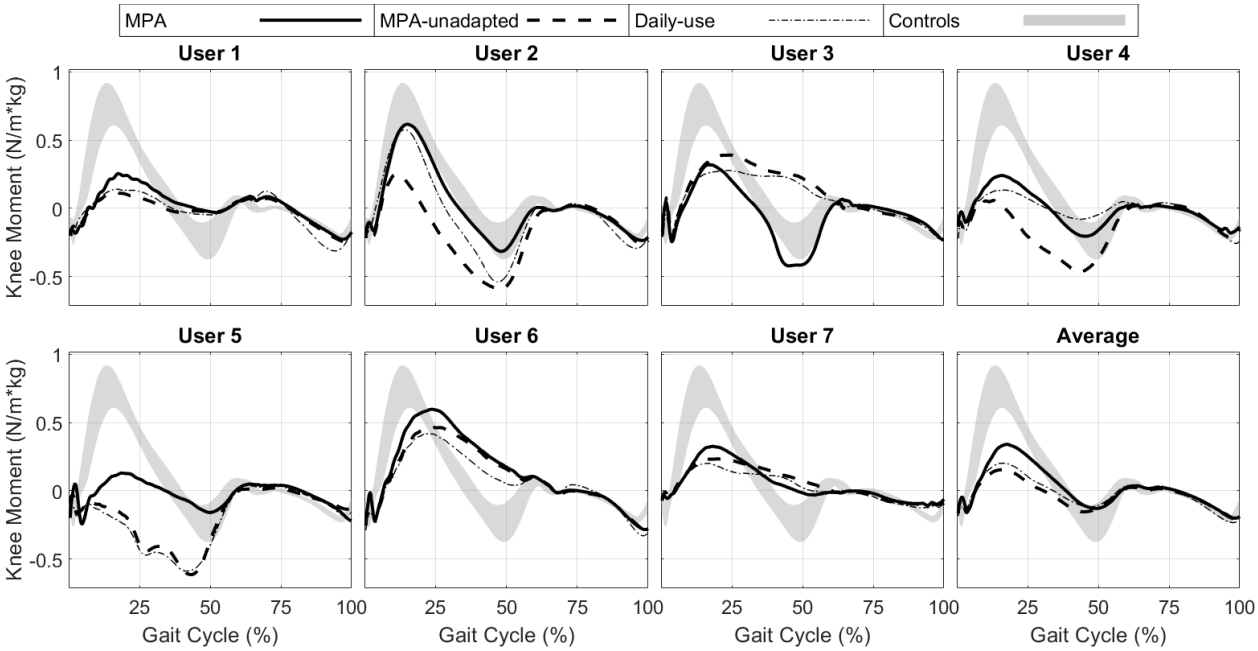

Figure 4.5: Prosthetic-side sagittal knee moment for each prosthesis user, as well as the seven-subject average during incline walking with the MPA (solid), MPA-unadapted (dashed), and daily-use (dash-dot) conditions. Positive values indicate knee extension moments. Six of seven users exhibited an increase in stance-phase knee extension moments when walking on the MPA vs. MPA-unadapted; however, there was substantial variability in waveforms between users. Shaded gray region represents control mean ± one standard deviation.

Table 4.1: Prosthesis user information. User 3 is female, the rest are males. All users have unilateral transtibial amputation.

User	Height (m)	Mass (kg)	Age (yrs.)	K-level	Daily-Use	Suspension	Cause	Yrs. Amp.	Side	Shoes
1	1.8	94	48	K4	All-Pro	Sleeve & Liner	Trauma	6 yrs.	L	Athletic
2	1.75	95	31	K4	All-Pro	1-way valve	Trauma	14 yrs.	L	Athletic
3	1.63	63	31	K4	Elation	Seal-in	Stroke	1 yr.	L	Casual
4	1.85	83	50	K4	All-Pro	Sleeve & linear	Trauma	10 yrs.	L	Athletic
5	1.72	83	42	K4	Re-Flex Shock	Pin-lock	Trauma	7 yrs.	R	Casual
6	1.8	105	63	K3	Rush 87	Sleeve & Liner	Trauma	2 yrs.	L	Athletic
7	1.75	100	25	K3	Pro-Flex XC	Passive Suction	Trauma	1 yr.	R	Athletic

Table 4.2: Subject-specific prosthesis set-point angles (i.e., sagittal plane dorsiflexion angle of the prosthetic foot relative to neutral). A neutral angle of 0 corresponds to the foot being orthogonal to the pylon. For MPA-unadapted this angle corresponds to the standard alignment made by the prosthetist for that individual. For the MPA, larger angles indicate that the ankle is more dorsiflexed (i.e., set-point adjusted to accommodate slope). Angles are reported in degrees. Subjects are ordered from most to least dorsiflexed set-point in MPAunadapted condition. Ankle angle is defined as the angle between the shank and the foot. The set-point angles for the MPA-unadapted and MPA were calculated as the ankle angle at terminal swing.

	MPA-unadapted		**MPA**	
User	**Set-point angle (°)**	**Landing pattern**	**Set-point angle (°)**	**Landing Pattern**
2	12	Rearfoot	18	Rearfoot
6	11	Forefoot	17	Forefoot
1	10	Forefoot	16	Rearfoot
7	5	Forefoot	12	Rearfoot
5	4	Forefoot	11	Rearfoot
4	2	Rearfoot	8	Rearfoot
3	4	Rearfoot	7	Rearfoot

4.4 Discussion

Despite the same intervention (increased dorsiflexion with the MPA during incline walking), changes in gait biomechanics across users were highly variable. Some users switched from a forefoot landing pattern on the MPA-unadapted to a rearfoot landing pattern when the MPA adapted to the slope, some exhibited a forefoot landing pattern regardless of the MPA ankle adaptation, and yet others exhibited a rearfoot landing pattern regardless of ankle adaptation (**Figure 4.3**). Rearfoot landing is more consistent with how healthy controls walked up the incline (**Figure 4.3**, shaded gray), and thus might be considered beneficial from a gait appearance or psychosocial standpoint [23]. Changes in knee kinematics and kinetics were also subject-specific (**Figure 4.4**-**Figure 4.5**). For instance, some users exhibited more knee flexion in early stance with the MPA, whereas

others exhibited less, and one individual showed negligible change (**Figure 4.4**).

As a result of high inter-subject variability, group-level biomechanical results (e.g., inter-subject means) did not reflect the behavior of each individual. For example, the 7-subject mean CoP curve suggests that users transitioned from a forefoot landing pattern on the MPA to a rearfoot landing pattern with the MPA (**Figure 4.3**, Average). At best, this mean curve only partially reflects the gait of a subset of users and largely misrepresents the remaining users. Furthermore, the mean knee angle curve suggests that the MPA condition had little effect on user knee flexion. In post-processing we performed a group-level statistical analysis and found that the negative peak at 10% gait cycle was not significantly different across users (**Figure 4.4**, p=0.468). Nonetheless, the majority (six of seven) of individual subjects exhibited changes $>5°$in knee flexion. One subset of individuals exhibited more knee flexion with the MPA, whereas another exhibited less knee flexion, such that averaging effectively canceled out these inverse effects in the average results. To summarize and report large amounts of biomechanical data from gait analysis studies, prior prosthesis studies – including our own – have primarily presented group-level results (e.g., [7, 33, 51, 162]), but this may inadvertently mask trends and important behaviors exhibited at an individual level. This highlights a contemporary challenge with prosthesis research [25], and more generally with human subject research [50, 152], namely that group mean results may not reflect the behaviors of individuals.

Observed discrepancies between inter-subject mean and individual responses call attention to prevailing experimental protocols that involve testing prosthesis users on one or more interventions, and then performing group-level statistical analyses to identify significant effects. One of the most common ways to evaluate prosthetic interventions involves controlled experiments (e.g., with parallel or cross-over design) to evaluate whether an intervention improves a given outcome for a group of prosthesis users. Group-level analyses may be appropriate when responses are known to be consistent

across a given population [50], and useful for certain practical purposes (e.g., to inform whether an intervention is beneficial enough, on average, to be covered by insurance). There are many circumstances when generalizability across prosthesis users is not expected (e.g., due to variability in residual limb length or pain, type of amputation surgery, fitness level, height, weight, age, etc.). Also, research on new prosthetic devices are often carried out on relatively small (and often statistically underpowered) sample sizes, due in part to constraints related to time, cost and access to study participants. Thus, typical sample sizes used in prosthetic gait analysis studies often preclude the use of statistical methods that help account for confounding variables between subjects. Furthermore, especially for new devices, the sub-population who will benefit may not be known a priori. As a result, it is common that some subset of users exhibits an intended outcome, while others may not. Finally, it is not clear that obtaining group-level statistical significance is always of critical importance for evaluating prosthetic interventions. Particularly for new interventions, and interventions designed for highly heterogeneous populations, it may be more important to determine if a subset of users can derive a substantial (e.g., clinically meaningful) benefit from the device and/or to determine the range of potential behavioral responses. From a clinical perspective, an intervention need not be beneficial for all individuals within a group, nor demonstrate statistically significant improvements on average across a group, in order to be beneficial for a single user or subset of users. A key question moving forward is whether group-level analysis should continue to be the de facto standard for evaluating prosthetic interventions (as it currently seems to be), particularly given the number of existing and emerging technologies and the practical constraints on testing large samples of prosthesis users using instrumented gait analysis. The field may benefit from supplementing conventional group-level analyses with alternative approaches such as single-subject study designs [11, 128] or from various improvements in data presentation [148, 147], such as depicting subject-specific data points within plots, enumerating the number of participants

who exhibited a key outcome or trend, reporting subject-specific results in supplementary material, or publicly archiving subject-specific data to empower other researchers to explore subject-specific responses.

There were several limitations to this study. First, we analyzed a limited sample, which included seven prosthesis users. This study included only K3-K4 prosthesis users due to the interest and availability of participants who were willing to devote two weeks to acclimating to a new device and several hours to in-lab testing. This challenge of self-selection and subject availability is common amongst prosthesis studies and itself can introduce a bias in the types of individuals tested. Subjects were given more time to acclimate to the MPA condition than to the MPA-unadapted condition. Participants were given at least two weeks to acclimate at home to the MPA, whereas the MPA-unadapted condition was introduced during initial training on the device and during the testing protocol. As such, participants were only given several minutes of walking time on this condition. However, because the ankle was locked at neutral configuration, the expectation was that the MPA-unadapted condition was sufficiently similar to commonly-prescribed prostheses, such that the participants did not need extensive time to acclimate. The order of the prosthesis conditions were not randomized possibly resulting in ordering effects. We did not enforce the same prosthesis alignment (foot relative to pylon angle) across MPA users. Each user had their MPA aligned by a trained prosthetist using typical standard of care procedures, which includes taking into account each user's comfort and preference. As a result the prosthesis alignment varied between users (**Table 4.2**). However, there was no indication that this subject-specific alignment explained differences observed in terms of rearfoot vs. forefoot landing pattern (**Figure 4.1**), or more vs. less knee flexion when using the MPA. Note that the subjects' daily-use prosthesis was fit by their standard care provider, and we did not change this alignment prior to testing; as a result the MPA and daily-use prostheses were fit by different prosthetists. However, the daily-use prosthesis condition was only intended as

a reference and thus does not affect the main conclusions of the study. The control group tested was not age-, size-, or weight-matched to the prosthesis users; however, as stated in Methods, the data set was non-dimensionalized and re-dimensionalized using the prosthesis users' average mass and leg length values. The results here inform the design of prosthetic feet, and the degree to which an ankle adaptation feature affects the gait of different individuals. The study was not intended to directly inform clinical decision-making for a prosthetist deciding between two different prostheses (e.g. one MPA vs. another non-MPA) on the market, since these feet will also differ in other aspects such as mass, inertia, shape or stiffness.

4.5 Conclusion

In this work we characterized how seven unilateral transtibial prosthesis users adapted to walking with an MPA that adapted its ankle to inclined slope, relative to the same MPA with ankle unadapted (i.e., fixed in its neutral alignment). Despite the MPA behaving similarly for each user (i.e., dorsiflexing the ankle to help accommodate to the slope), we observed marked differences in user gait patterns (rearfoot vs. forefoot landing) and in gait biomechanics (as evidenced by changes in knee angle and moment). Comprehensive subject-specific kinematics and kinetics are presented in the Appendix for reference. Although the prevailing experimental paradigm in prosthetic gait analysis studies is to focus on group-level (inter-subject mean) analysis, these results call attention to the high inter-subject variability which may necessitate alternative experimental approaches and alternative data visualization strategies to better understand and assess the effects of emerging prosthetic interventions.

Chapter 5

Design, Modeling and Demonstration of a New Dual-Mode Back-Assist Exosuit

Occupational exoskeletons and exosuits have been shown to reduce muscle demands and fatigue for physical tasks relevant to a variety of industries (e.g. logistics, construction, manufacturing, military, healthcare). However, adoption of these devices into the workforce has been slowed by practical factors related to comfort, form-factor, weight and not interfering with movement or posture. We previously introduced an un-motorized, low-profile, dual-mode exosuit comprised of textile and elastic materials to address these adoption barriers. Here we build upon this prior work by introducing an extension mechanism that increases the moment arm of a exosuit while in engaged mode, then collapses in disengaged mode to retain key benefits related to being lightweight, low-profile and unobstructive. Here we demonstrate both analytically and empirically how this extensible exosuit concept can (i) reduce device-to-body forces (which can improve comfort for some users and situations), or (ii) increase the magnitude of torque assistance about the low back (which may be valuable for heavy-lifting jobs) without increasing shoulder or leg forces relative to the prior form-fitting exosuit. We also introduce a novel mode-switching mechanism, as well as a human-exosuit biomechanical model to elucidate how individual design parameters affect exosuit assistance torque and device-to-body forces. The proof-of-concept prototype, case study and modeling work provide a foundation for understanding and implementing extensible exosuits for a broad range of applications. We envision promising opportunities to apply this new dual-mode extensible exosuit concept to assist heavy-lifting, to further enhance user comfort, and to address the unique needs of last-mile delivery workers

5.1 Introduction

Occupational exoskeletons and exosuits have been developed for industrial applications such as manufacturing, construction and material handling [48], and have been demonstrated to reduce physical demands, muscle activity and fatigue during a variety of tasks [89]. Despite the promising potential of these technologies to alleviate physical strain on workers, their adoption into industry has been slowed by practical factors such as comfort, weight and form-factor [149, 12]. The challenge is that users are generally unwilling to adopt a wearable device if it is uncomfortable or if it protrudes out from their body in a way that is obstructive, unsafe or restricts movements needed to perform their job [13, 151].

To overcome these adoption barriers we previously developed a back-assist exosuit that was lightweight and sufficiently low-profile to fit underneath clothing, and was primarily made of soft textile and elastic materials to minimize pressure points, discomfort and movement interference. We also demonstrated its ability to reduce low-back muscle activity during lifting and bending tasks [82], and to reduce the rate of muscle fatigue [83]. This exosuit (detailed in previous work [82]) uses elastic bands along the back, which stretch when the user bends forward or crouches down, creating an assistive torque about the low-back and hips that offloads the lumbar and hip extensor muscles. In a variation of this exosuit design we integrated a mode-switching clutch (both manual and motorized versions), which allowed the user to quickly engage and disengage the exosuit assistance on demand [84, 160]. Users disengaged the exosuit to have full and unrestricted range of motion when assistance was not needed.

The prior exosuit was designed to fit close to the body and therefore had a relatively short moment arm ($\sim$8 cm) relative to the lumbosacral joint (hereafter referred to as the L5-S1 joint). To provide an assistive torque of 20 Newton $\cdot$ meters (Nm) with the exosuit would require approximately 250 Newtons (N) of device-to-body forces on the shoulders and legs. Although this is far below the force comfort limit observed on the shoulders

and legs in a previous study (∼600-1000 N, [153]), we highlight two compelling cases here. First, there may be individuals who are particularly sensitive to shoulder or leg forces and for whom we may want to achieve the same 20 Nm assistive torque but with reduced device-to-body forces to ensure comfort. Second, there may be individuals who are comfortable with the nominal device-to-body forces, but who are engaged in heavy lifting, and would like to increase the magnitude of exosuit assistance (e.g. to 40 Nm), but maintain the same magnitude of device-to-body forces on the shoulders and legs.

One simple solution is to increase the moment arm of the exosuit by adding a spacer between the elastic band and the back or buttocks. In this configuration, assistive torque could be maintained while decreasing the force through the elastic bands and applied to the shoulders and legs. Alternatively, in this configuration, if force through the elastic bands is held constant (at 250 N) then the assistive torque about the low-back would be increased. Devices such as the Personal Lift Assist Device have implemented this style of design, and have demonstrated that this simple solution works as expected [3, 2]. However, this solution re-introduces the problem of form-factor: the device now protrudes out from the back or buttocks in a way that can interfere with movement, various postures (e.g. sitting), and the work environment.

In this work we sought to model, develop and show proof-of-concept for a new patent-pending exosuit design [159] that could temporarily increase the exosuit's moment arm using an extension mechanism during lifting and bending tasks. The extension mechanism could then collapse and switch back to a low-profile configuration during unassisted tasks (e.g. walking, sitting, (**Figure 5.1**, left)) to avoid interfering with movement or the environment. The low-profile configuration is important because most of the time the primary goal of an exosuit is simply to not get in the way of the user. Even in jobs that are characterized by frequent or intensive lifting, workers spend only a fraction of their time bent over and lifting (e.g. $\sim$ 10 percent of the time for retail workers, [57]) and are otherwise performing tasks which do not require exosuit assistance. For

most situations and occupations we would not expect a temporary protrusion (e.g. an extension mechanism) from the back during lifting or bending to interfere with the task or surrounding environment. This is because generally when a person is executing a manual lifting or bending task, there is not another person or object immediately behind them or encroaching on their backside. We have found this to be true in our personal experiences and also observations of industrial workplaces such as warehouses, airports, distribution centers and construction sites. In this manuscript we detail computational modeling used to gain insight on exosuit design parameters, followed by design details on an exosuit prototype with an extension mechanism. We then present a case study demonstration of its function in engaged (assistive) mode with the mechanism extended, and in disengaged (stay-out-of-the-way) mode with the mechanism collapsed (**Figure 5.1**). For the remainder of this paper, we refer to the exosuit design detailed in our previous work as the *form-fitting exosuit*, and we refer to the newly proposed concept as the *extensible exosuit*.

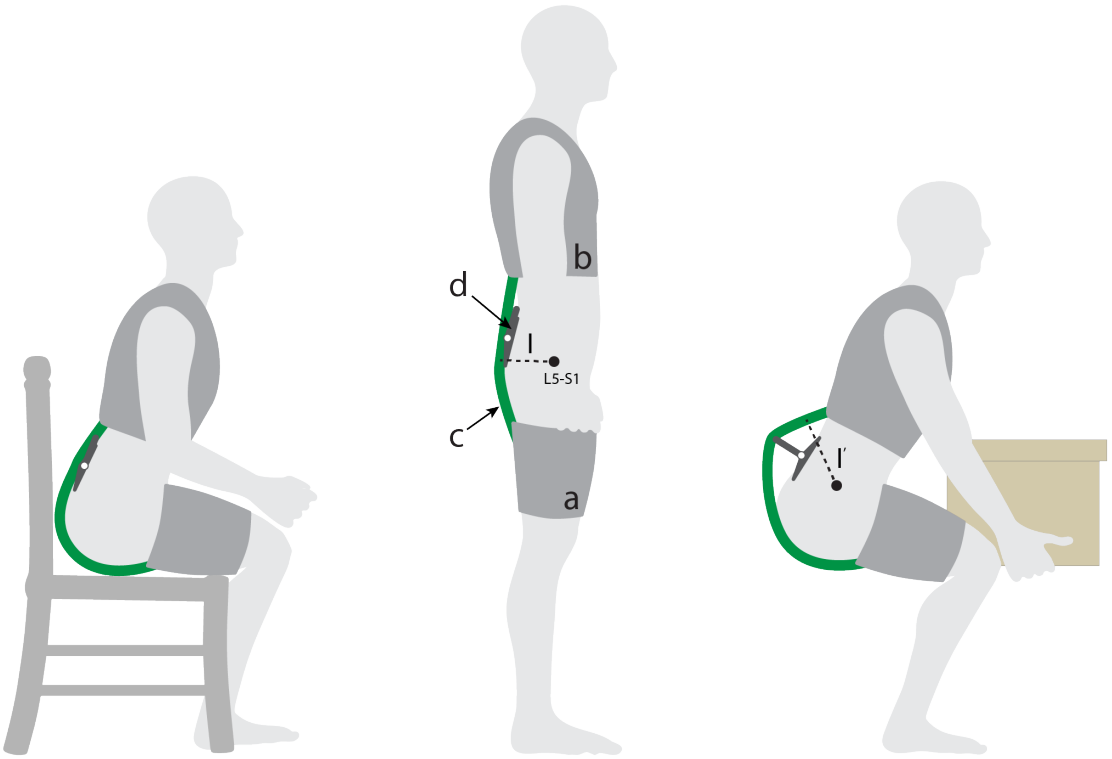

Figure 5.1: **Conceptual depiction of the extensible exosuit.** This concept is shown in disengaged (collapsed) mode during seated and standing postures, and in engaged (extended) mode during lifting. The extensible exosuit is composed of a leg (a) and trunk (b) interface, an elastic band (c), and a mechanism that can switch between an extended (larger moment arm l') and collapsed state (smaller moment arm l). The elastic band (green) runs along the user's posterior, over the moment arm mechanism, and connects the leg interface to the trunk interface. In engaged mode, as the user bends forward or crouches down, the elastic band stretches, applying tension forces to the leg and trunk interfaces. The addition of the extension mechanism redirects the path of the elastic band, increasing the exosuit moment arm (from l to l') of the exosuit relative to the lumbosacral (L5-S1) joint. This simplified image is only intended to introduce the basic concept, and additional aspects of the design are detailed later in **Section 5.4**)

5.2 Design Approach Overview

Our approach involved a sequence of biomechanical modeling (**Section 5.3**), followed by prototype design (**Section 5.4**), and then a proof-of-concept demonstration of an extensible exosuit prototype via a human subject case study (**Section 5.5**). We developed a biomechanical exosuit-human model to gain insight on which design parameters were

most important and how they interplay to affect device-to-body forces. Next we used these model insights to inform design parameter selection, and fabricated an exosuit prototype with an extension mechanism. Finally we performed a human subject case study to demonstrate mechanical function of the prototype. Specifically, we sought to confirm experimentally (i) that the extensible exosuit could provide the same L5-S1 joint torque assistance as the form-fitting exosuit but with lower device-to-body forces on the shoulders and legs, and (ii) that the extensible exosuit could remain sufficiently low-profile when it was disengaged such that it did not interfere with common movements and postures like walking and sitting.

5.3 Modeling

Previous biomechanical models of wearable back-assist devices [3, 135, 74, 82] explain the underlying physics of how these devices offload the lumbar muscles and spine. We sought to build upon this prior work by characterizing how to adjust specific exosuit design parameters to affect device-to-body forces and the exosuit moment arm about the spine. The rationale for this modeling is readily apparent in **Figure 5.2** where we note that there are number of inter-related design choices such as where to anchor to each body segment, where to place the base of the extension mechanism along the back, and how to select the extension length of the mechanism. The effects of and the interplay between these parameters on device-to-body forces was unknown, but important for us to understand in order to inform the design and fabrication of a prototype. We therefore developed a model of the human and exosuit that estimates the device-to-body forces (**Figure 5.2**, $\overrightarrow{F_T}$, $\overrightarrow{F_M}$, $\overrightarrow{F_L}$) needed to create a desired torque about the L5-S1 joint (**Figure 5.2**, p_0). The model is a static, sagittal plane model of the exosuit and human system. We use a static model for simplicity since the goal was general design insight, and since exosuit mass is low and inertial effects are negligible. The model only considers the sagittal plane because the majority of the biological lumbar moment and exosuit assistive torque

(τ_{exo}) are observed in the sagittal plane [82], and these dynamics typically dominate even in the presence of twisting or other non-sagittal trunk motions [55]. The model primarily considers the exosuit assistance torque created about the L5-S1 joint because it commonly experiences the highest flexion torques along the spine [20]. The model considers the exosuit and human mechanics when the exosuit is engaged (i.e. extension mechanism is lengthened and elastic bands are under tension) and the user is leaning forward (as in **Figure 5.2**). We focus on the device-to-body forces at the trunk ($\overrightarrow{F_T}$), legs ($\overrightarrow{F_L}$) and waist (via the extension mechanism, $\overrightarrow{F_M}$) because we have noted from experience that these tend to be areas that are more sensitive to external loads. Whereas we were not concerned about the device-to-body force on the buttocks because this area can comfortably sustain external forces on the order of a body weight (e.g. during sitting), and the device-to-body forces from our exosuits are far below this magnitude. The human body is modeled as a series of linked rigid-body segments. In this modeling section, we also assume negligible friction and thus that the magnitude of tension is constant throughout the elastic element (i.e. the tension magnitude at the trunk, $\|\overrightarrow{F_T}\|$, is equal to the tension magnitude at the leg, $\|\overrightarrow{F_L}\|$). We supplement this model by adding a routing point (**Figure 5.2**, p_2), which redirects the path of the elastic band (**Figure 5.2**, green curve) and introduces a device-to-body force ($\overrightarrow{F_M}$). This routing point (which is modeled as a friction-less pulley) is the main element which alters the exosuit moment arm about the spine.

We identified design parameter candidates to manipulate, which included: routing point location along the spine, routing point offset from the skin surface, number of routing points, elastic band attachment point on the trunk interface and the elastic band attachment point on the leg interface. We narrowed the options (based on initial modeling findings, physical intuition and expected end-user applications and constraints) to three key parameters: the routing point position along the back (**Figure 5.2**, x_2), the routing point offset normal to the back (**Figure 5.2**, y_2), and the position of the elastic

anchoring point on the trunk interface (**Figure 5.2**, x_1).

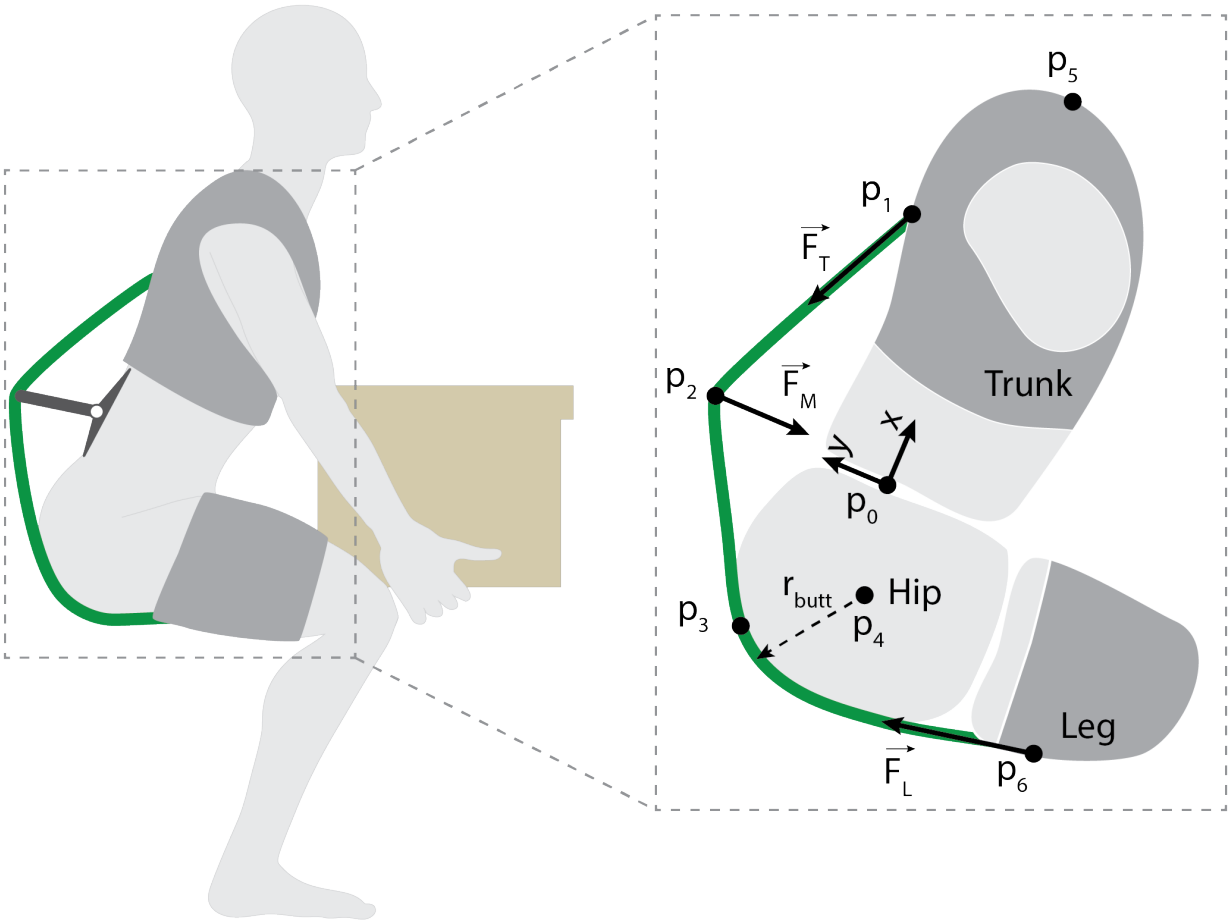

Figure 5.2: **Static model of the exosuit-human system.** The exosuit is comprised of a leg interface, a trunk interface, an elastic band (green curve) and an extension mechanism. The leg interface and trunk interface attach to the leg and trunk respectively, and are coupled by an elastic band. The exosuit creates an assistive torque by applying forces at the trunk ($\overrightarrow{F_T}$) and waist ($\overrightarrow{F_M}$) and legs ($\overrightarrow{F_L}$,). p_0 is the location of the L5-S1 joint and coordinate system origin. p_1 is the point at which the elastic band attaches to the trunk interface (and applies $\overrightarrow{F_T}$). p_2 is the routing point for the elastic band on the extension mechanism (and where $\overrightarrow{F_M}$ is applied). Note that when p_2 sits flush with the trunk/waist, there is no extension mechanism and the device behaves like the previous form-fitting exosuit detailed in [82]. p_3 is the point at which the elastic band first makes contact with the posterior waist (simplified as a tangency point with a circle of radius r_{butt}). p_4 is the hip center of rotation, p_5 is the top most point on the shoulder, and p_6 is the anchoring point on the leg

5.3.1 Model Development

The torque created about the L5-S1 joint (τ_{exo}, in the z-axis coming out of the page) by the exosuit is:

$$\tau_{exo} = \tau_T + \tau_M \tag{5.1}$$

Where τ_T is the torque created by the device-to-body trunk force vector ($\overrightarrow{F_T}$), and τ_M is the torque contribution from the device-to-body force vector from the extension mechanism ($\overrightarrow{F_M}$):

$$\tau_T = \overrightarrow{r_{10}} \times \overrightarrow{F_T} = (\overrightarrow{r_{10}} \times \overrightarrow{u_{21}}) \cdot \|\overrightarrow{F_T}\| \tag{5.2}$$

$$\tau_M = \overrightarrow{r_{20}} \times \overrightarrow{F_M} = (\overrightarrow{r_{20}} \times (\overrightarrow{u_{32}} + \overrightarrow{u_{12}})) \cdot \|\overrightarrow{F_T}\| \tag{5.3}$$

In equation **Equation** (5.2), $\overrightarrow{r_{10}}$ is the position vector from p_0 to p_1, and $\overrightarrow{u_{21}}$ is the unit vector from p_1 to p_2, and $\|\overrightarrow{F_T}\|$ is the tension magnitude in the elastic band. In **Equation** (5.3), $\overrightarrow{r_{20}}$ is the position vector from p_0 to p_2, and $\overrightarrow{u_{32}}$ is the unit vector from p_2 to p_3, and $\overrightarrow{u_{12}}$ is the unit vector from p_2 to p_1. The device-to-body forces ($\overrightarrow{F_T}$ and $\overrightarrow{F_M}$) only create torque about the L5-S1 joint if their line-of-action intersects the trunk body segment (e.g. at a point $> p_{0_x}$). The trunk interface anchoring point p_1 (and therefore $\overrightarrow{F_T}$) in this model is constrained to sit on the trunk above the L5-S1 joint and create an extension torque about p_0 because $\overrightarrow{F_T}$ is applied by an elastic band that can generate tension but not compression force. An extension mechanism supports the routing point (represented by p_2), and this mechanism is allowed to sit anywhere along the posterior side of the waist or trunk. This model assumes that the extension mechanism will only bear compression loads (i.e. no bending moments). Physically, this means that the extension mechanism is assumed to be co-linear with $\overrightarrow{F_M}$ and will be anchored at the

location on the back where $\overrightarrow{F_M}$ intersects the back. Note that $\overrightarrow{F_M}$ only creates a flexion (clockwise) torque about p_0 when $\overrightarrow{F_M}$ intersects the trunk above p_0, but otherwise $\overrightarrow{F_M}$ does not create torque about p_0.

After minor algebraic manipulations of **Equations** (5.1) to (5.3) we can calculate the exosuit moment arm (r_T) about the L5-S1 joint with **Equation** (5.4):

$$r_T = \frac{\tau_{exo}}{\|\overrightarrow{F_T}\|} = (\overrightarrow{r_{10}} \times \overrightarrow{u_{21}} + \overrightarrow{r_{20}} \times (\overrightarrow{u_{32}} + \overrightarrow{u_{12}}))^{-1} \tag{5.4}$$

Where this moment arm moment arm (r_T) represents the Euclidean (straight-line) distance between the L5-S1 joint (p_0) and the line of action of the elastic band from p_1 to p_2. Also, take note that (r_T) is inversely proportional to $\|\overrightarrow{F_T}\|$. This means that for a fixed magnitude of τ_{exo} increasing (or maximizing) the moment arm r_T is analytically equivalent to decreasing (or minimizing) the device-to-body forces on the legs and trunk ($\overrightarrow{F_T}$).

Equation (5.5) below is an expression for the magnitude of the device-to-body force from the extension mechanism $\|\overrightarrow{F_M}\|$:

$$\|\overrightarrow{F_M}\| = \|\overrightarrow{u_{32}} + \overrightarrow{u_{12}}\| \cdot \|\overrightarrow{F_T}\| = k_R \cdot \|\overrightarrow{F_T}\| \tag{5.5}$$

Where we note that k_R is the ratio of force magnitude on the extension mechanism to the trunk force magnitude in the elastic band.

5.3.2 Model Parameter Exploration

A parameter exploration was performed by systematically varying the exosuit design parameters and characterizing the effects on the exosuit moment arm and device-to-body forces. Using **Equations** (5.4) and (5.5) we performed a series of parameter sweeps: varying the trunk anchoring point (x_1), the extension mechanism position along the back (x_2) and the extension mechanism offset from the back (y_2) across their respective

domains as determined from anthropometric tables. Anthropometric data were used to scale the model to a 50^{th} percentile male stature (**Table 5.1**, [75, 58]).

Our primary goal was to understand parameter combinations that increase the exosuit moment arm (r_T), which as noted above and shown analytically in **Equation** (5.4), corresponds to decreasing device-to-body forces on the trunk and legs. Another way to conceptualize the exosuit moment arm (r_T) is that it is the ratio of exosuit torque (τ_{exo}) per elastic band tension ($\|\overrightarrow{F_T}\|$); therefore increasing the moment arm means that the exosuit can provide more torque for the same tension (or alternatively the same torque for less tension). Our secondary goal was to understand parameter combinations that minimize the extension mechanism force itself ($\|\overrightarrow{F_M}\|$), since this is an additional device-to-body force applied to the back or waist. Reducing $\|\overrightarrow{F_M}\|$ is achieved by reducing k_R, which is the ratio of the extension mechanism force magnitude per tension magnitude. To inform our prototype design we were most interested in exosuit parameter combinations that resulted in a relatively large r_T but a relatively small k_R. There is a trade-off between these two variables, such that it is not possible to simultaneously maximize one and minimize the other. Therefore, we performed a parameter exploration to quantitatively map out these trade-offs, and inform the exosuit design.

5.3.3 Key Model Findings

The maximum exosuit moment arm r_T across the explored parameter space was 0.22 meters (m). For instance, this occurred when the extension mechanism was below the L5-S1 joint (x_2 = -0.13 m), the extension mechanism was offset from the back (y_2 = 0.28 m), and the elastic bands were attached to the trunk interface at the top of the shoulders (x_1 = 0.41 m, **Figure 5.3**). The k_R at this parameter combination was 1.4 (**Figure 5.4**). We assumed a baseline r_T of of 0.08 m based on previous estimates (i.e. the approximate moment arm of the elastic band in our prior form-fitting exosuit [84]. Therefore, The maximum observed increase in r_T was 175% (0.08 to 0.22 m). Extended details about

the exosuit parameters explored in this work can be found in appendix **C.0.1**. Below we briefly summarize the key findings used to inform prototype design:

[H]The main effect of the extension mechanism position (x_2) was to change the location and orientation of the extension mechanism force vector along the back ($\overrightarrow{F_M}$). The x_2 value which resulted in the largest moment arm (r_T) was near or slightly below the x-position of the L5-S1 joint (x_0). The main effect of the extension mechanism offset (y_2) was to change the moment arm (r_T) and extension mechanism force magnitude (k_R) where increasing y_2 would increase both r_T and k_R. However, increasing y_2 beyond about 0.3 m had only minor effects on increasing the exosuit moment arm, which plateaued around 0.22 m (**Figure C.3**). The main effect of increasing the trunk interface anchoring point (x_1) was to reduce the extension mechanism force magnitude ($\|\overrightarrow{F_M}\|$); however, this effect (benefit) of increasing x_1 plateaued around $x_1 = 0.2$ m.

Measurement	Value
r_{butt}	0.1 m
x_4	-0.135 m
x_5	0.4 m
d_{skin}	0.08 m

Parameter	Minimum	Maximum
trunk interface anchoring point (x_1)	L5-S1 (x_0)	shoulder (x_5)
ext. mech. position (x_2)	buttocks (x_4 - r_{butt})	shoulder (x_5)
ext. mech. offset (y_2)	skin surface (d_{skin})	d_{skin} + 0.2 m

Table 5.1: **Top**: Anthropometric measurements used to scale the model to a 50^{th} percentile male [75, 58]. **Bottom**: Domain of the parameters with respect to the L5-S1 joint (coordinate system defined in **Figure 5.2**) used for the parameter exploration. The trunk interface anchoring point (x_1) was restricted to sit at or above the L5-S1 (x_0) and at or below the shoulder (d_{50}). The extension mechanism position along the back (x_2) was restricted to sit at or above the apex of the buttocks (x_4-r_{butt}) and at or below the shoulder (d_{50}). The extension mechanism offset (y_2) was restricted to sit at or above the skin surface (d_{skin}) and at or below 0.2 m offset from the skin surface (note: in a secondary analysis we explored y_2 out to 0.5 m offset from the skin surface and this extended parameter sweep is presented in **Figure C.3**).

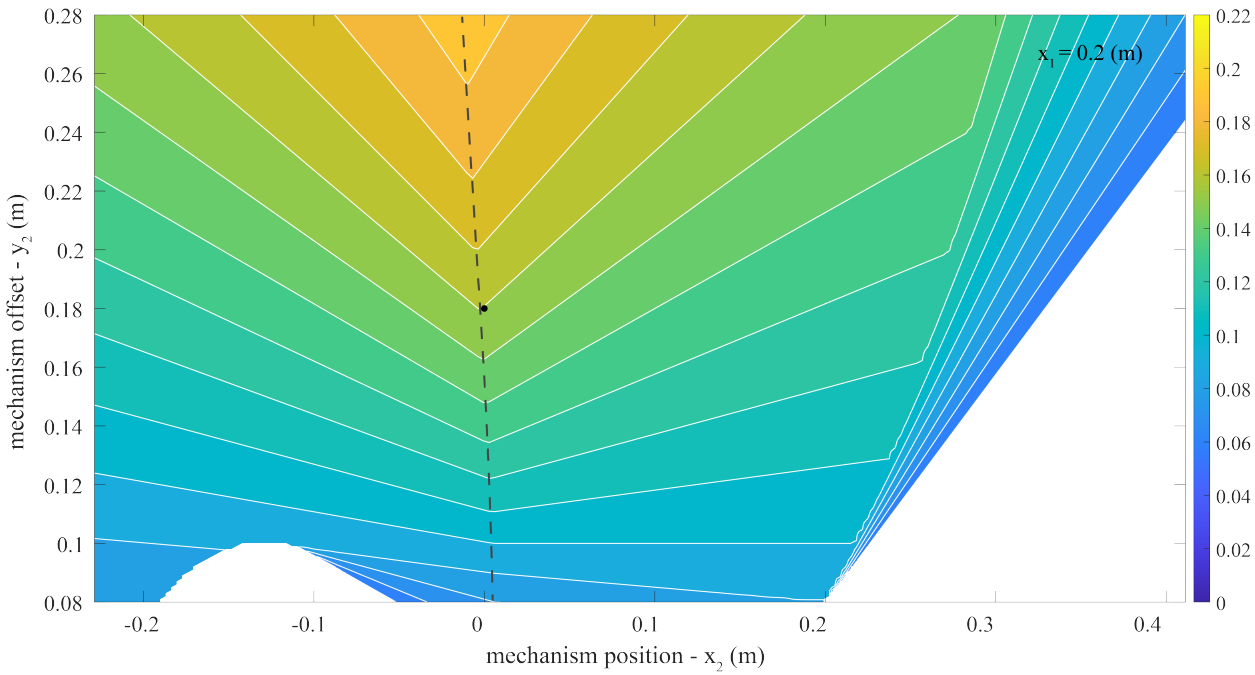

Figure 5.3: **Extensible exosuit moment arm (r_T) contour plot**. Plotted is the extensible exosuit moment arm calculated with **Equation** (5.4). As a reminder, in this model higher values of r_T signify lower device-to-body forces on the shoulders and legs. This contour plot covers the parameter space of the extension mechanism location (x_2) and offset (y_2) specified in **Table 5.1**, with a constant trunk interface anchoring point (x_1 = 0.2 m). The target parameter combination selected for the proof-of-concept design in **Section 5.4.1** is plotted as a black dot (x_2 = 0.0 m, y_2 = 0.18 m). The dashed line represents extension mechanism parameter combinations (i.e. x_2 and y_2) with the smallest extension mechanism footprint (i.e. minimum y_2) for a given r_T (i.e. contour line). Additional parameter exploration results which include the full range of x_1 can be found in appendix **C.0.1**

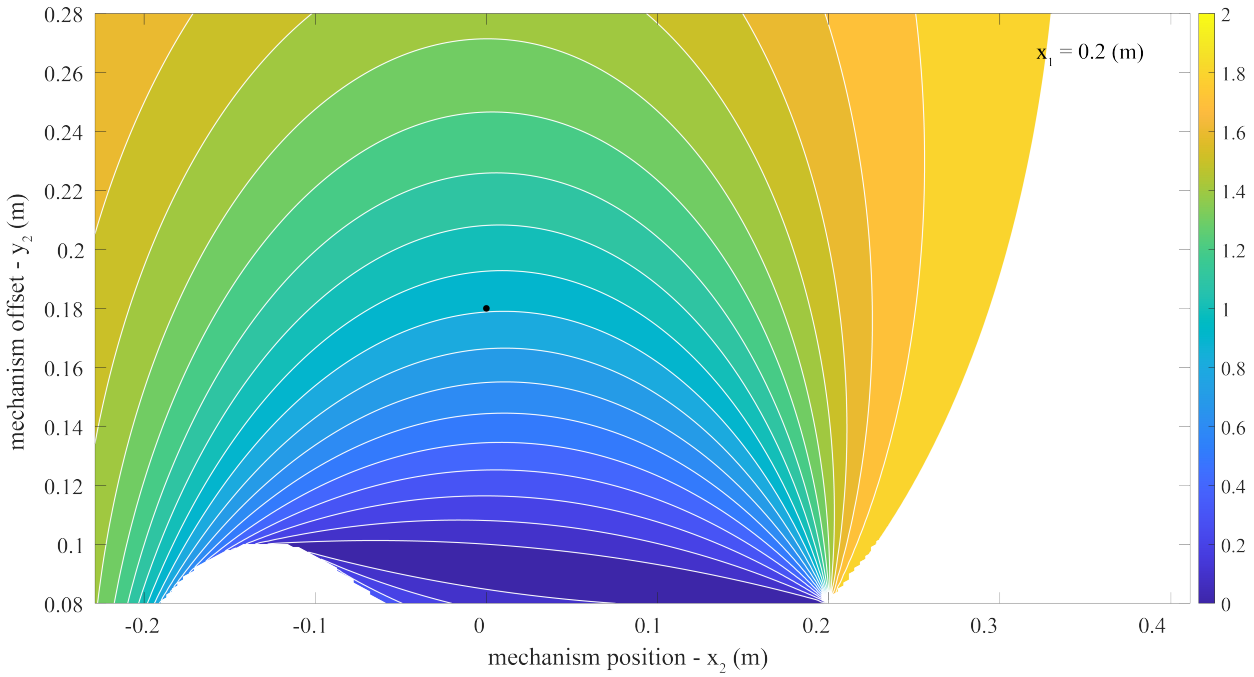

Figure 5.4: k_R **contour plot**. Plotted is the extension mechanism force scaling constant (k_R) calculated with **Equation** (5.5). As a reminder, in this model lower values of k_R signify lower device-to-body forces from the extension mechanism onto the back or waist. This contour plot covers the parameter space of the extension mechanism location (x_2) and offset (y_2) specified in **Table 5.1**, and a constant trunk interface anchoring point (x_1 = 0.2 m). The parameter combination selected for the proof-of-concept design in **Section 5.4.1** is plotted as a black dot (x_2 = 0.0 m, y_2 = 0.18 m). Additional parameter exploration results which include the full range of x_1 can be found in appendix **C.0.1**

5.4 Design

5.4.1 Design Criteria

For the proof-of-concept prototype we aimed to design an extensible exosuit that would reduce $\|\vec{F_T}\|$ by about 50% and minimize the exosuit footprint (i.e. minimum extension mechanism offset y_2) for the average male user (e.g. 50^{th} percentile). Using the model results, we followed the process detailed in appendix **C.0.2** to choose appropriate exosuit design parameters (i.e. target design criteria) for the extensible exosuit proof-of-concept prototype as follows:

[H]The distance from the extension mechanism (and L5-S1) to the trunk interface

anchoring point should be about 0.2 m (x_1 = 0.2 m). The mechanism should sit approximately over the L5-S1 joint (x_2 = 0.0 m). When engaged, the extension mechanism should be offset from the L5-S1 joint by about 0.18 m (y_2 = 0.18 m).

5.4.2 Softgoods Design

The extensible exosuit softgoods (i.e. textiles) consist of a trunk interface, two leg interfaces, and two elastic bands (**Figure 5.5**). The trunk interface includes breathable shoulder straps and a waist belt which are sewn together along the back. The shoulder straps (similar to backpack shoulder straps) transmit the trunk interface force to the users' shoulders. The waist belt serves as a mounting point for the extension mechanism, and transmits a force at the users' waist. The leg interfaces are conical fabric sleeves that transmit force to the user's legs. The leg is shaped approximately like a conical frustum, which prevents the leg interfaces from migrating up the leg when upward forces are applied by the elastic bands. The elastic bands attach to the trunk interface about 0.2 m above the extension mechanism, according to the target parameters selected (**Figure 5.5**, x_1). The elastic bands consist of fabric elastic (adapted from fabric resistance bands) sewn in series with non-stretch polyester webbing (**Figure 5.5**, c). The elastic bands are routed through the extension mechanism (**Figure 5.5**, e).

5.4.3 Extension Mechanism Design

The purpose of the extension mechanism is to move the elastic bands between two stable positions. In one position the mechanism and elastic bands should sit close to the body and the exosuit should be transparent to the user (i.e. not restrict or interfere with movement or posture). In the other position, the mechanism and elastic bands should be extended from the back (according to the exosuit parameters in **Section 5.4.1**), and the elastic bands should stretch and apply torque about the L5-S1 joint as the user bends

or lifts. Numerous extension mechanism designs were considered (e.g. four-bar mechanism, hinge [159]). The benefits/drawbacks of each ultimately depend on the intended end-user and use case (making this more of a later-stage product development choice). The goal of this work was simply to demonstrate one embodiment of the concept, so we prioritized simplicity in form and function, and opted for a dual-flap, hinge-lever design, which we detail here. The extension mechanism is made of two 3D printed flaps (**Figure 5.5**). Each flap attaches to the waist belt at about the L5-S1 level (target: x_2 = 0.0 m). The flaps are 15 cm apart, centered over the mid-line of the spine (**Figure 5.5**, w_1). Two elastic bands (one on the left and and one on the right) are routed through each respective flap (**Figure 5.5**, e). The flaps are anchored to the waist belt with fabric hinges, which allow the flaps to rotate about an axis parallel to the spine. The flaps are designed to have a disengaged and an engaged mode. In disengaged mode, the extension mechanism flaps rest on the sides of the user's waist (**Figure 5.5**, left). In engaged mode, the flaps are rotated to the posterior (bringing the elastic bands with them) until the flaps connect (held together via hook and loop), forming an offset from the L5-S1 (target: y_2 = 0.18 m, (**Figure 5.5**, right). The elastic bands then stretch during movements such as bending and lifting to assist the low back and hip extensor muscles. Moving the flaps from disengaged to engaged mode creates the desired moment arm extension effect. Moving the flaps back into the disengaged mode causes the elastic bands to run along the side of the waist (i.e. along the neutral axis of body in the sagittal plane) and thus to experience negligible displacement during movements (e.g. lifting, walking, stair ascent/descent) and postures (e.g. standing, sitting, crouching). We note that this new dual-mode flap design that utilizes the neutral axis of the body [157] differs from the clutch mechanisms used in our previous form-fitting exosuit [84], but they each accomplish the same goal of achieving one mode in which the device stays out of the way (disengaged state) and one that assists the user (engaged state). A physical prototype of this design was fabricated and is shown in **Figure 5.6**). In total this extensible exosuit

prototype weighs 1.5 kg (**Figure 5.6**).

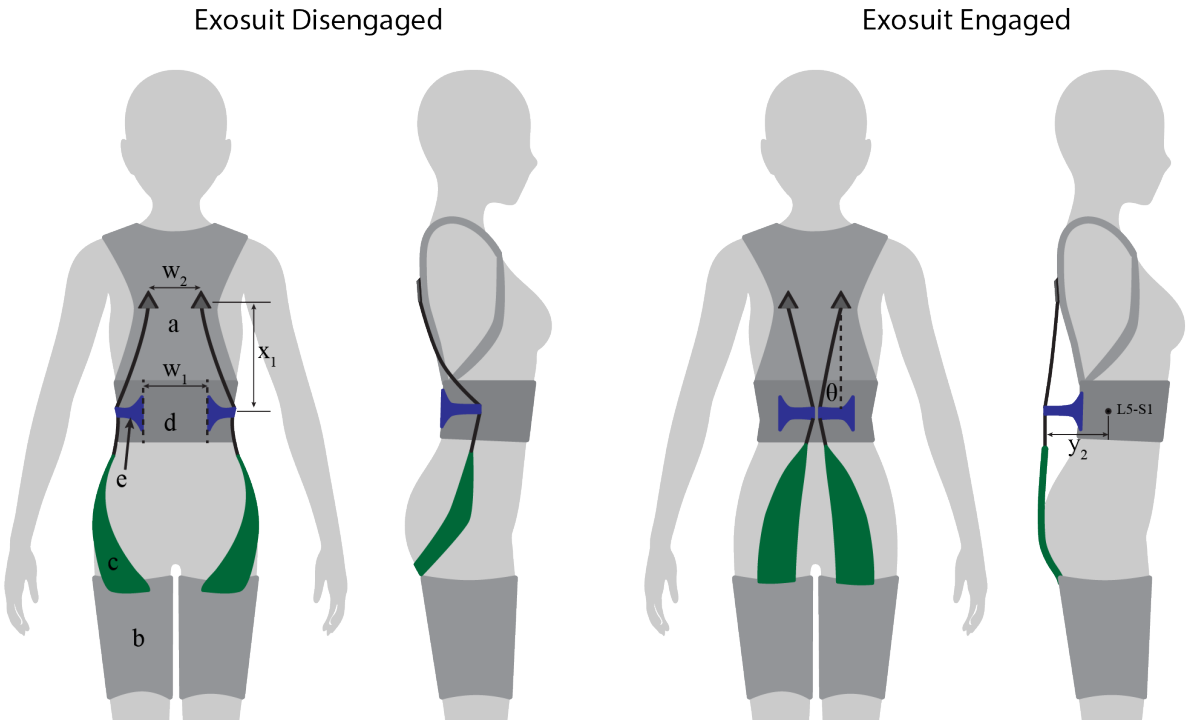

Figure 5.5: **Extensible exosuit prototype schematic.** This extensible exosuit design consists of a trunk interface (**a**), two leg interfaces (**b**), two elastic bands (**c**), a waist belt (**d**), and the extension mechanism flaps (**e**). The trunk interface is coupled with the leg interfaces via the elastic bands, which each consist of an elastic (green) and inelastic (black) segment in series. The elastic bands were routed through the flaps. **Exosuit disengaged:** the mechanism flaps (and the elastic bands) are folded to the user's sides so that the elastic bands do not stretch or apply device-to-body forces during movement. **Exosuit engaged:** the mechanism flaps are folded to the users' back (creating the offset y_2) so that the elastic bands stretch and apply torque about the back and hips during tasks like lifting, bending, and stooping. The flaps rotate about hinges (dashed lines) which were spaced apart by 0.15 m (w_1). The trunk interface anchoring points were spaced apart by 0.15 m as well (w_2)

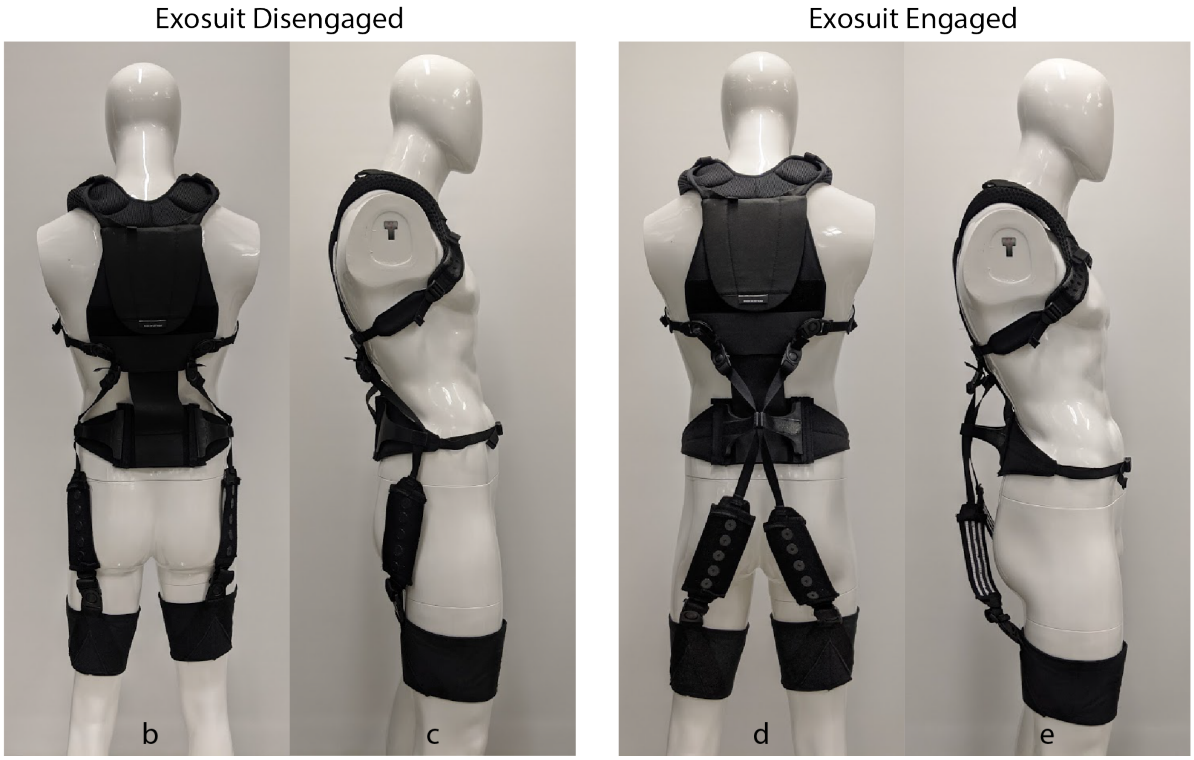

Figure 5.6: **Photos of the extensible exosuit prototype** in disengaged mode (two photos on the left), and in engaged mode (two photos on the right). Refer to the schematic in **Figure 5.5** for call-outs to each component

5.5 Case Study Demonstration

A single-subject case study was performed to demonstrate and confirm the mechanical function of the extensible exosuit prototype. The first test (**Section 5.5.1**) sought to confirm that the extensible exosuit in engaged mode (i.e., extended mechanism) could provide the same torque assistance but with reduced device-to-body forces ($\|\overrightarrow{F_T}\|$ on the shoulders and legs) compared to the form-fitting exosuit during a manual lifting task. The second test (**Section 5.5.2**) sought to to confirm that the user could perform common movements and postures (e.g. walking, carrying, leaning, twisting, sitting) without feeling restricted while wearing the extensible exosuit in disengaged mode. The subject provided written consent prior to testing according to the approved Vanderbilt University Institutional Review Board protocol.

5.5.1 Exosuit Assistance Demonstration

A single subject (female, 64 kg, 1.74 m, 26 yr.) performed a lifting and lowering task while wearing the extensible exosuit vs. the form-fitting exosuit. User and exosuit kinematics and elastic band tension data were collected. The subject performed 8 lifting and 8 lowering movements with a 13 kg box, paced at 15 lifting/lowering movements per minute. The subject performed the task with the extensible exosuit and with the form-fitting exosuit. The elastic band stiffness was adjusted between both exosuit conditions (i.e. different elastic bands were installed on the extensible vs. form fitting exosuit) to ensure that the same peak exosuit torque assistance (τ_{exo}) was provided for both conditions.

Motion capture markers were placed on the following segments to measure their kinematics: the subject's trunk, the subject's pelvis, the trunk interface, the extension mechanism, the elastic bands, and the leg interfaces. One of the elastic bands was instrumented with a load cell to measure the trunk force. The trunk force in the non-instrumented elastic band was matched to the instrumented elastic band by matching the slack length of the two elastic bands and confirming with the subject that the tension of the two elastic bands felt equivalent during the movement. Motion capture (Vicon) and load cell (Futek) data were collected synchronously at 200 Hz and 1000 Hz, respectively. Motion and load cell data were low-pass filtered at 6 Hz and 10 Hz, respectively, with a 4^{th} order, dual-pass Butterworth filter [161]. τ_{exo} was calculated using motion capture and load cell data collected during the lifting and lowering trials. Motion capture markers placed on the elastic bands and extension mechanism provided orientation data, and the load cell provided the magnitude of force along the elastic band, which enabled us to calculate force vectors ($\overrightarrow{F_T}$) and ($\overrightarrow{F_M}$). Motion capture markers on the pelvis' anatomical landmarks were used to estimate the location of the L5-S1 joint [109]. Time series τ_{exo} was calculated for all trials and cycles using **Equations** (5.1) to (5.3). Kinematic and kinetic analysis were performed using the Visual3D software package

(C-Motion). Time series kinematic and kinetic data were divided into individual cycles, time-normalized to 1000 data points and then averaged across cycles. Peak τ_{exo}, $\overrightarrow{F_T}$ and $\overrightarrow{F_M}$ were calculated for individual cycles, and then averaged. The two key outcome metrics were: τ_{exo} (to confirm assistance magnitudes were similar for each exosuit condition), and $\overrightarrow{F_T}$ (to confirm that the extensible exosuit reduced device-to-body forces vs. the form-fitting exosuit). We also used the experimental motion capture data to measure the actual design parameters (x_1, x_2 and y_2) that resulted when the prototype was worn by this specific case study participant.

5.5.2 Exosuit Non-Interference Demonstration

Next the subject performed a series of common movement tasks while wearing the extensible exosuit in disengaged mode. The subject performed the following tasks: level treadmill walking, walking while carrying a 13 kg box, stair ascent/descent, sitting, sit-to-stand, twisting at the torso in the coronal plate, leaning left and right in the frontal plane, leaning forward and backward in the sagittal plane. Immediately after completing each movement the subject filled out a questionnaire (see **Table C.1** in the Appendix) in which they rated how much they felt that the extensible exosuit interfered with the task on a five point Likert scale.

5.5.3 Case Study Results

The extensible exosuit parameters during the lifting and lowering trials (measured using the motion capture data), were 0.15 m for the trunk interface anchoring point (x_1), -0.025 m for the extension mechanism location on the back (x_2), and 0.19 m for the extension mechanism offset (y_2). These parameters differed slightly from our target design criteria (see **Section 5.4.1** above), which was not unexpected since these parameters depend on each person's body dimensions and precisely how the prototype fits onto

their body. Nonetheless the parameters were deemed adequate to achieve our proof-of-concept demonstration goals. When disengaged, the extension mechanism protruded $<$ 2 cm away from the body **Figure 5.6**.

The peak exosuit torques while wearing the extensible and form-fitting exosuits were similar, 17.2 $\pm$ 0.5 Nm and 16.7 $\pm$ 0.6 Nm, respectively (**Figure 5.7**, a). The peak trunk force magnitude for the extensible and form-fitting exosuit were 159 $\pm$ 6 N and 249 $\pm$ 7 N, respectively (a 36% reduction when wearing the extensible exosuit prototype, **Figure 5.7**, b). This reduction was similar to the model predictions when we plugged the measured design parameters (x_1, x_2 and y_2) back into the model. Also of note, this subject reported that they felt the extensible exosuit was more comfortable than the form-fitting exosuit, consistent with the observed reduction in force. For reference, the peak extension mechanism force on the extensible moment arm was 157 $\pm$ 7 N. While in disengaged mode, the subject reported that she was able to complete all movement tasks without interference from the extensible exosuit (survey responses are provided in **Table C.1**).

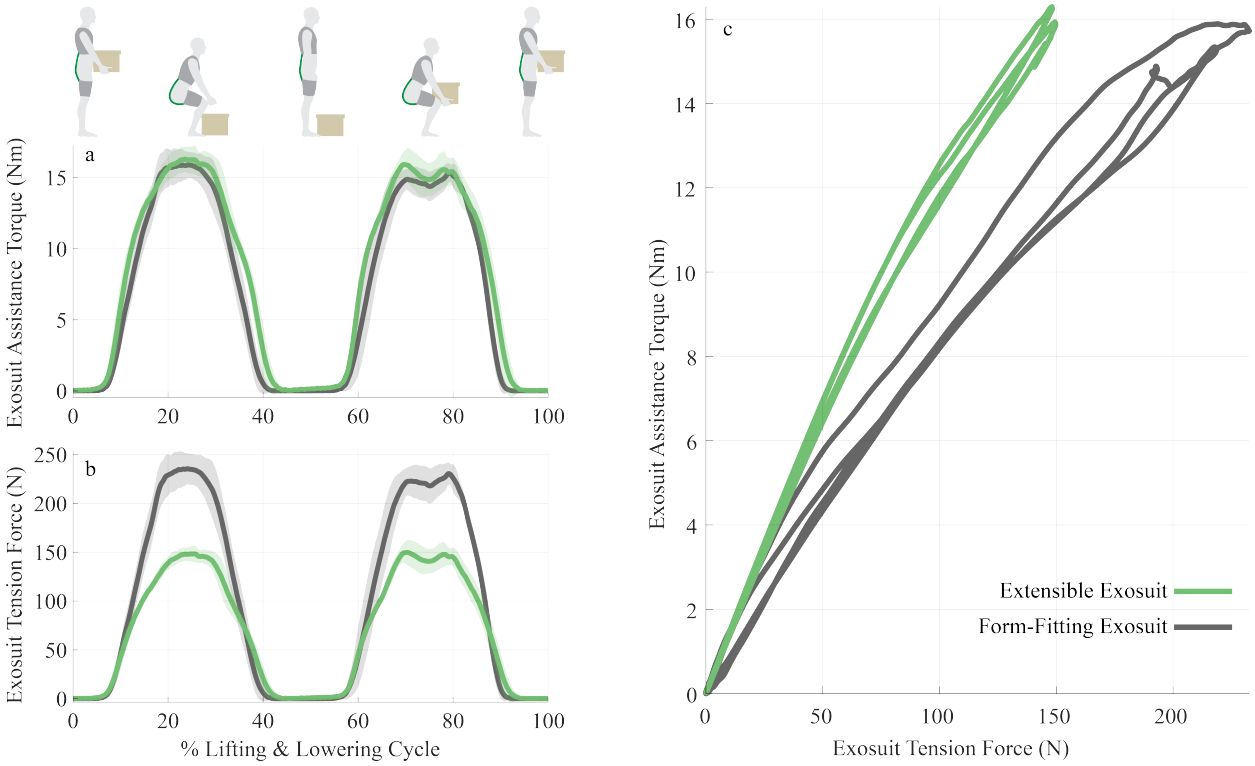

Figure 5.7: **Mechanics of extensible vs. form-fitting exosuit from case study**. The extensible exosuit (green curves) provided similar assistance torque (**a**) as the form-fitting exosuit (gray curves), but with lower device-to-body force on the shoulders and legs (**b**, reduced peak force magnitude by 36%). The slopes of the curves in **c** show the relationship between the trunk force magnitude ($\|\overrightarrow{F_T}\|$, x-axis) and the assistive torque (τ_{exo}, y-axis). This slope is analytically equivalent to the exosuit moment arm r_T. The moment arm r_T for the extensible exosuit (based on a linear least squares fit of each curve) is 0.109 $\frac{Nm}{N}$, which is 63% greater than the slope for the form-fitting exosuit (0.067 $\frac{Nm}{N}$). Curves in (**a**) and (**b**) depict the mean (solid lines) $\pm$ standard deviation (shaded area around mean) across the lifting cycles

5.6 Discussion

5.6.1 Summary

In this work we developed a human-exosuit biomechanical model which was used to understand how various design parameters affected exosuit assistance torque and device-to-body forces. We used these model findings to inform the design and fabrication of an extensible exosuit prototype. We then demonstrated in a human subject case

study that the extensible exosuit could provide the same low back assistance torque as a form-fitting exosuit, but with reduced device-to-body forces on the shoulders and legs (reduced by 36% in the case study, but the model provides insight on how to adjust design parameters to increase or decrease this magnitude as desired). User feedback confirmed that the extensible exosuit successfully provided assistance during lifting, reduced device-to-body forces on the shoulders and legs, improved perceived comfort, and allowed for full freedom of movement and posture (including sitting) when disengaged.

5.6.2 Applications of an Extensible Exosuit

The extensible exosuit offers a way to increase the moment arm of form-fitting exosuits (while in engaged mode), without sacrificing key benefits related to being lightweight, low-profile and unobstructive (in disengaged mode). The extensible exosuit can reduce device-to-body forces on the shoulders and legs, as shown analytically in the model and confirmed empirically in the case study, which can be used to improve comfort for some users or situations. Alternatively, the extensible exosuit can be used to increase the magnitude of assistance without increasing these device-to-body forces (relative to the form-fitting exosuit), which may be valuable for heavy-lifting jobs. Furthermore, although this exosuit was designed to assist the low back, this extension mechanism concept could be used to assist other joints or segments as well (e.g., ankle, knee, neck or shoulder). An extension mechanism could be used in unpowered (e.g., spring) or powered (e.g., motorized) exosuits to selectively increase the moment arm, or it could be controlled in powered exosuits to actively assist movement (e.g., to inject energy by using a motor to extend the mechanism as the user is lifting).

The dual-mode design detailed here may be well-suited for a variety of occupations and work environments. One worth highlighting is last-mile delivery, which typically involves extended periods of sitting (while driving) and intermittent lifting and carrying. In these types of jobs the ability to shift or rotate rigid/semi-rigid components away

from the posterior of the back while in disengaged mode may be beneficial (or critical) to ensure comfort while sitting in delivery vehicles. This style of mode-switching is unique amongst existing back-assist exoskeletons and exosuits, which typically have rigid components along the back or waist that interfere with and may cause discomfort during prolonged sitting. We highlight this application because we are not aware of any commercial or research exoskeletons or exosuits that are particularly well-suited for last-mile delivery, which is a fast-growing market segment. Also of note, this dual-mode flap design can be used with or without an extensible moment arm (i.e. it could also be implemented within a form-fitting exosuit, [157]).

5.6.3 Alternative and Future Designs

The goal of this prototype was to demonstrate proof-of-concept of an extensible exosuit. However, there are numerous alternative designs and implementations of an extensible moment arm mechanism (i.e. alternative to the flap design used in this work), such as a four-bar mechanism, an inflatable pneumatic pouch, or a simple hinged lever. Additionally there may be alternative design objectives such as simultaneously increasing the moment arm about multiple joints (e.g., about both the low back and the hip joints), or creating a non-linear assistance torque profile (appendix **C.0.3**). These objectives could be achieved by relocating and/or reorienting the extension mechanism, by using multiple extension mechanisms, by changing the shape or trajectory of the extension mechanism, or by adjusting where the elastic bands are affixed along the length of the extension mechanism. Therefore, in addition to increasing the exosuit's moment arm, an extension mechanism could also be designed to provide a custom torque profile for a given application.

We opted to use the flap extension mechanism design for this proof-of-concept prototype because the design and construction was simple, low-profile (flaps were $<$6 mm thick), and because the flaps served the dual purpose of mode-switching and extend-

ing/collapsing the exosuit extension mechanism. In the future, if we were to build a prototype for the purposes of field testing, then we would update the design in the follow ways. First, we would upgrade the mode-switching behavior to improve the user experience. The current prototype was sufficient for proof-of-concept but it requires two hands to manually move both flaps from engaged to disengaged position, and vice versa. In future iterations this could be simplified by coupling the two flaps such that the user only needs to perform a single movement (e.g. with one hand) to more quickly and easily move the flaps between the engaged and disengaged modes. We have previously built and demonstrated a variety of these mode-switching controls to easily engage and disengage assistance [84]; some have used small motors (muscle activity control, voice control, phone app) and others have been purely passive (manual button, switch, knob). These are straightforward to implement and the choice is driven by the intended use case of the exosuit. Second, we would improve the ease of adjustability of the elastic band length in order to ensure exosuit could fit more people of varying body shapes and sizes. In future designs this could be addressed by integrating a mechanism that allows each user to adjust the slack length of the elastic bands in both engaged and disengaged modes, which is important to ensure proper fit and function. This sizing adjustability aspect of the design is more closely related to product design (or a later stage prototype), and therefore was not optimized for in this proof-of-concept demonstration.

We achieved our intended goal with this extensible exosuit prototype: we reduced the device-to-body forces on the trunk and legs, while providing the same exosuit assistance torque about the low back (**Figure 5.7**). However, the extension mechanism in this prototype did not alter the moment arm with respect to the hip joint. Because the exosuit moment arm about the hip remained the same and the force in the elastic bands was reduced, the assistance torque (and work) about the hips was also reduced with the extensible exosuit, relative to the form-fitting exosuit. Consistent with this biomechanical effect at the hips, the subject reported that they felt like they were get-

ting more assistance during the lift when wearing the form-fitting exosuit. This makes sense: during a squat lifting movement, the lumbar spine undergoes relatively small angular displacement, so the exosuit is primarily providing what we might term a support torque (i.e., reducing force demands on the back extensor muscles which are contracting near-isometrically). In contrast, the hip joints experience large angular displacements during the lifting movement. As the elastic bands stretch and recoil, elastic potential energy is stored and returned to the users as assistive work about the hip joints (i.e., offsetting mechanical work that would otherwise need to be done by the hip extensor muscles). If we were to match tension in the elastic bands instead of matching torque between the extensible and form-fitting exosuits, then we would expect to see the same hip assistance torque (and work) between both exosuits during lifting, but greater L5-S1 support torque in the extensible exosuit. Or if our design goal had been to increase the moment arms about both the L5-S1 and hip joints, then we could have used the same modeling approach we outlined in **Section 5.3** to identify the proper exosuit and extension mechanism design parameters to achieve these goals (appendix **C.0.3**). This highlights the benefit of using biomechanical modeling to identify design parameters that achieve a specified assistance goal, and also provides a reminder that the prototype demonstrated is simply an example, and that this concept of using an extensible mechanism to increase the moment arm can be adapted to assist one or more body joints or segments.

5.6.4 Additional Model Insights

One insight from the model is that the theoretical upper limit of the moment arm relative to the L5-S1 joint is equal to the distance between the trunk interface anchoring point (x_1) and the L5-S1 joint (i.e. the moment arm $r_T \leq \|p_1 - p_0\|$). This makes intuitive sense: if you imagine an infinitely long extension mechanism ($y_2 \to \infty$), then the force vector on the trunk $\overrightarrow{F_T}$ would be perpendicular to the trunk segment itself. This

configuration is analytically equivalent to a rigid exoskeleton comprised of a rotational spring and a rigid strut from L5-S1 to the trunk interface anchoring point. This is also a useful reminder that despite the common distinction made between rigid exoskeletons and soft exosuits they both operate on the same physical principles. They are springs (or actuators) acting in parallel with the body, and from a physics perspective they represent different sets of parameters along a continuum of possibilities. In a sense, our extensible exosuit concept is a design somewhere in the middle of this continuum, in which we blend some of the benefits of exosuits (e.g. using flexible textiles to minimize weight, movement interference, pressure points and associated discomfort) with some of the benefits of rigid exoskeletons (e.g. they typically have larger moment arms by nature of applying more perpendicular device-to-body forces farther away from the biological joint center of rotation).

A second interesting model insight is that: when the extension mechanism is placed on the low back, the force ($\overrightarrow{F_M}$) it exerts on the body causes the moment arm to plateau at around 0.22 m, which is considerably lower than the theoretical upper limit of 0.41 m. This holds true even as the extension mechanism offset is increased (e.g. up to 0.58 m, **Figure C.3**). This happens because $\overrightarrow{F_M}$ changes orientation as y_2 increases, such that it creates a flexion torque component (clockwise) about the L5-S1 which directly opposes the extension torque component (counter-clockwise) of $\overrightarrow{F_T}$. This may be a limitation for this particular proof-of-concept design implementation (i.e. mechanism sitting on the low back); however, there are alternative ways to configure the extensible mechanism (or mechanisms) that would create an even larger moment arm (see appendix **C.0.3** for examples of alternatives). However, in practice, this limitation may be moot, because if the extension mechanism becomes too large, then it will be considered by the users as too bulky and impractical to adopt.

A final insight is related to the physical design of the exosuit, and specifically the placement of the elastic elements (materials) within the bands. While the model de-

picts an elastic material running continuously between the trunk and leg interfaces (**Figure 5.1**), fabricating the physical device often requires this band to be comprised of a combination of elastic/stretch and inelastic/non-stretch materials in series (**Figure 5.6**). This introduces practical design choices, such as deciding whether the elastic element (within the band) should be located near the middle of the back vs. behind the buttocks vs. behind the legs, etc. For this extensible exosuit prototype (**Figure 5.6**) and for our previous exosuit designs [82] we chose to place the elastic elements over the buttocks and the non-stretch webbing over the user's back. From our own experience in testing and designing these exosuits, we have found that this placement of the elastic elements makes the exosuit subjectively feel more comfortable and assistive to us. To provide insight on this topic we extended our biomechanical model to consider the effects of friction between the exosuit and the user. The model (detailed in appendix **C.0.4**) suggests that the benefit of placing the elastic element over the buttocks is that it minimizes relative motion between the band and the buttocks. This in turn minimizes dissipative energy losses due to friction. In contrast, placing an non-stretch material (e.g. non-stretch webbing) over the buttocks results in frictional losses each time a person bends or lifts. Interestingly, most people are already familiar with this physical phenomenon from their own personal life experience: When you bend forward or squat down while wearing non-stretch pants (e.g. denim jeans), your pants tend to slide down in the back (potentially exposing your intergluteal cleft, i.e. your butt crack). Whereas this sliding effect does not happen (or is greatly reduced) when wearing elastic or stretch pants (e.g. spandex leggings) because the elastic fabric deforms with your buttocks as you bend. Consistent with this shared human experience, the key takeaway from our model is that placing the elastic element over the buttocks likely reduces friction force and dissipative work, which may explain why this configuration subjectively feels more comfortable and assistive than alternative configurations (e.g. placing the non-stretch element over the buttocks and the elastic element in the middle of the back). Additional technical

details and visual illustrations related to elastic band placement, buttocks friction and dissipative work are provided in appendix **C.0.4**.

5.6.5 Scope of Work and Limitations

First, regarding the scope of work, we chose not to assess back muscle activity in the case study. This is because over the last 15 years there have already been over a dozen independent studies consistently showing that these types of exosuits reduce back muscle loading and fatigue during lifting and bending tasks, and also that the magnitude of back offloading scales with the magnitude of exosuit torque assistance (see appendix **C.0.5** for a table summarizing the evidence). To be specific: when in engaged mode, the extensible exosuit presented here is functionally similar to previous exosuits in the way that they provide assistance torque about the low-back. As such, a case study would not meaningfully advance our understanding beyond the current state of knowledge. The innovations here were the extensible/collapsible nature of the moment arm, the novel mode-switching behavior, and the modeling work that better informs the selection of design parameters.

Second, we employed a simple model of the human and exosuit system, which neglects some 3D geometrical details, curvature of the spine, and soft-body mechanics. Despite these assumptions, our model was adequate for its intended purpose: to provide general insight on design parameters which we could use to inform fabrication of a prototype.

Third, we only tested the extensible exosuit on a single-subject. However, this was sufficient for our purposes: to demonstrate proof-of-concept. Future work includes development of a field testable prototype, and multi-user field test evaluation, in particular to better understand user perceptions and preferences across a larger number of people. For instance, while there may be some individuals who prefer the lower shoulder and leg forces afforded by the extensible exosuit, we have anecdotal evidence that suggests

others may find the form-fitting exosuit sufficiently comfortable such that they prefer the higher shoulder forces over an additional force (albeit lower) on their lower back or waist. Of note, we previously used this same research-development-translation progression (i.e., modeling and feasibility test, followed by field prototype and field testing, followed by technology translation) to translate the form-fitting exosuit into a commercial product (HeroWear Apex). We hope to follow a similar progression with this extensible exosuit, and this manuscript represents the first stage of that progression.

Finally we note that the biomechanical estimates of L5-S1 torque may be susceptible to errors in absolute magnitude, because the L5-S1 joint location was estimated using external reference markers and regression equations derived from cadaveric pelvises [109]. However, in this work we only look at differences between the extensible exosuit vs. the form-fitting exosuit (i.e., relative differences), which use the same estimated L5-S1 location, and therefore absolute errors in the magnitude of the torque assistance do not affect the relative comparisons or any of our conclusions.

5.7 Conclusion

The dual-mode extensible exosuit introduced here provides a practical and effective way to enhance the moment arm of exosuits, while also retaining key benefits of not interfering with movement and being low-profile while disengaged. A proof-of-concept prototype was demonstrated, and the modeling work provides the foundation for broad applications and various implementations of extensible exosuits to enhance human health and safety, for the back and other body segments. We envision promising opportunities to apply this extensible exosuit concept to assist heavy-lifting, to further enhance user comfort, and to address the unique needs of last-mile delivery workers.

Chapter 6

Future Work and Conclusions

6.1 Conclusion

This dissertation highlights my scientific and engineering contributions to the development and understanding of quasi-passive wearable assistive devices. I developed a novel textile-based exosuit and showed that it is an effective way to assist various demanding movements (e.g. lifting and leaning) by reducing back extensor muscle effort (in terms of EMG magnitude) and rates of fatigue (in terms of EMG median frequency). I also show through novel modeling, design, and experimental demonstration that this type of exosuit can be enhanced with an extension mechanism to further improve user comfort or assistance. Finally, I quantified the potential benefits of a commercially available adaptive prosthesis for lower-limb prosthesis users during sloped walking, and elucidated key methodological considerations when performing biomechanical assessment of this population. Together these contributions have advanced the engineering development of quasi-passive wearable assistive devices and furthered our scientific understanding of how they affect end-users and how they can be improved to sustain health and augment performance.

6.2 Future Work

In the following paragraph I highlight a number of research avenues related to my work that I find particularly interesting and important for future work.

First, the approach I used in this work (i.e. textile-based, passive or quasi-passive exosuits) can be extended to other joints (e.g. the ankle [151], knee, hip [67], shoulder, etc.). In future designs, these exosuits could span multiple [15], or even most of the

joints (e.g. the exosuit could be worn like a spandex base-layer that covers the upper and lower body). Textile-based, low-power clutching (e.g. textile electrostatic clutching [70]) and computing (e.g. via e-textiles), could then be used to engaged, disengaged and tune elastic and damping elements [107] all along the body to augment movements involving multiple joints. This single exosuit then would be able to assist during many different functional and mobility tasks like walking and running (e.g. by engaging elastic elements across the hip, and ankle), lifting (e.g. by engaging elastic elements across the back, hip and knee), overhead manual work (e.g. by engaging elastic elements across the shoulders), and stair descent (e.g. by engaging damping elements across the knee). This type of exosuit would require biomechanical insights (to identify movements that can be assisted with passive springs and dampers [36]), predictive biomechanical modeling (to anticipate the users movement and engage the passive elements accordingly), and softgoods expertise (to create a comfortable, form-fitting garment with woven fabrics, elastics, and e-textiles).

Second, my motivation for using softgoods (e.g. fabric and elastic) was to create a wearable assistive device that people would want to wear because it would look and feel like clothing. Our understanding of how to design clothing-like exosuits which apply assistance to the body has advanced in recent years ([10, 153, 118, 155]), however, many of these exosuits are still research prototypes, and will require considerable product design work in order become clothing-like. I believe the success of these exosuits (especially in a commercial space) will hinge on a deep understanding of textiles, clothing and ongoing partnerships with softgoods and clothing experts, because exosuits face many barriers to adoption which are intimately related to softgoods design (e.g. comfort, mobility, durability, breath-ability, don-doff ease, aesthetic appeal, etc.). It is also worth noting that there are promising advancements in softgoods such as textile based sensors, actuators, and computing which could be used to expand the capabilities of exosuits [27, 62, 14, 112, 30].

Finally, the next crucial step after the development and validation a device is to determine whether it can affect outcomes that are most directly relevant to the intended end-users in the real world (e.g. nurses, package-handlers, last-miler delivery workers). End-user outcomes might include: reducing perceived exhaustion (e.g. after a full work shift), increasing productivity (e.g. for a logistics floor manager), alleviating pain or discomfort, reducing injury or injury recurrence risk (i.e. primary or secondary prevention [139]), or improving long-term musculoskeletal health. These outcomes are important for assuring that in-lab measurements and estimates (e.g. changes in muscle activity, reduced loading of the spine) translate to relevant user outcomes, and more generally that the wearable assistive device is a valuable tool for improving the physical health of society. Real-world, long-term research (e.g. longitudinal randomized experiments) of wearable assistive devices has largely been limited to back braces (and conclusive evidence shows they do not help prevent back pain [145]). Wearable assistive devices which provide mechanical assistance are younger technologies and have not yet been tested on the same scale as back belts, for example. The real-world testing that has been conducted thus far on these wearable assistive devices is promising ([154, 60]), but the long-term impact of these devices on relevant end-user outcomes remains to be explored.

Bibliography

[1]• Mohammad Abdoli-E, Michael J. Agnew, and Joan M. Stevenson. "An on-body personal lift augmentation device (PLAD) reduces EMG amplitude of erector spinae during lifting tasks". In: *Clinical Biomechanics* 21.5 (June 2006), pp. 456–465. ISSN: 0268-0033. DOI: 10.1016/j.clinbiomech.2005.12.021. URL: http://www.sciencedirect.com/science/article/pii/S0268003306000064 (visited on 01/07/2016).

[2] Mohammad Abdoli-E and Joan M. Stevenson. "The effect of on-body lift assistive device on the lumbar 3D dynamic moments and EMG during asymmetric freestyle lifting". In: *Clinical Biomechanics* 23.3 (Mar. 1, 2008), pp. 372–380. ISSN: 0268-0033. DOI: 10.1016/j.clinbiomech.2007.10.012. URL: http://www.sciencedirect.com/science/article/pii/S0268003307002458 (visited on 08/05/2020).

[3] Mohammad Abdoli-Eramaki et al. "Mathematical and empirical proof of principle for an on-body personal lift augmentation device (PLAD)". In: *Journal of Biomechanics* 40.8 (Jan. 1, 2007), pp. 1694–1700. ISSN: 0021-9290. DOI: 10.1016/j.jbiomech.2006.09.006. URL: http://www.sciencedirect.com/science/article/pii/S0021929006003228.

[4] M. A. Adams, W. C. Hutton, and J. R. Stott. "The resistance to flexion of the lumbar intervertebral joint". In: *Spine* 5.3 (June 1980), pp. 245–253. ISSN: 0362-2436.

[5] M. A. Adams et al. "Mechanical initiation of intervertebral disc degeneration". In: *Spine* 25.13 (July 1, 2000), pp. 1625–1636. ISSN: 0362-2436.

[6] Michael A. Adams, Kim Burton, and Nikolai Bogduk. *The Biomechanics of Back Pain*. Google-Books-ID: SKAuZkQ10zoC. Elsevier Health Sciences, 2006. 331 pp. ISBN: 978-0-443-10068-0.

[7] Vibhor Agrawal et al. "Comparison of four different categories of prosthetic feet during ramp ambulation in unilateral transtibial amputees". In: *Prosthetics and Orthotics International* 39.5 (Oct. 1, 2015), pp. 380–389. ISSN: 0309-3646. DOI: 10.1177/0309364614536762. URL: https://doi.org/10.1177/0309364614536762 (visited on 04/04/2018).

[8] Merkur Alimusaj et al. "Kinematics and kinetics with an adaptive ankle foot system during stair ambulation of transtibial amputees". In: *Gait & Posture* 30.3 (Oct. 2009), pp. 356–363. ISSN: 0966-6362. DOI: 10.1016/j.gaitpost.2009.06.009. URL: http://www.sciencedirect.com/science/article/pii/S0966636209001805 (visited on 03/27/2017).

[9] Gunnar BJ Andersson. "Epidemiological features of chronic low-back pain". In: *The Lancet* 354.9178 (Aug. 14, 1999), pp. 581–585. ISSN: 0140-6736. DOI: 10.1016/S0140-6736(99)01312-4. URL: http://www.sciencedirect.com/science/article/pii/S0140673699013124 (visited on 08/09/2016).

[10] Alan T. Asbeck et al. "A biologically inspired soft exosuit for walking assistance". In: *The International Journal of Robotics Research* 34.6 (May 1, 2015), pp. 744–762. ISSN: 0278-3649. DOI: 10.1177/0278364914562476. URL: http://journals.sagepub.com/doi/abs/10.1177/0278364914562476 (visited on 01/30/2017).

[11] Catherine L. MS Backman and Susan R. Harris. "CASE STUDIES, SINGLE-SUBJECT RESEARCH, AND N OF 1 RANDOMIZED TRIALS: Comparisons and Contrasts1. [Miscellaneous Article]". In: *Journal of Physical Medicine* 78.2 (Apr. 1999), pp. 170–176. ISSN: 0894-9115.

[12] S. J. Baltrusch et al. "The effect of a passive trunk exoskeleton on functional performance in healthy individuals". In: *Applied Ergonomics* 72 (2018), pp. 94–106. ISSN: 0003-6870. DOI: 10.1016/j.apergo.2018.04.007. URL: https://www.sciencedirect.com/science/article/pii/S0003687018300930 (visited on 05/29/2018).

[13] Saskia J. Baltrusch et al. “Perspectives of End Users on the Potential Use of Trunk Exoskeletons for People With Low-Back Pain: A Focus Group Study”. In: *Human Factors* (Jan. 8, 2020), p. 0018720819885788. ISSN: 0018-7208. DOI: 10.1177/0018720819885788. URL: https://doi.org/10.1177/0018720819885788 (visited on 01/17/2020).

[14] Yoseph Bar-Cohen. *Electroactive Polymer (EAP) Actuators as Artificial Muscles: Reality, Potential, and Challenges*. Google-Books-ID: uxqgkdqE9FIC. SPIE Press, 2004. 790 pp. ISBN: 978-0-8194-5297-9.

[15] Hamid Barazesh and Maziar Ahmad Sharbafi. “A biarticular passive exosuit to support balance control can reduce metabolic cost of walking”. In: *Bioinspiration & Biomimetics* 15.3 (Mar. 2020). Publisher: IOP Publishing, p. 036009. ISSN: 1748-3190. DOI: 10.1088/1748-3190/ab70ed. URL: https://doi.org/10.1088%2F1748-3190%2Fab70ed (visited on 08/17/2020).

[16] B. Bazrgari and A. Shirazi-Adl. “Spinal stability and role of passive stiffness in dynamic squat and stoop lifts”. In: *Computer Methods in Biomechanics and Biomedical Engineering* 10.5 (Oct. 1, 2007), pp. 351–360. ISSN: 1025-5842. DOI: 10.1080/10255840701436974. URL: https://doi.org/10.1080/10255840701436974 (visited on 04/03/2018).

[17] Rezaul Begg et al. “Minimum foot clearance during walking: Strategies for the minimisation of trip-related falls”. In: *Gait & Posture* 25.2 (Feb. 1, 2007), pp. 191–198. ISSN: 0966-6362. DOI: 10.1016/j.gaitpost.2006.03.008. URL: http://www.sciencedirect.com/science/article/pii/S0966636206000476.

[18] Bruce P Bernard, Vern Putz-Anderson, and Susan E. Burt. “Musculoskeletal Disorders and Workplace Factors - A Critical Review of Epidemiologic Evidence for Work-Related Musculoskeletal Disorders of the Neck, Upper Extremity, and Low

Back". In: *Cincinnati: Centers for Disease Control and Prevention National Institute for Occupational Safety and Health* (July 1997), pp. 97–141.

[19] Nikolai Bogduk. *Clinical Anatomy of the Lumbar Spine and Sacrum*. Google-Books-ID: UYC_NpoFfAsC. Elsevier Health Sciences, 2005. 262 pp. ISBN: 978-0-443-10119-9.

[20] NIKOLAI BSc(Med) Bogduk and JANET E. Macintosh. "The Applied Anatomy of the Thoracolumbar Fascia". In: *Spine* 9.2 (Mar. 1984), pp. 164–170. ISSN: 0362-2436.

[21] Nikolai Bogduk, Garth Johnson, and Deborah Spalding. "The morphology and biomechanics of latissimus dorsi". In: *Clinical Biomechanics* 13.6 (Sept. 1, 1998), pp. 377–385. ISSN: 0268-0033. DOI: 10.1016/S0268-0033(98)00102-8. URL: http://www.sciencedirect.com/science/article/pii/S0268003398001028 (visited on 10/11/2018).

[22] Tim Bosch et al. "The effects of a passive exoskeleton on muscle activity, discomfort and endurance time in forward bending work". In: *Applied Ergonomics* 54 (May 2016), pp. 212–217. ISSN: 0003-6870. DOI: 10.1016/j.apergo.2015.12.003. URL: http://www.sciencedirect.com/science/article/pii/S0003687015301241 (visited on 08/26/2016).

[23] James W. Breakey. "Body Image: The Lower-Limb Amputee". In: *JPO: Journal of Prosthetics and Orthotics* 9.2 (Apr. 1997), p. 58. ISSN: 1040-8800. URL: https://journals.lww.com/jpojournal/Abstract/1997/00920/Body_Image__The_Lower_Limb_Amputee.5.aspx (visited on 08/20/2018).

[24] P Brinckmann, M Biggemann, and D Hilweg. "Fatigue fracture of human lumbar vertebrae". In: *Clinical Biomechanics* 3 (Jan. 1, 1988), i–S23. ISSN: 0268-0033. DOI: 10.1016/S0268-0033(88)80001-9. URL: http://www.sciencedirect.com/science/article/pii/S0268003388800019 (visited on 12/05/2016).

[25] Joshua M. Caputo and Steven H. Collins. "Prosthetic ankle push-off work reduces metabolic rate but not collision work in non-amputee walking". In: *Scientific Reports* 4.1 (May 2015). ISSN: 2045-2322. DOI: 10.1038/srep07213. URL: http://www.nature.com/articles/srep07213 (visited on 05/31/2018).

[26] André Cardoso, Ana Colim, and Nuno Sousa. "The Effects of a Passive Exoskeleton on Muscle Activity and Discomfort in Industrial Tasks". In: *Occupational and Environmental Safety and Health II*. Ed. by Pedro M. Arezes et al. Studies in Systems, Decision and Control. Cham: Springer International Publishing, 2020, pp. 237–245. ISBN: 978-3-030-41486-3. DOI: 10.1007/978-3-030-41486-3_26. URL: https://doi.org/10.1007/978-3-030-41486-3_26 (visited on 02/27/2020).

[27] Lina M. Castano and Alison B. Flatau. "Smart fabric sensors and e-textile technologies: a review". In: *Smart Materials and Structures* 23.5 (Apr. 2014). Publisher: IOP Publishing, p. 053001. ISSN: 0964-1726. DOI: 10.1088/0964-1726/23/5/053001. URL: https://doi.org/10.1088%2F0964-1726%2F23%2F5%2F053001 (visited on 08/18/2020).

[28] Don B. Chaffin. "Localized Muscle Fatigue - Definition and Measurement". In: *Journal of Occupational Medicine* 15.4 (Apr. 1973), pp. 346–354. ISSN: 0096-1736.

[29] DON B. CHAFFIN and KYUNG S. PARK. "A Longitudinal Study of Low-Back Pain as Associated with Occupational Weight Lifting Factors". In: *American Industrial Hygiene Association Journal* 34.12 (Dec. 1, 1973), pp. 513–525. ISSN: 0002-8894. DOI: 10.1080/0002889738506892. URL: http://www.tandfonline.com/doi/abs/10.1080/0002889738506892 (visited on 08/09/2016).

[30] Min Chen et al. "Smart Clothing: Connecting Human with Clouds and Big Data for Sustainable Health Monitoring". In: *Mobile Networks and Applications* 21.5 (Oct. 1, 2016), pp. 825–845. ISSN: 1572-8153. DOI: 10.1007/s11036-016-0745-1. URL: https://doi.org/10.1007/s11036-016-0745-1 (visited on 08/18/2020).

[31] W. Lee Childers and Kota Z. Takahashi. "Increasing prosthetic foot energy return affects whole-body mechanics during walking on level ground and slopes". In: *Scientific Reports* 8 (Mar. 29, 2018). ISSN: 2045-2322. DOI: 10.1038/s41598-018-23705-8. URL: https://www.ncbi.nlm.nih.gov/pmc/articles/PMC5876366/ (visited on 04/04/2018).

[32] Pieter Coenen et al. "Cumulative Low Back Load at Work as a Risk Factor of Low Back Pain: A Prospective Cohort Study". In: *Journal of Occupational Rehabilitation* 23.1 (Mar. 1, 2013), pp. 11–18. ISSN: 1053-0487, 1573-3688. DOI: 10.1007/s10926-012-9375-z. URL: http://link.springer.com/article/10.1007/s10926-012-9375-z (visited on 11/17/2016).

[33] Benjamin J. Darter and Jason M. Wilken. "Energetic consequences of using a prosthesis with adaptive ankle motion during slope walking in persons with a transtibial amputation". In: *Prosthetics and Orthotics International* 38.1 (Feb. 1, 2014), pp. 5–11. ISSN: 0309-3646, 1746-1553. DOI: 10.1177/0309364613481489. URL: http://poi.sagepub.com/content/38/1/5 (visited on 05/23/2016).

[34] D Daynard et al. "Biomechanical analysis of peak and cumulative spinal loads during simulated patient-handling activities: a substudy of a randomized controlled trial to prevent lift and transfer injury of health care workers". In: *Applied Ergonomics* 32.3 (June 1, 2001), pp. 199–214. ISSN: 0003-6870. DOI: 10.1016/S0003-6870(00)00070-3. URL: http://www.sciencedirect.com/science/article/pii/S0003687000000703 (visited on 07/10/2018).

[35] Alan R De Asha and John G Buckley. "The effects of walking speed on minimum toe clearance and on the temporal relationship between minimum clearance and peak swing-foot velocity in unilateral trans-tibial amputees". In: *Prosthetics and Orthotics International* 39.2 (Apr. 1, 2015), pp. 120–125. ISSN: 0309-3646. DOI:

10.1177/0309364613515493. URL: https://doi.org/10.1177/0309364613515493 (visited on 05/08/2018).

[36] W. van Dijk, H. van der Kooij, and E. Hekman. "A passive exoskeleton with artificial tendons: Design and experimental evaluation". In: *2011 IEEE International Conference on Rehabilitation Robotics*. 2011 IEEE International Conference on Rehabilitation Robotics. June 2011, pp. 1–6. DOI: 10.1109/ICORR.2011.5975470.

[37] Wietse van Dijk and Herman Van der Kooij. "XPED2: A Passive Exoskeleton with Artificial Tendons". In: *IEEE Robotics Automation Magazine* 21.4 (Dec. 2014). Conference Name: IEEE Robotics Automation Magazine, pp. 56–61. ISSN: 1558-223X. DOI: 10.1109/MRA.2014.2360309.

[38] P Dolan and M. A Adams. "Repetitive lifting tasks fatigue the back muscles and increase the bending moment acting on the lumbar spine". In: *Journal of Biomechanics* 31.8 (Aug. 1, 1998), pp. 713–721. ISSN: 0021-9290. DOI: 10.1016/S0021-9290(98)00086-4. URL: http://www.sciencedirect.com/science/article/pii/S0021929098000864 (visited on 07/05/2018).

[39] Aaron M. Dollar and Hugh Herr. "Design of a quasi-passive knee exoskeleton to assist running". In: *2008 IEEE/RSJ International Conference on Intelligent Robots and Systems*. 2008 IEEE/RSJ International Conference on Intelligent Robots and Systems. ISSN: 2153-0866. Sept. 2008, pp. 747–754. DOI: 10.1109/IROS.2008.4651202.

[40] Joan E. Edelstein. "Prosthetic feet: State of the art". In: *Physical Therapy* (1988), pp. 1874–1881.

[41] R. H. Edwards. "Human muscle function and fatigue". In: *Ciba Foundation Symposium* 82 (1981), pp. 1–18. ISSN: 0300-5208.

[42] Britt Elfving et al. "Recovery of electromyograph median frequency after lumbar muscle fatigue analysed using an exponential time dependence model". In: *European Journal of Applied Physiology* 88.1 (Nov. 1, 2002), pp. 85–93. ISSN: 1439-

6319, 1439-6327. DOI: 10.1007/s00421-002-0685-2. URL: https://link-springer-com.proxy.library.vanderbilt.edu/article/10.1007/s00421-002-0685-2 (visited on 02/16/2018).

[43] R. M. Enoka and D. G. Stuart. "Neurobiology of muscle fatigue". In: *Journal of Applied Physiology* 72.5 (May 1, 1992), pp. 1631–1648. ISSN: 8750-7587. DOI: 10.1152/jappl.1992.72.5.1631. URL: https://www.physiology.org/doi/abs/10.1152/jappl.1992.72.5.1631 (visited on 09/27/2018).

[44] Johann Albert Eytelwein. *Handbuch der Statik fester Körper: mit vorzüglicher Rücksicht auf ihre Anwendung in der Architektur*. Google-Books-ID: i9ZZAAAAcAAJ. Reimer, 1832. 528 pp.

[45] Dario Farina, Marco Gazzoni, and Roberto Merletti. "Assessment of low back muscle fatigue by surface EMG signal analysis: methodological aspects". In: *Journal of Electromyography and Kinesiology*. Muscle function and dysfunctional in the spine 13.4 (Aug. 1, 2003), pp. 319–332. ISSN: 1050-6411. DOI: 10.1016/S1050-6411(03)00040-3. URL: http://www.sciencedirect.com/science/article/pii/S1050641103000403.

[46] SA Ferguson and WS Marras. "A literature review of low back disorder surveillance measures and risk factors". In: *Clinical Biomechanics* 12.4 (June 1, 1997), pp. 211–226. ISSN: 0268-0033. DOI: 10.1016/S0268-0033(96)00073-3. URL: http://www.sciencedirect.com/science/article/pii/S0268003396000733 (visited on 09/22/2016).

[47] DANIEL P. FERRIS, GREGORY S. SAWICKI, and MONICA A. DALEY. "A PHYSIOLOGIST'S PERSPECTIVE ON ROBOTIC EXOSKELETONS FOR HUMAN LOCOMOTION". In: *International journal of HR : humanoid robotics* 4.3 (Sept. 2007), pp. 507–528. ISSN: 0219-8436. DOI: 10.1142/S0219843607001138. URL: https://www.ncbi.nlm.nih.gov/pmc/articles/PMC2185037/ (visited on 02/21/2020).

[48] Daniel P. Ferris, Bryan R. Schlink, and Aaron J. Young. "Robotics: Exoskeletons". In: *Encyclopedia of Biomedical Engineering*. Ed. by Roger Narayan. Oxford: Elsevier, 2019, pp. 645–651. ISBN: 978-0-12-805144-3. DOI: 10.1016/B978-0-12-801238-3.99906-9. URL: http://www.sciencedirect.com/science/article/pii/B9780128012383999069 (visited on 02/21/2020).

[49] Gene S Fisch. "Evaluating data from behavioral analysis: visual inspection or statistical models?" In: *Behavioural Processes* 54.1 (May 3, 2001), pp. 137–154. ISSN: 0376-6357. DOI: 10.1016/S0376-6357(01)00155-3. URL: http://www.sciencedirect.com/science/article/pii/S0376635701001553 (visited on 12/04/2019).

[50] Aaron J. Fisher, John D. Medaglia, and Bertus F. Jeronimus. "Lack of group-to-individual generalizability is a threat to human subjects research". In: *Proceedings of the National Academy of Sciences* (June 18, 2018), p. 201711978. ISSN: 0027-8424, 1091-6490. DOI: 10.1073/pnas.1711978115. URL: http://www.pnas.org/content/early/2018/06/15/1711978115 (visited on 06/20/2018).

[51] Laetitia Fradet et al. "Biomechanical analysis of ramp ambulation of transtibial amputees with an adaptive ankle foot system". In: *Gait & Posture* 32.2 (June 2010), pp. 191–198. ISSN: 0966-6362. DOI: 10.1016/j.gaitpost.2010.04.011. URL: http://www.sciencedirect.com/science/article/pii/S0966636210001177 (visited on 05/25/2016).

[52] Jason R. Franz and Rodger Kram. "The effects of grade and speed on leg muscle activations during walking". In: *Gait & Posture* 35.1 (Jan. 1, 2012), pp. 143–147. ISSN: 0966-6362. DOI: 10.1016/j.gaitpost.2011.08.025. URL: http://www.sciencedirect.com/science/article/pii/S0966636211002827 (visited on 05/17/2018).

[53] Freburger JK et al. "The rising prevalence of chronic low back pain". In: *Archives of Internal Medicine* 169.3 (Feb. 9, 2009), pp. 251–258. ISSN: 0003-9926. DOI: 10.1001/

archinternmed.2008.543. URL: http://dx.doi.org/10.1001/archinternmed.2008.543 (visited on 07/17/2016).

[54] David M. Frost, Mohammad Abdoli-E, and Joan M. Stevenson. "PLAD (personal lift assistive device) stiffness affects the lumbar flexion/extension moment and the posterior chain EMG during symmetrical lifting tasks". In: *Journal of Electromyography and Kinesiology* 19.6 (Dec. 1, 2009), e403–e412. ISSN: 1050-6411. DOI: 10.1016/j.jelekin.2008.12.002. URL: http://www.sciencedirect.com/science/article/pii/S1050641108002034 (visited on 05/25/2018).

[55] Denis Gagnon and Micheline Gagnon. "The influence of dynamic factors on triaxial net muscular moments at the L5S1 joint during asymmetrical lifting and lowering". In: *Journal of Biomechanics* 25.8 (Aug. 1, 1992), pp. 891–901. ISSN: 0021-9290. DOI: 10.1016/0021-9290(92)90229-T. URL: http://www.sciencedirect.com/science/article/pii/002192909290229T (visited on 08/05/2020).

[56] Robert S. Gailey et al. "The Amputee Mobility Predictor: An instrument to assess determinants of the lower-limb amputee's ability to ambulate". In: *Archives of Physical Medicine and Rehabilitation* 83.5 (May 1, 2002), pp. 613–627. ISSN: 0003-9993, 1532-821X. DOI: 10.1053/apmr.2002.32309. URL: https://www.archives-pmr.org/article/S0003-9993(02)47460-6/abstract (visited on 01/09/2019).

[57] Jack Geissinger et al. "Quantification of Postures for Low-Height Object Manipulation Conducted by Manual Material Handlers in a Retail Environment". In: *IISE transactions on occupational ergonomics and human factors* (July 21, 2020), pp. 1–11. ISSN: 2472-5846. DOI: 10.1080/24725838.2020.1793825.

[58] Claire C. Gordon et al. *2012 Anthropometric Survey of U.S. Army Pilot Personnel: Methods and Summary Statistics*. NATICK/TR-16/013. ARMY NATICK SOLDIER RESEARCH DEVELOPMENT AND ENGINEERING CENTER MA, May 2016. URL: https://apps.dtic.mil/docs/citations/ADA634277 (visited on 04/27/2020).

[59] S. J. Gordon et al. “Mechanism of disc rupture. A preliminary report”. In: *Spine* 16.4 (Apr. 1991), pp. 450–456. ISSN: 0362-2436.

[60] Ryan B. Graham, Michael J. Agnew, and Joan M. Stevenson. “Effectiveness of an on-body lifting aid at reducing low back physical demands during an automotive assembly task: Assessment of EMG response and user acceptability”. In: *Applied Ergonomics* 40.5 (Sept. 1, 2009), pp. 936–942. ISSN: 0003-6870. DOI: 10.1016/j.apergo.2009.01.006. URL: http://www.sciencedirect.com/science/article/pii/S0003687009000118 (visited on 08/17/2020).

[61] Kevin P. Granata and W. S. Marras. “The Influence of Trunk Muscle Coactivity on Dynamic Spinal Loads”. In: *Spine* 20.8 (Apr. 1995), pp. 913–919. ISSN: 0362-2436.

[62] Jianglong Guo et al. “Electroactive textile actuators for wearable and soft robots”. In: *2018 IEEE International Conference on Soft Robotics (RoboSoft)*. 2018 IEEE International Conference on Soft Robotics (RoboSoft). Apr. 2018, pp. 339–343. DOI: 10.1109/ROBOSOFT.2018.8404942.

[63] Andrew H. Hansen, Dudley S. Childress, and Steve C. Miff. “Roll-over characteristics of human walking on inclined surfaces”. In: *Human Movement Science* 23.6 (Dec. 1, 2004), pp. 807–821. ISSN: 0167-9457. DOI: 10.1016/j.humov.2004.08.023. URL: http://www.sciencedirect.com/science/article/pii/S0167945704000661.

[64] Andrew H. Hansen et al. “The human ankle during walking: implications for design of biomimetic ankle prostheses”. In: *Journal of Biomechanics* 37.10 (Oct. 2004), pp. 1467–1474. ISSN: 0021-9290. DOI: 10.1016/j.jbiomech.2004.01.017. URL: http://www.sciencedirect.com/science/article/pii/S0021929004000478 (visited on 11/20/2015).

[65] T. H. Hansson, T. S. Keller, and D. M. Spengler. “Mechanical behavior of the human lumbar spine. II. Fatigue strength during dynamic compressive loading”. In: *Journal of Orthopaedic Research* 5.4 (Jan. 1, 1987), pp. 479–487. ISSN: 1554-527X.

DOI: 10.1002/jor.1100050403. URL: http://onlinelibrary.wiley.com/doi/10.1002/jor.1100050403/abstract (visited on 11/22/2016).

[66] H. Hara and Y. Sankai. "HAL equipped with passive mechanism". In: *2012 IEEE/SICE International Symposium on System Integration (SII)*. 2012 IEEE/SICE International Symposium on System Integration (SII). Dec. 2012, pp. 1–6. DOI: 10.1109/SII.2012.6427323.

[67] Florian L. Haufe et al. "Biomechanical effects of passive hip springs during walking". In: *Journal of Biomechanics* 98 (Jan. 2, 2020), p. 109432. ISSN: 0021-9290. DOI: 10.1016/j.jbiomech.2019.109432. URL: http://www.sciencedirect.com/science/article/pii/S0021929019306797 (visited on 08/17/2020).

[68] Hans Heneweer et al. "Physical activity and low back pain: a systematic review of recent literature". In: *European Spine Journal* 20.6 (June 1, 2011), pp. 826–845. ISSN: 0940-6719, 1432-0932. DOI: 10.1007/s00586-010-1680-7. URL: https://link.springer.com/article/10.1007/s00586-010-1680-7 (visited on 06/28/2017).

[69] HJ eds. HERMENS. "European Recommendations for Surface Electromyography". In: *Results of the SENIAM (Surface EMG for Noninvasive Assessment of Muscles) Project* (1999). URL: https://ci.nii.ac.jp/naid/10016394449/ (visited on 11/14/2018).

[70] Ronan Hinchet and Herbert Shea. "High Force Density Textile Electrostatic Clutch". In: *Advanced Materials Technologies* 5.4 (2020). _eprint: https://onlinelibrary.wiley.com/doi/pdf/ p. 1900895. ISSN: 2365-709X. DOI: 10.1002/admt.201900895. URL: http://onlinelibrary.wiley.com/doi/abs/10.1002/admt.201900895 (visited on 08/17/2020).

[71] Damian Hoy et al. "Measuring the global burden of low back pain". In: *Best Practice & Research Clinical Rheumatology*. Back Pain and Non-Inflammatory Spinal Disorders 24.2 (Apr. 2010), pp. 155–165. ISSN: 1521-6942. DOI: 10.1016/j.berh.2009.11.

002. URL: http://www.sciencedirect.com/science/article/pii/S1521694209001259 (visited on 08/16/2016).

[72] Ling Hui et al. "Evaluation of physiological work demands and low back neuromuscular fatigue on nurses working in geriatric wards". In: *Applied Ergonomics* 32.5 (Oct. 1, 2001), pp. 479–483. ISSN: 0003-6870. DOI: 10.1016/S0003-6870(01)00025-4. URL: http://www.sciencedirect.com/science/article/pii/S0003687001000254 (visited on 11/14/2018).

[73] Kirsten Huysamen, Valerie Power, and Leonard O'Sullivan. "Elongation of the surface of the spine during lifting and lowering, and implications for design of an upper body industrial exoskeleton". In: *Applied Ergonomics* 72 (Oct. 1, 2018), pp. 10–16. ISSN: 0003-6870. DOI: 10.1016/j.apergo.2018.04.011. URL: http://www.sciencedirect.com/science/article/pii/S0003687018300978 (visited on 11/14/2018).

[74] Y. Imamura et al. "Motion-based design of elastic belts for passive assistive device using musculoskeletal model". In: *2011 IEEE International Conference on Robotics and Biomimetics*. 2011 IEEE International Conference on Robotics and Biomimetics. 2011, pp. 1343–1348. DOI: 10.1109/ROBIO.2011.6181475.

[75] Roger P. Jackson et al. "Compensatory Spinopelvic Balance Over the Hip Axis and Better Reliability in Measuring Lordosis to the Pelvic Radius on Standing Lateral Radiographs of Adult Volunteers and Patients". In: *Spine* 23.16 (Aug. 15, 1998), p. 1750. ISSN: 0362-2436. URL: https://journals.lww.com/spinejournal/Fulltext/1998/08150/Compensatory_Spinopelvic_Balance_Over_the_Hip_Axis.8.aspx?casa_token=lCBG3gVooEcAAAAA:2b_Fg-wNZuuZXHzubQatMqDxScWzJa8VFbqbUp4HRTo-hxYH8yVm-bP_V4wNrmyLgfkKnc9kkUx-gTAf_iVRo (visited on 12/18/2019).

[76] Jeffrey N. Katz. "Lumbar Disc Disorders and Low-Back Pain: Socioeconomic Factors and Consequences". In: *J Bone Joint Surg Am* 88 (suppl 2 Apr. 1, 2006), pp. 21–

24. ISSN: 0021-9355, 1535-1386. DOI: 10.2106/JBJS.E.01273. URL: http://jbjs.org/content/88/suppl_2/21 (visited on 07/17/2016).

[77] Florence Peterson Kendall et al. *Muscles: Testing and Function, with Posture and Pain*. Fifth, North American edition. Baltimore, MD: LWW, Mar. 4, 2005. 560 pp. ISBN: 978-0-7817-4780-6.

[78] Wayne Koniuk. "Self-adjusting prosthetic ankle apparatus". U.S. pat. 6443993B1. Conexant Inc. Sept. 3, 2002. URL: https://patents.google.com/patent/US6443993B1/en (visited on 09/24/2018).

[79] Judith I. Kuiper et al. "Epidemiologic evidence on manual materials handling as a risk factor for back disorders:a systematic review". In: *International Journal of Industrial Ergonomics* 24.4 (Aug. 23, 1999), pp. 389–404. ISSN: 0169-8141. DOI: 10.1016/S0169-8141(99)00006-2. URL: http://www.sciencedirect.com/science/article/pii/S0169814199000062 (visited on 11/15/2018).

[80] S. Kumar. "Cumulative load as a risk factor for back pain". In: *Spine* 15.12 (Dec. 1990), pp. 1311–1316. ISSN: 0362-2436.

[81] M. Kuster, S. Sakurai, and G. A. Wood. "Kinematic and kinetic comparison of downhill and level walking". In: *Clinical Biomechanics* 10.2 (Mar. 1, 1995), pp. 79–84. ISSN: 0268-0033, 1879-1271. DOI: 10.1016/0268-0033(95)92043-L. URL: https://www.clinbiomech.com/article/0268-0033(95)92043-L/abstract (visited on 04/30/2018).

[82] Erik P. Lamers, Aaron J. Yang, and Karl E. Zelik. "Feasibility of a Biomechanically-Assistive Garment to Reduce Low Back Loading During Leaning and Lifting". In: *IEEE Transactions on Biomedical Engineering* 65.8 (Aug. 2018). Conference Name: IEEE Transactions on Biomedical Engineering, pp. 1674–1680. ISSN: 1558-2531. DOI: 10.1109/TBME.2017.2761455.

[83] Erik P. Lamers et al. “Low-Profile Elastic Exosuit Reduces Back Muscle Fatigue”. In: *Scientific Reports* (2020). DOI: InPress.

[84] Erik P Lamers, Aaron J Yang, and Karl E Zelik. “Biomechanically-Assistive Garment Offloads Low Back During Leaning and Lifting”. In: International Society of Biomechanics. Brisbane, Austrailia, 2017.

[85] Ute Latza et al. “Cohort study of occupational risk factors of low back pain in construction workers”. In: *Occupational and Environmental Medicine* 57.1 (Jan. 1, 2000), pp. 28–34. ISSN: 1351-0711, 1470-7926. DOI: 10.1136/oem.57.1.28. URL: https://oem.bmj.com/content/57/1/28 (visited on 11/15/2018).

[86] Andrea N. Lay, Chris J. Hass, and Robert J. Gregor. “The effects of sloped surfaces on locomotion: A kinematic and kinetic analysis”. In: *Journal of Biomechanics* 39.9 (Jan. 1, 2006), pp. 1621–1628. ISSN: 0021-9290, 1873-2380. DOI: 10.1016/j.jbiomech.2005.05.005. URL: https://www.jbiomech.com/article/S0021-9290(05)00215-0/abstract (visited on 04/30/2018).

[87] Alain Leroux, Joyce Fung, and H. Barbeau. “Adaptation of the walking pattern to uphill walking in normal and spinal-cord injured subjects”. In: *Experimental Brain Research* 126.3 (May 1, 1999), pp. 359–368. ISSN: 0014-4819, 1432-1106. DOI: 10.1007/s002210050743. URL: http://link.springer.com/article/10.1007/s002210050743 (visited on 05/01/2018).

[88] Paolo de Leva. “Adjustments to Zatsiorsky-Seluyanov’s segment inertia parameters”. In: *Journal of Biomechanics* 29.9 (Sept. 1996), pp. 1223–1230. ISSN: 0021-9290. DOI: 10.1016/0021-9290(95)00178-6. URL: http://www.sciencedirect.com/science/article/pii/0021929095001786 (visited on 04/26/2016).

[89] Michiel P. de Looze et al. “Exoskeletons for industrial application and their potential effects on physical work load”. In: *Ergonomics* 59.5 (May 3, 2016), pp. 671–681. ISSN: 0014-0139, 1366-5847. DOI: 10.1080/00140139.2015.1081988. URL: https:

//www.tandfonline.com/doi/full/10.1080/00140139.2015.1081988 (visited on 05/30/2018).

[90] Christy A. Lotz et al. "The effect of an on-body personal lift assist device (PLAD) on fatigue during a repetitive lifting task". In: *Journal of Electromyography and Kinesiology* 19.2 (Apr. 2009), pp. 331–340. ISSN: 1050-6411. DOI: 10.1016/j.jelekin.2007.08.006. URL: http://www.sciencedirect.com/science/article/pii/S1050641107001447 (visited on 05/10/2016).

[91] Brian D. Lowe, William G. Billotte, and Donald R. Peterson. "ASTM F48 Formation and Standards for Industrial Exoskeletons and Exosuits". In: *IISE Transactions on Occupational Ergonomics and Human Factors* 7.3 (Oct. 2, 2019). Publisher: Taylor & Francis _eprint: https://doi.org/10.1080/24725838.2019.1579769, pp. 230–236. ISSN: 2472-5838. DOI: 10.1080/24725838.2019.1579769. URL: https://doi.org/10.1080/24725838.2019.1579769 (visited on 02/27/2020).

[92] Z. Luo and Y. Yu. "Wearable stooping-assist device in reducing risk of low back disorders during stooped work". In: *2013 IEEE International Conference on Mechatronics and Automation*. 2013 IEEE International Conference on Mechatronics and Automation. Aug. 2013, pp. 230–236. DOI: 10.1109/ICMA.2013.6617923.

[93] Anne F. Mannion and Patricia Dolan. "Electromyographic Median Frequency Changes During Isometric Contraction of the Back Extensors to Fatigue". In: *Spine* 19.11 (June 1994), pp. 1223–1229. ISSN: 0362-2436.

[94] Anne F. Mannion et al. "The use of surface EMG power spectral analysis in the evaluation of back muscle function". In: *Journal of Rehabilitation Research and Development; Washington* 34.4 (Oct. 1997), pp. 427–39. ISSN: 07487711. URL: https://search.proquest.com/docview/215294830/abstract/C678393E03424440PQ/1 (visited on 02/15/2018).

[95] William S. Marras and Carolyn M. Sommerich. "A Three-Dimensional Motion Model of Loads on the Lumbar Spine: I. Model Structure". In: *Human Factors: The Journal of the Human Factors and Ergonomics Society* 33.2 (Apr. 1, 1991), pp. 123–137. ISSN: 0018-7208, 1547-8181. DOI: 10.1177/001872089103300201. URL: http://hfs.sagepub.com/content/33/2/123 (visited on 06/08/2016).

[96] Brook I. Martin et al. "Expenditures and Health Status Among Adults With Back and Neck Problems". In: *JAMA* 299.6 (Feb. 13, 2008), pp. 656–664. ISSN: 0098-7484. DOI: 10.1001/jama.299.6.656. URL: http://jamanetwork.com/journals/jama/fullarticle/181453 (visited on 08/04/2017).

[97] H. Matsui et al. "Risk indicators of low back pain among workers in Japan. Association of familial and physical factors with low back pain". In: *Spine* 22.11 (June 1, 1997), 1242–1247, discussion 1248. ISSN: 0362-2436.

[98] S. M. McGill and R. W. Norman. "Partitioning of the L4-L5 dynamic moment into disc, ligamentous, and muscular components during lifting". In: *Spine* 11.7 (Sept. 1986), pp. 666–678. ISSN: 0362-2436.

[99] S. M. McGill and R. W. Norman. "Potential of lumbodorsal fascia forces to generate back extension moments during squat lifts". In: *Journal of Biomedical Engineering* 10.4 (July 1, 1988), pp. 312–318. ISSN: 0141-5425. DOI: 10.1016/0141-5425(88)90060-X. URL: http://www.sciencedirect.com/science/article/pii/014154258890060X (visited on 06/09/2016).

[100] Andrew Stuart McIntosh et al. "Gait dynamics on an inclined walkway". In: *Journal of Biomechanics* 39.13 (2006), pp. 2491–2502. ISSN: 0021-9290. DOI: 10.1016/j.jbiomech.2005.07.025. URL: http://www.sciencedirect.com/science/article/pii/S0021929005003659 (visited on 11/17/2015).

[101] R. Merletti, M. Knaflitz, and C. J. De Luca. "Myoelectric manifestations of fatigue in voluntary and electrically elicited contractions". In: *Journal of Applied Physiology*

69.5 (Nov. 1, 1990), pp. 1810–1820. ISSN: 8750-7587, 1522-1601. URL: http://jap.physiology.org.proxy.library.vanderbilt.edu/content/69/5/1810 (visited on 12/01/2017).

[102] A. L. Nachemson. "Disc pressure measurements". In: *Spine* 6.1 (Feb. 1981), pp. 93–97. ISSN: 0362-2436.

[103] Antoni V. F. Nargol et al. "Factors in the Reproducibility of Electromyographic Power Spectrum Analysis of Lumbar Paraspinal Muscle Fatigue". In: *Spine* 24.9 (May 1, 1999), p. 883. ISSN: 0362-2436. URL: https://journals.lww.com/spinejournal/Abstract/1999/05010/Factors_in_the_Reproducibility_of.9.aspx (visited on 02/16/2018).

[104] K. Naruse et al. "Development of wearable exoskeleton power assist system for lower back support". In: *Proceedings 2003 IEEE/RSJ International Conference on Intelligent Robots and Systems (IROS 2003) (Cat. No.03CH37453)*. Proceedings 2003 IEEE/RSJ International Conference on Intelligent Robots and Systems (IROS 2003) (Cat. No.03CH37453). Vol. 4. Oct. 2003, 3630–3635 vol.3. DOI: 10.1109/IROS.2003.1249719.

[105] Randy MA Neblett et al. "Quantifying the Lumbar Flexion-Relaxation Phenomenon: Theory, Normative Data, and Clinical Applications". In: *Spine* 28.13 (July 2003), pp. 1435–1446. ISSN: 0362-2436.

[106] GUNNAR Nemeth and HANS Ohlsen. "Moment Arm Lengths of Trunk Muscles to the Lumbosacral Joint Obtained In Vivo with Computed Tomography". In: *Spine* 11.2 (Mar. 1986), pp. 158–160. ISSN: 0362-2436.

[107] Paul T. Nenno and Eric D. Wetzel. "Design and properties of a rate-dependent 'dynamic ligament' containing shear thickening fluid". In: *Smart Materials and Structures* 23.12 (Oct. 2014). Publisher: IOP Publishing, p. 125019. ISSN: 0964-1726. DOI: 10.1088/0964-1726/23/12/125019. URL: https://doi.org/10.1088%2F0964-1726%2F23%2F12%2F125019 (visited on 08/18/2020).

[108] L. I. Oddsson et al. "Development of new protocols and analysis procedures for the assessment of LBP by surface EMG techniques". In: *Journal of Rehabilitation Research and Development* 34.4 (Oct. 1997), pp. 415–426. ISSN: 0748-7711.

[109] Junfeng Peng et al. "Methods for determining hip and lumbosacral joint centers in a seated position from external anatomical landmarks". In: *Journal of Biomechanics* 48.2 (Jan. 21, 2015), pp. 396–400. ISSN: 0021-9290. DOI: 10.1016/j.jbiomech.2014.11.040. URL: http://www.sciencedirect.com/science/article/pii/S0021929014006290 (visited on 07/16/2020).

[110] Ornella Pinzone, Michael H. Schwartz, and Richard Baker. "Comprehensive non-dimensional normalization of gait data". In: *Gait & Posture* 44 (Supplement C Feb. 1, 2016), pp. 68–73. ISSN: 0966-6362. DOI: 10.1016/j.gaitpost.2015.11.013. URL: http://www.sciencedirect.com/science/article/pii/S0966636215009625.

[111] José L. Pons. *Wearable Robots: Biomechatronic Exoskeletons*. Google-Books-ID: ovCk-TEKEmkkC. John Wiley & Sons, Apr. 15, 2008. 361 pp. ISBN: 978-0-470-98765-0.

[112] E. R. Post et al. "E-broidery: Design and fabrication of textile-based computing". In: *IBM Systems Journal; Armonk* 39.3 (2000). Num Pages: 21 Place: Armonk, United States, Armonk Publisher: International Business Machines Corporation, pp. 840–860. ISSN: 00188670. URL: http://search.proquest.com/docview/222414501/abstract/570DC42A118F4F6CPQ/1 (visited on 08/18/2020).

[113] J. R. Potvin, S. M. McGill, and R. W. Norman. "Trunk muscle and lumbar ligament contributions to dynamic lifts with varying degrees of trunk flexion". In: *Spine* 16.9 (Sept. 1991), pp. 1099–1107. ISSN: 0362-2436.

[114] J. R. Potvin and R. W. Norman. "Quantification of erector spinae muscle fatigue during prolonged, dynamic lifting tasks". In: *European Journal of Applied Physiology and Occupational Physiology* 67.6 (Dec. 1, 1993), pp. 554–562. ISSN: 0301-5548, 1439-

6327. DOI: 10.1007/BF00241654. URL: https://link.springer.com/article/10.1007/BF00241654 (visited on 08/28/2017).

[115] J. R. Potvin and P. R. O'Brien. "Trunk muscle co-contraction increases during fatiguing, isometric, lateral bend exertions. Possible implications for spine stability". In: *Spine* 23.7 (Apr. 1, 1998), 774–780, discussion 781. ISSN: 0362-2436.

[116] Mohamad Amin Pourhoseingholi, Ahmad Reza Baghestani, and Mohsen Vahedi. "How to control confounding effects by statistical analysis". In: *Gastroenterology and Hepatology From Bed to Bench* 5.2 (2012), pp. 79–83. ISSN: 2008-2258. URL: https://www.ncbi.nlm.nih.gov/pmc/articles/PMC4017459/ (visited on 01/03/2019).

[117] Laura Punnett et al. "Back disorders and nonneutral trunk postures of automobile assembly workers". In: *Scandinavian Journal of Work, Environment & Health* 17.5 (1991), pp. 337–346. ISSN: 0355-3140. URL: https://www.jstor.org/stable/40965914 (visited on 10/24/2018).

[118] Brendan Quinlivan et al. "Force Transfer Characterization of a Soft Exosuit for Gait Assistance". In: (Aug. 2, 2015), V05AT08A049. DOI: 10.1115/DETC2015-47871. URL: http://dx.doi.org/10.1115/DETC2015-47871 (visited on 10/25/2018).

[119] Ronald Rosenburg and Helmut Seidel. "Electromyography of lumbar erector spinae muscles — influence of posture, interelectrode distance, strength, and fatigue". In: *European Journal of Applied Physiology and Occupational Physiology* 59.1 (Sept. 1, 1989), pp. 104–114. ISSN: 0301-5548, 1439-6327. DOI: 10.1007/BF02396587. URL: https://link.springer.com/article/10.1007/BF02396587 (visited on 03/08/2018).

[120] SERGE H. MS Roy, CARLO J. De Luca, and DAVID A. MS Casavant. "Lumbar Muscle Fatigue and Chronic Lower Back Pain". In: *Spine* 14.9 (Sept. 1989), pp. 992–1001. ISSN: 0362-2436.

[121] Mark S. Redfern and James DiPasquale. "Biomechanics of descending ramps". In: *Gait & Posture* 6.2 (Oct. 1997), pp. 119–125. ISSN: 0966-6362. DOI: 10.1016/S0966-

6362(97)01117-X. URL: http://www.sciencedirect.com/science/article/pii/S096663629701117X (visited on 02/13/2016).

[122] David J Sanderson and Philip E Martin. "Lower extremity kinematic and kinetic adaptations in unilateral below-knee amputees during walking". In: *Gait & Posture* 6.2 (Oct. 1, 1997), pp. 126–136. ISSN: 0966-6362. DOI: 10.1016/S0966-6362(97)01112-0. URL: http://www.sciencedirect.com/science/article/pii/S0966636297011120 (visited on 03/11/2019).

[123] H. Schechtman and D. L. Bader. "Fatigue damage of human tendons". In: *Journal of Biomechanics* 35.3 (Mar. 2002), pp. 347–353. ISSN: 0021-9290. DOI: 10.1016/S0021-9290(01)00177-4. URL: http://www.sciencedirect.com/science/article/pii/S0021929001001774 (visited on 11/23/2016).

[124] A. Schultz et al. "Loads on the lumbar spine. Validation of a biomechanical analysis by measurements of intradiscal pressures and myoelectric signals." In: *J Bone Joint Surg Am* 64.5 (June 1, 1982), pp. 713–720. ISSN: 0021-9355, 1535-1386. URL: http://jbjs.org/content/64/5/713 (visited on 06/08/2016).

[125] Helmut Seidel, Helga Beyer, and Dieter Bräuer. "Electromyographic evaluation of back muscle fatigue with repeated sustained contractions of different strengths". In: *European Journal of Applied Physiology and Occupational Physiology* 56.5 (Sept. 1, 1987), pp. 592–602. ISSN: 1439-6327. DOI: 10.1007/BF00635375. URL: https://doi.org/10.1007/BF00635375 (visited on 11/28/2018).

[126] Max K. Shepherd and Elliott J. Rouse. "The VSPA Foot: A Quasi-Passive Ankle-Foot Prosthesis With Continuously Variable Stiffness". In: *IEEE Transactions on Neural Systems and Rehabilitation Engineering* 25.12 (Dec. 2017). Conference Name: IEEE Transactions on Neural Systems and Rehabilitation Engineering, pp. 2375–2386. ISSN: 1558-0210. DOI: 10.1109/TNSRE.2017.2750113.

[127] Max K. Shepherd et al. "Amputee perception of prosthetic ankle stiffness during locomotion". In: *Journal of NeuroEngineering and Rehabilitation* 15.1 (Nov. 8, 2018), p. 99. ISSN: 1743-0003. DOI: 10.1186/s12984-018-0432-5. URL: https://doi.org/10.1186/s12984-018-0432-5 (visited on 02/22/2019).

[128] A. H. Shultz and M. Goldfarb. "A Unified Controller for Walking on Even and Uneven Terrain With a Powered Ankle Prosthesis". In: *IEEE Transactions on Neural Systems and Rehabilitation Engineering* 26.4 (Apr. 2018), pp. 788–797. ISSN: 1534-4320. DOI: 10.1109/TNSRE.2018.2810165.

[129] J. Smedley et al. "Manual handling activities and risk of low back pain in nurses." In: *Occupational and Environmental Medicine* 52.3 (Mar. 1, 1995), pp. 160–163. ISSN: , 1470-7926. DOI: 10.1136/oem.52.3.160. URL: http://oem.bmj.com/content/52/3/160 (visited on 09/22/2016).

[130] A. Soueid et al. "The pain of surgery: Pain experienced by surgeons while operating". In: *International Journal of Surgery* 8.2 (Jan. 1, 2010), pp. 118–120. ISSN: 1743-9191. DOI: 10.1016/j.ijsu.2009.11.008. URL: http://www.sciencedirect.com/science/article/pii/S1743919109001708 (visited on 11/16/2018).

[131] Walter F. Stewart et al. "Lost Productive Work Time Costs From Health Conditions in the United States: Results From the American Productivity Audit". In: *Journal of Occupational* 45.12 (Dec. 2003), pp. 1234–1246. ISSN: 1076-2752.

[132] Simo Taimela, Markku Kankaanpaa, and Satu Luoto. "The Effect of Lumbar Fatigue on the Ability to Sense a Change in Lumbar Position: A Controlled Study. [Miscellaneous Article]". In: *Spine* 24.13 (July 1999). ISSN: 0362-2436.

[133] Kota Z. Takahashi, Thomas M. Kepple, and Steven J. Stanhope. "A unified deformable (UD) segment model for quantifying total power of anatomical and prosthetic below-knee structures during stance in gait". In: *Journal of Biomechanics* 45.15 (Oct. 11, 2012), pp. 2662–2667. ISSN: 0021-9290. DOI: 10.1016/j.jbiomech.2012.

08.017. URL: http://www.sciencedirect.com/science/article/pii/S0021929012004630 (visited on 07/21/2015).

[134] Takayuki Tanaka et al. "Smart Suit: Soft power suit with semi-active assist mechanism - prototype for supporting waist and knee joint -". In: *2008 International Conference on Control, Automation and Systems*. 2008 International Conference on Control, Automation and Systems. Oct. 2008, pp. 2002–2005. DOI: 10.1109/ICCAS.2008.4694428.

[135] S. Toxiri et al. "A wearable device for reducing spinal loads during lifting tasks: Biomechanics and design concepts". In: *2015 IEEE International Conference on Robotics and Biomimetics (ROBIO)*. 2015 IEEE International Conference on Robotics and Biomimetics (ROBIO). 2015, pp. 2295–2300. DOI: 10.1109/ROBIO.2015.7419116.

[136] Brent L. Ulrey and Fadi A. Fathallah. "Effect of a personal weight transfer device on muscle activities and joint flexions in the stooped posture". In: *Journal of Electromyography and Kinesiology* 23.1 (Feb. 2013), pp. 195–205. ISSN: 1050-6411. DOI: 10.1016/j.jelekin.2012.08.014. URL: http://www.sciencedirect.com/science/article/pii/S1050641112001502 (visited on 08/26/2016).

[137] BETHANY Valachi and KEITH Valachi. "Mechanisms leading to musculoskeletal disorders in dentistry". In: *The Journal of the American Dental Association* 134.10 (Oct. 1, 2003), pp. 1344–1350. ISSN: 0002-8177. DOI: 10.14219/jada.archive.2003.0048. URL: http://www.sciencedirect.com/science/article/pii/S0002817714651163 (visited on 11/16/2018).

[138] H. der Linde Van et al. "A systematic literature review of the effect of different prosthetic components on human functioning with a lower-limb prosthesis." In: *Journal of rehabilitation research and development* 41.4 (July 2004), pp. 555–570. ISSN: 0748-7711. URL: http://europepmc.org/abstract/med/15558384 (visited on 01/03/2019).

[139] J. Verbeek et al. “Manual material handling advice and assistive devices for preventing and treating back pain in workers: a Cochrane Systematic Review”. In: *Occupational and Environmental Medicine* 69.1 (Jan. 1, 2012). Publisher: BMJ Publishing Group Ltd Section: Cochrane corner, pp. 79–80. ISSN: 1351-0711, 1470-7926. DOI: 10.1136/oemed-2011-100214. URL: https://oem.bmj.com/content/69/1/79 (visited on 06/27/2020).

[140] Rino Versluys et al. “Prosthetic feet: State-of-the-art review and the importance of mimicking human ankle–foot biomechanics”. In: *Disability and Rehabilitation: Assistive Technology* 4.2 (Jan. 2009), pp. 65–75. ISSN: 1748-3107, 1748-3115. DOI: 10.1080/17483100802715092. URL: http://www.tandfonline.com/doi/full/10.1080/17483100802715092 (visited on 08/17/2020).

[141] Deborah R. Vickers et al. “Elderly unilateral transtibial amputee gait on an inclined walkway: A biomechanical analysis”. In: *Gait & Posture* 27.3 (Apr. 2008), pp. 518–529. ISSN: 0966-6362. DOI: 10.1016/j.gaitpost.2007.06.008. URL: http://www.sciencedirect.com/science/article/pii/S0966636207001701 (visited on 05/25/2016).

[142] Slavka Viteckova, Patrik Kutilek, and Marcel Jirina. “Wearable lower limb robotics: A review”. In: *Biocybernetics and Biomedical Engineering* 33.2 (Jan. 1, 2013), pp. 96–105. ISSN: 0208-5216. DOI: 10.1016/j.bbe.2013.03.005. URL: http://www.sciencedirect.com/science/article/pii/S0208521613000065 (visited on 02/27/2020).

[143] A. H. Vrieling et al. “Uphill and downhill walking in unilateral lower limb amputees”. In: *Gait & Posture* 28.2 (Aug. 2008), pp. 235–242. ISSN: 0966-6362. DOI: 10.1016/j.gaitpost.2007.12.006. URL: http://www.sciencedirect.com/science/article/pii/S0966636207003074 (visited on 11/16/2015).

[144] Conor James Walsh, Ken Endo, and Hugh Herr. “A QUASI-PASSIVE LEG EXOSKELETON FOR LOAD-CARRYING AUGMENTATION”. In: *International Jour-*

nal of Humanoid Robotics 04.3 (Sept. 2007), pp. 487–506. ISSN: 0219-8436, 1793-6942. DOI: 10.1142/S0219843607001126. URL: https://www.worldscientific.com/doi/abs/10.1142/S0219843607001126 (visited on 08/17/2020).

[145] James T. Wassell et al. "A Prospective Study of Back Belts for Prevention of Back Pain and Injury". In: *JAMA* 284.21 (Dec. 6, 2000). Publisher: American Medical Association, pp. 2727–2732. ISSN: 0098-7484. DOI: 10.1001/jama.284.21.2727. URL: http://jamanetwork.com/journals/jama/fullarticle/193330 (visited on 08/17/2020).

[146] Michael Wehner, David Rempel, and Homayoon Kazerooni. "Lower Extremity Exoskeleton Reduces Back Forces in Lifting". In: (Jan. 1, 2009), pp. 49–56. DOI: 10.1115/DSCC2009-2644. URL: http://dx.doi.org/10.1115/DSCC2009-2644 (visited on 01/14/2016).

[147] Tracey L. Weissgerber et al. "From Static to Interactive: Transforming Data Visualization to Improve Transparency". In: *PLOS Biology* 14.6 (June 22, 2016), e1002484. ISSN: 1545-7885. DOI: 10.1371/journal.pbio.1002484. URL: http://journals.plos.org/plosbiology/article?id=10.1371/journal.pbio.1002484 (visited on 08/22/2018).

[148] Tracey L. Weissgerber et al. "Transparent reporting for reproducible science". In: *Journal of Neuroscience Research* 94.10 (Oct. 1, 2016), pp. 859–864. ISSN: 1097-4547. DOI: 10.1002/jnr.23785. URL: https://onlinelibrary.wiley.com/doi/abs/10.1002/jnr.23785 (visited on 09/25/2018).

[149] Jamie Wolff et al. "A survey of stakeholder perspectives on exoskeleton technology". In: *Journal of NeuroEngineering and Rehabilitation* 11.1 (Dec. 19, 2014), p. 169. ISSN: 1743-0003. DOI: 10.1186/1743-0003-11-169. URL: https://doi.org/10.1186/1743-0003-11-169 (visited on 02/21/2020).

[150] Keijiro Yamamoto et al. “Development of Power Assisting Suit for Assisting Nurse Labor”. In: *JSME International Journal Series C Mechanical Systems, Machine Elements and Manufacturing* 45.3 (2002), pp. 703–711. DOI: 10.1299/jsmec.45.703.

[151] Matthew B. Yandell, Joshua R. Tacca, and Karl E. Zelik. “Design of a Low Profile, Unpowered Ankle Exoskeleton That Fits Under Clothes: Overcoming Practical Barriers to Widespread Societal Adoption”. In: *IEEE Transactions on Neural Systems and Rehabilitation Engineering* 27.4 (Apr. 2019). Conference Name: IEEE Transactions on Neural Systems and Rehabilitation Engineering, pp. 712–723. ISSN: 1558-0210. DOI: 10.1109/TNSRE.2019.2904924.

[152] Matthew B. Yandell and Karl E. Zelik. “Preferred Barefoot Step Frequency is Influenced by Factors Beyond Minimizing Metabolic Rate”. In: *Scientific Reports* 6 (Mar. 18, 2016), p. 23243. ISSN: 2045-2322. DOI: 10.1038/srep23243. URL: https://www.nature.com/articles/srep23243 (visited on 08/17/2018).

[153] Matthew B. Yandell et al. “Characterizing the comfort limits of forces applied to the shoulders, thigh and shank to inform exosuit design”. In: *PLOS ONE* 15.2 (Feb. 12, 2020), e0228536. ISSN: 1932-6203. DOI: 10.1371/journal.pone.0228536. URL: https://journals.plos.org/plosone/article?id=10.1371/journal.pone.0228536 (visited on 02/21/2020).

[154] Matthew B. Yandell et al. “Effect of A Back-Assist Exosuit on Logistics Worker Perceptions, Acceptance and Muscle Activity”. In: The International Symposium on Wearable Robotics. 2020.

[155] Matthew B. Yandell et al. “Physical interface dynamics alter how robotic exosuits augment human movement: implications for optimizing wearable assistive devices”. In: *Journal of NeuroEngineering and Rehabilitation* 14 (May 18, 2017), p. 40. ISSN: 1743-0003. DOI: 10.1186/s12984-017-0247-9. URL: https://doi.org/10.1186/s12984-017-0247-9.

[156] Aaron J. Young and Daniel P. Ferris. "State of the Art and Future Directions for Lower Limb Robotic Exoskeletons". In: *IEEE Transactions on Neural Systems and Rehabilitation Engineering* 25.2 (Feb. 2017), pp. 171–182. ISSN: 1558-0210. DOI: 10.1109/TNSRE.2016.2521160.

[157] Karl E. Zelik, J. S. Fine, and Anna Wolfe. "Bimodal Exosuit". U.S. pat. 63039869. Vanderbilt University. 2020.

[158] Karl E. Zelik and Eric C. Honert. "Ankle and foot power in gait analysis: Implications for science, technology and clinical assessment". In: *Journal of Biomechanics* 75 (June 25, 2018), pp. 1–12. ISSN: 0021-9290. DOI: 10.1016/j.jbiomech.2018.04.017. URL: http://www.sciencedirect.com/science/article/pii/S0021929018302902 (visited on 08/30/2018).

[159] Karl E. Zelik, Erik P. Lamers, and Keaton L. Scherpereel. "Moment arm extension system for exosuit". U.S. pat. 2020034999. Vanderbilt University. 2020.

[160] Karl E. Zelik, Matthew B. Yandell, and Dustin Howser. "Wearable exoskeleton for reducing low back loading and other applications". Pat. 62448102. 2017.

[161] Karl E. Zelik et al. "Coordination of intrinsic and extrinsic foot muscles during walking". In: *European Journal of Applied Physiology* 115.4 (Nov. 25, 2014), pp. 691–701. ISSN: 1439-6319, 1439-6327. DOI: 10.1007/s00421-014-3056-x. URL: http://link.springer.com/article/10.1007/s00421-014-3056-x (visited on 06/05/2015).

[162] Karl E. Zelik et al. "Systematic variation of prosthetic foot spring affects center-of-mass mechanics and metabolic cost during walking". In: *IEEE transactions on neural systems and rehabilitation engineering : a publication of the IEEE Engineering in Medicine and Biology Society* 19.4 (Aug. 2011), pp. 411–419. ISSN: 1534-4320. DOI: 10.1109/TNSRE.2011.2159018. URL: https://www.ncbi.nlm.nih.gov/pmc/articles/PMC4286327/ (visited on 08/28/2018).

[163] Haohan Zhang, Abhijit Kadrolkar, and IV Sup Frank C. "Design and Preliminary Evaluation of a Passive Spine Exoskeleton". In: *Journal of Medical Devices* 10.1 (Nov. 16, 2015), pp. 011002–011002–8. ISSN: 1932-6181. DOI: 10.1115/1.4031798. URL: http://dx.doi.org/10.1115/1.4031798 (visited on 03/03/2017).

[164] Ziqing Zhuang et al. "Biomechanical evaluation of assistive devices for transferring residents". In: *Applied Ergonomics* 30.4 (Aug. 1, 1999), pp. 285–294. ISSN: 0003-6870. DOI: 10.1016/S0003-6870(98)00035-0. URL: http://www.sciencedirect.com/science/article/pii/S0003687098000350 (visited on 11/05/2018).

[165] Kathryn Ziegler-Graham et al. "Estimating the Prevalence of Limb Loss in the United States: 2005 to 2050". In: *Archives of Physical Medicine and Rehabilitation* 89.3 (Mar. 1, 2008), pp. 422–429. ISSN: 0003-9993. DOI: 10.1016/j.apmr.2007.11.005. URL: http://www.sciencedirect.com/science/article/pii/S0003999307017480 (visited on 02/17/2020).

[166] A.B. Zoss, H. Kazerooni, and A. Chu. "Biomechanical design of the Berkeley lower extremity exoskeleton (BLEEX)". In: *IEEE/ASME Transactions on Mechatronics* 11.2 (Apr. 2006), pp. 128–138. ISSN: 1083-4435. DOI: 10.1109/TMECH.2006.871087. URL: http://ieeexplore.ieee.org/lpdocs/epic03/wrapper.htm?arnumber=1618670 (visited on 08/23/2016).

Appendix A

Chapter 3 Appendix

A.1 Subject-Specific Fatigue Results

This Appendix depicts MDF vs. time results for each individual subject. The decrease in median frequency (MDF) over the duration of leaning is fit by linear regression lines. The slope of the regression line (i.e., MDF slope) is commonly used as a measurement of the rate of muscle fatigue [31]. Data are plotted for each muscle and each trial condition; control trial A1 (black line, open black circles), intervention trial B (green line, shaded green circles), control trial A2 (gray line, open gray circles).

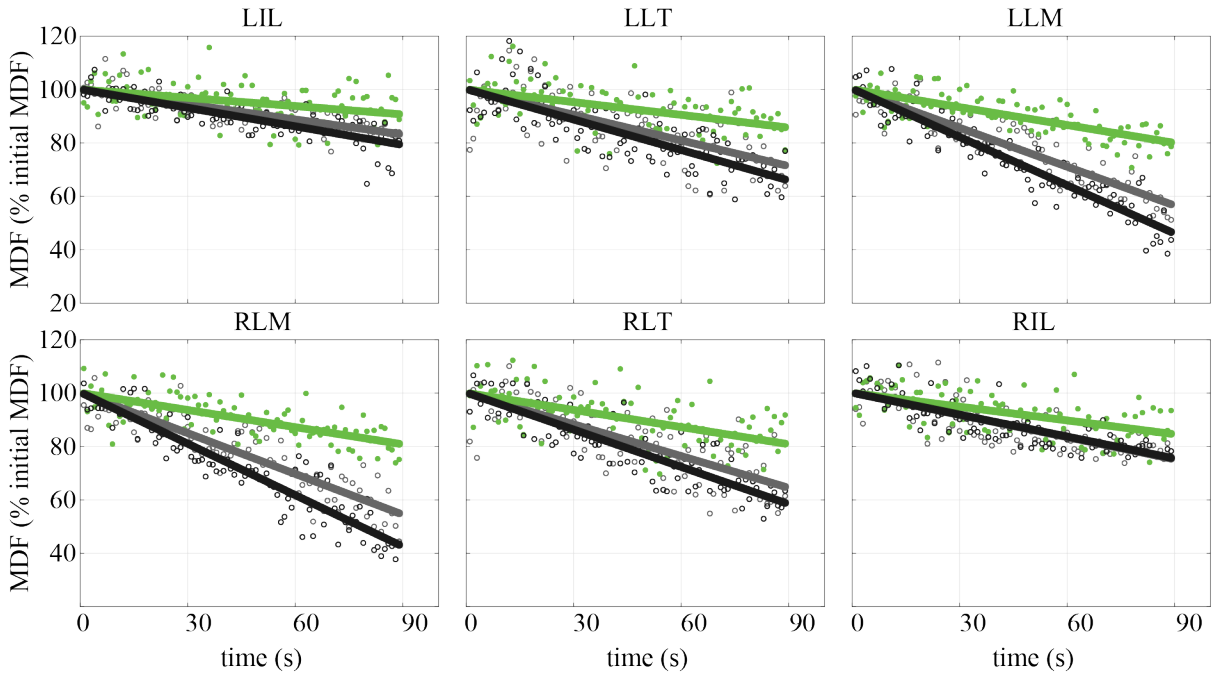

Figure A.1: Subject 1, individual muscle MDF vs. time. Figure layout is identical to **Figure 3.3** in the main text.

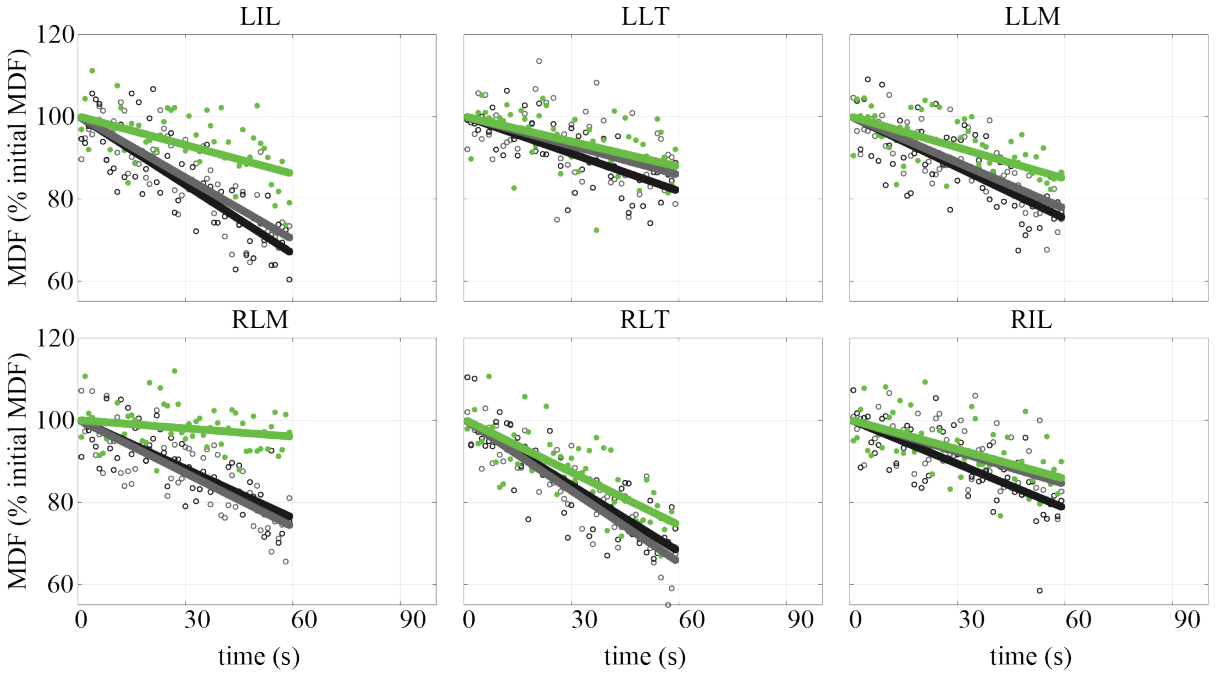

Figure A.2: Subject 2, individual muscle MDF vs. time. Figure layout is identical to **Figure 3.3** in the main text.

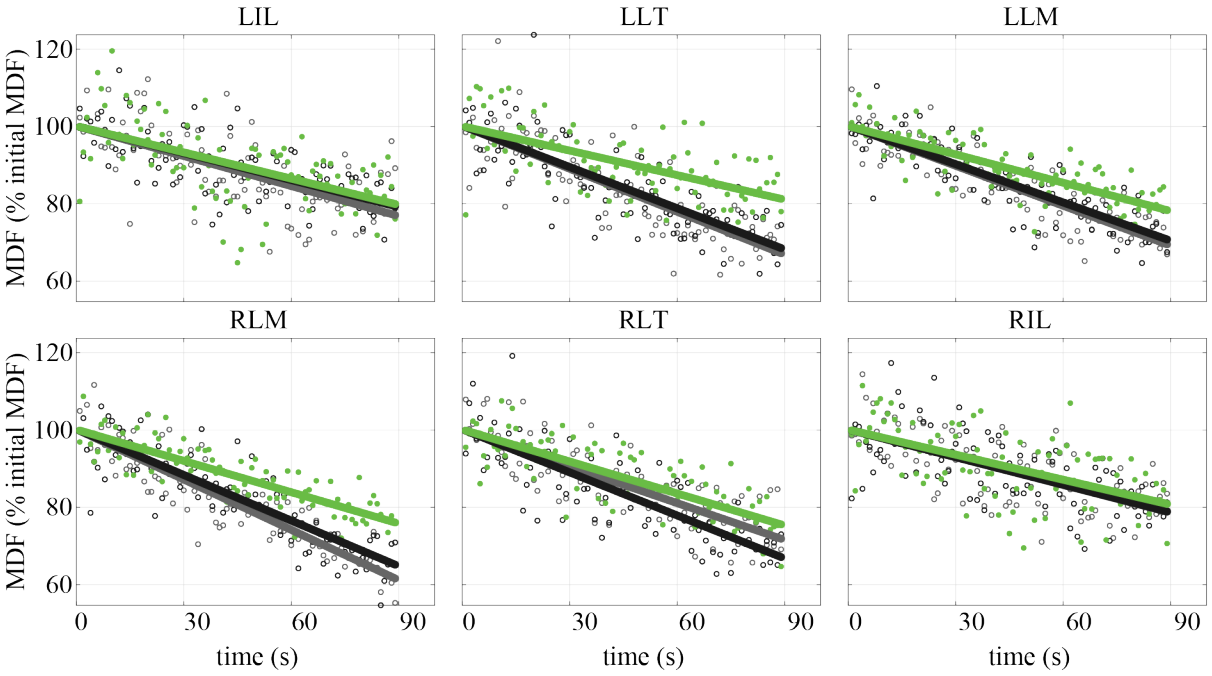

Figure A.3: Subject 3, individual muscle MDF vs. time. Figure layout is identical to **Figure 3.3** in the main text.

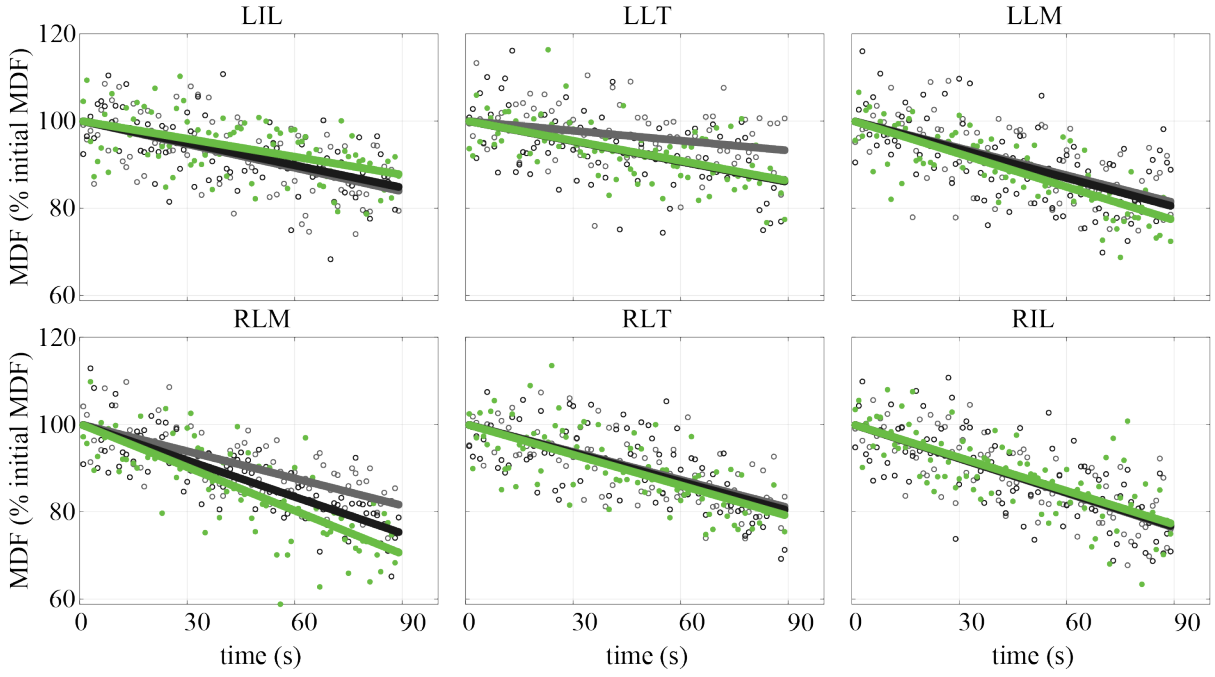

Figure A.4: Subject 4, individual muscle MDF vs. time. Figure layout is identical to **Figure 3.3** in the main text.

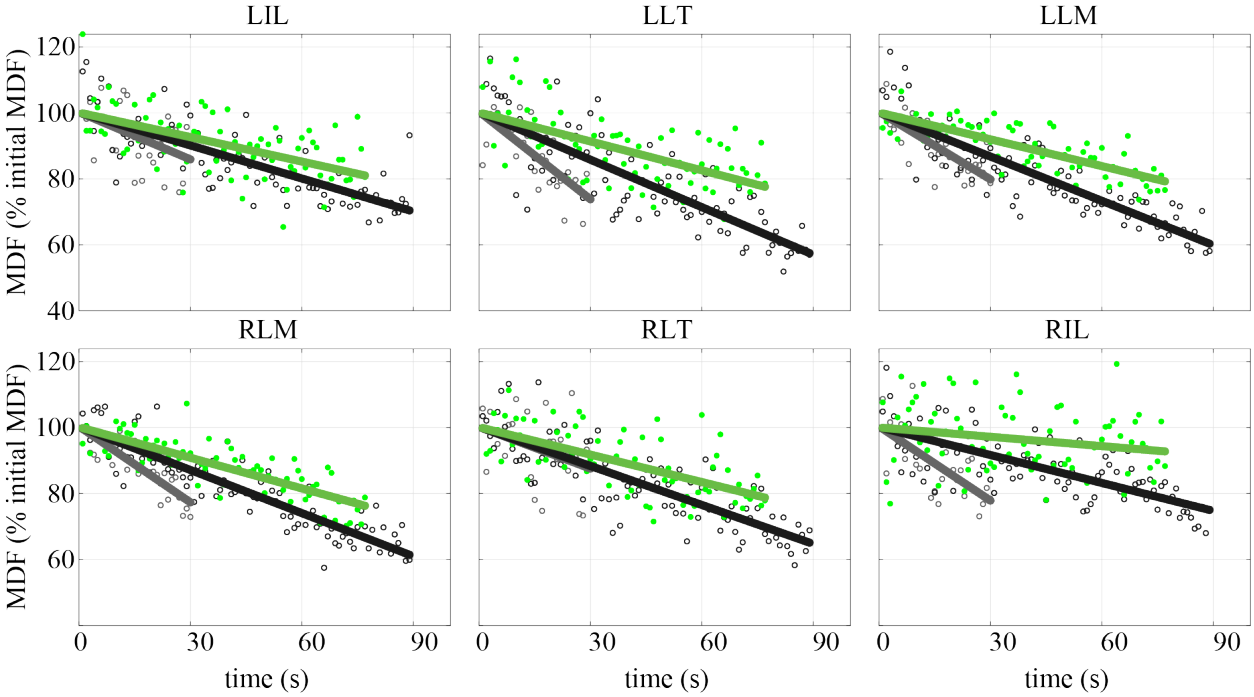

Figure A.5: Subject 5, individual muscle MDF vs. time. Figure layout is identical to **Figure 3.3** in the main text.

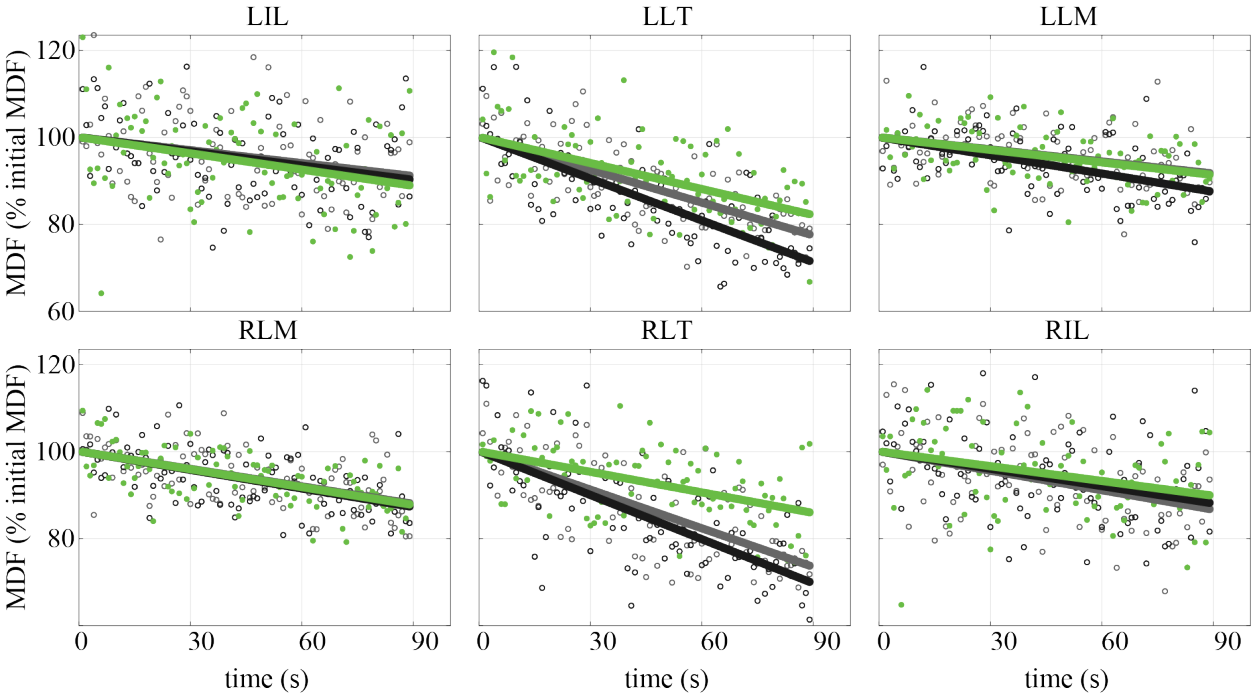

Figure A.6: Subject 6, individual muscle MDF vs. time. Figure layout is identical to **Figure 3.3** in the main text.

Appendix B

Chapter 4 Appendix

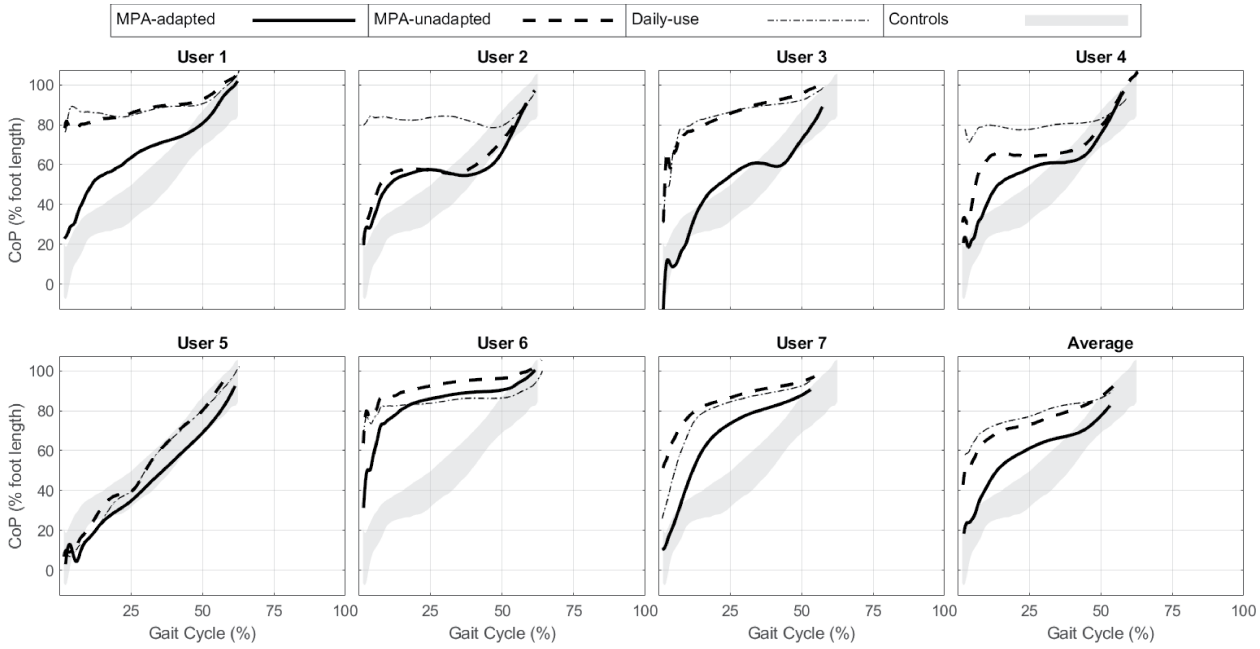

Figure B.1: Prosthetic-side sagittal center of pressure (CoP) for each prosthesis user, as well as the seven-subject average during incline walking, where 0% and 100% correspond to the heel and toe respectively.

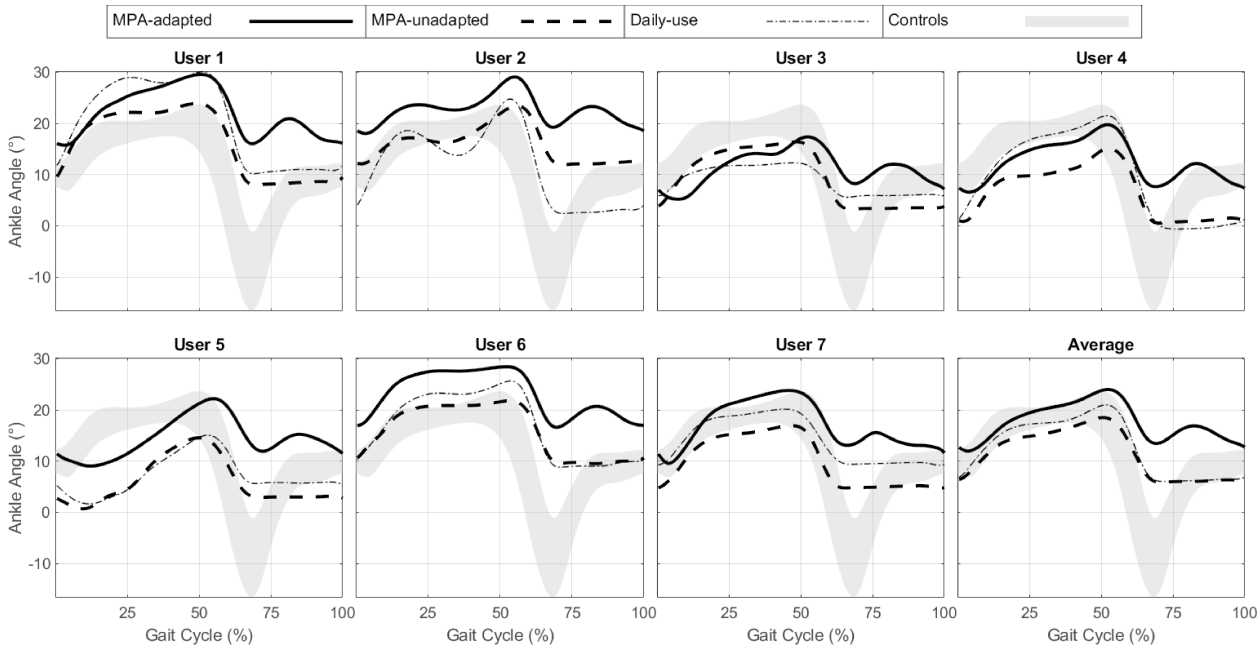

Figure B.2: Prosthetic-side sagittal ankle angle for each user, as well as the seven-subject average during incline walking. Positive values indicate ankle dorsiflexion.

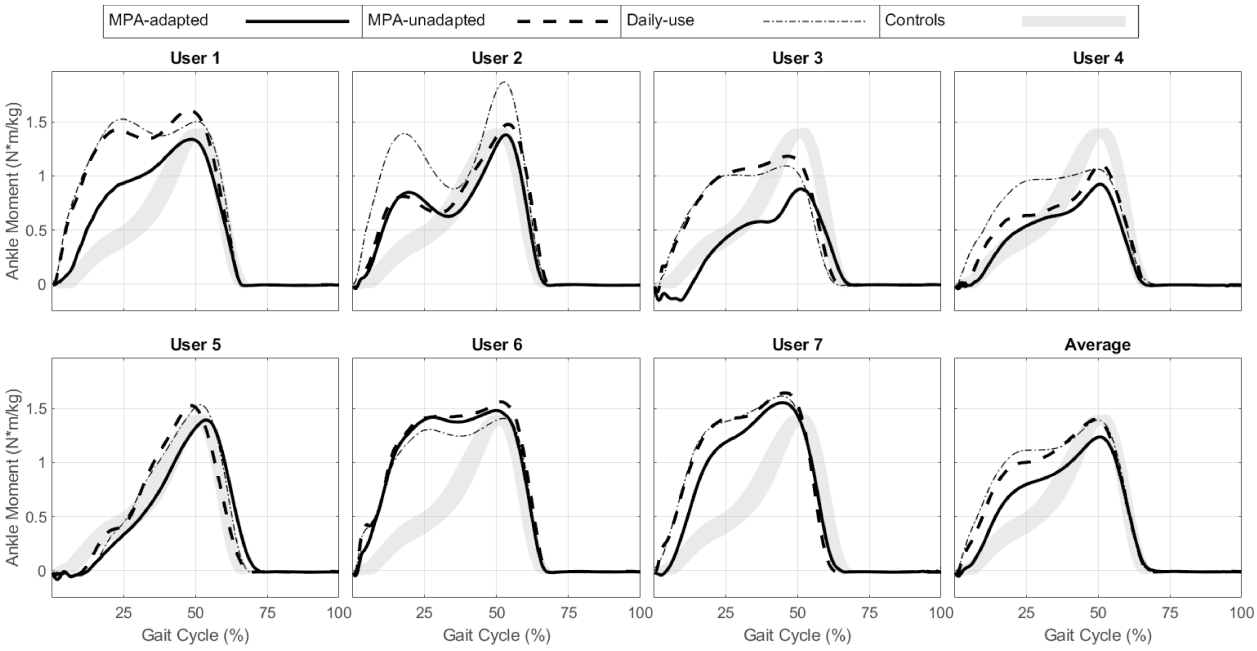

Figure B.3: Prosthetic-side sagittal ankle moment for each user, as well as the seven-subject average during incline walking. Negative values indicate ankle plantarflexion moments.

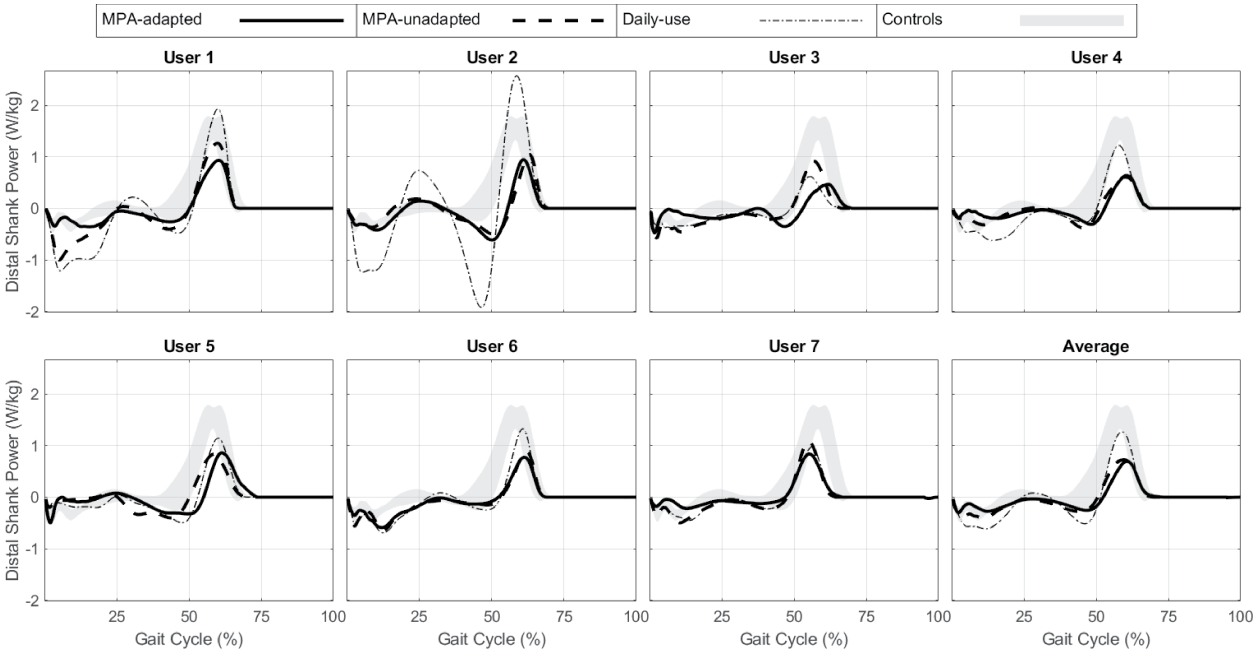

Figure B.4: Prosthetic-side distal shank power for each prosthesis user, as well as the seven-subject average during incline walking. Positive values indicate power generation.

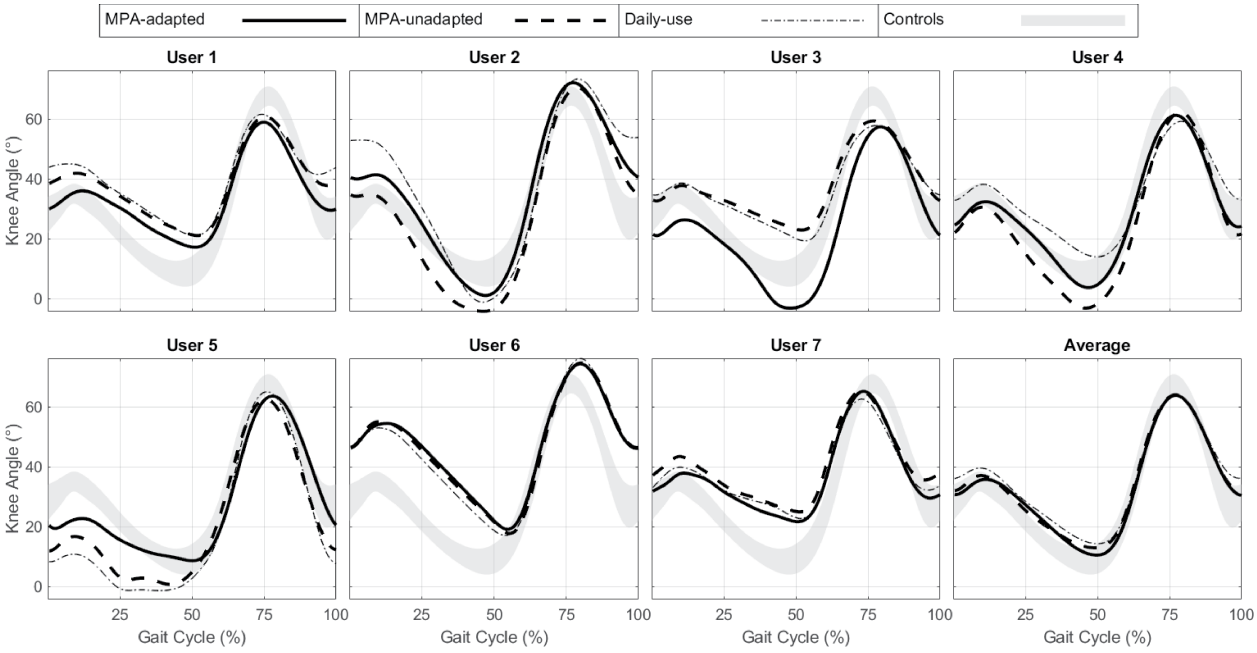

Figure B.5: Prosthetic-side sagittal knee angle for each prosthesis user, as well as the seven-subject average during incline walking. Positive values indicate knee flexion.

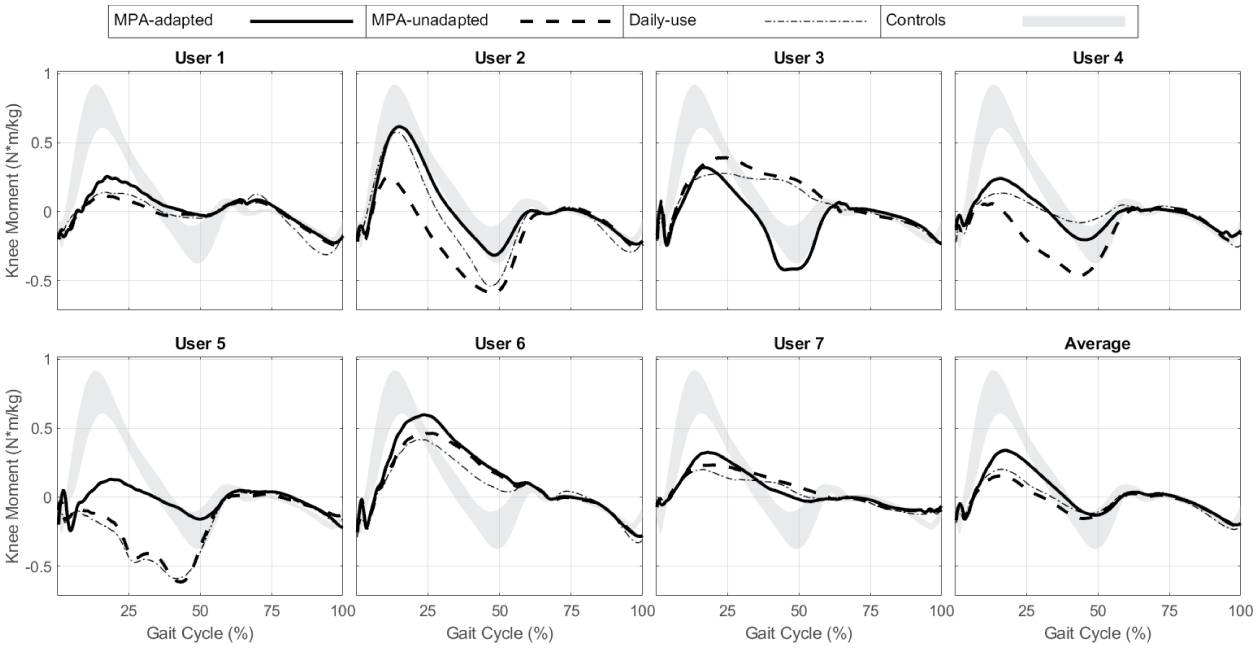

Figure B.6: Prosthetic-side sagittal knee moment for each prosthesis user, as well as the seven-subject average during incline walking. Positive values indicate knee extension moments.

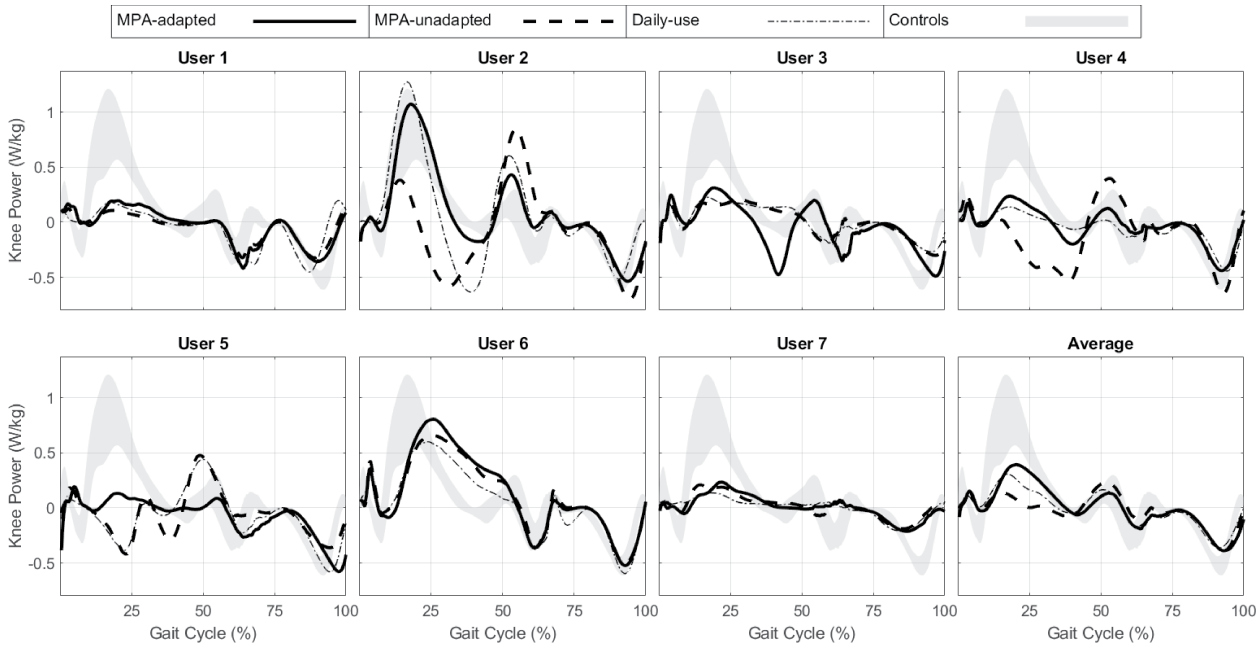

Figure B.7: Prosthetic-side sagittal knee power for each prosthesis user, as well as the seven-subject average during incline walking. Positive values indicate power generation.

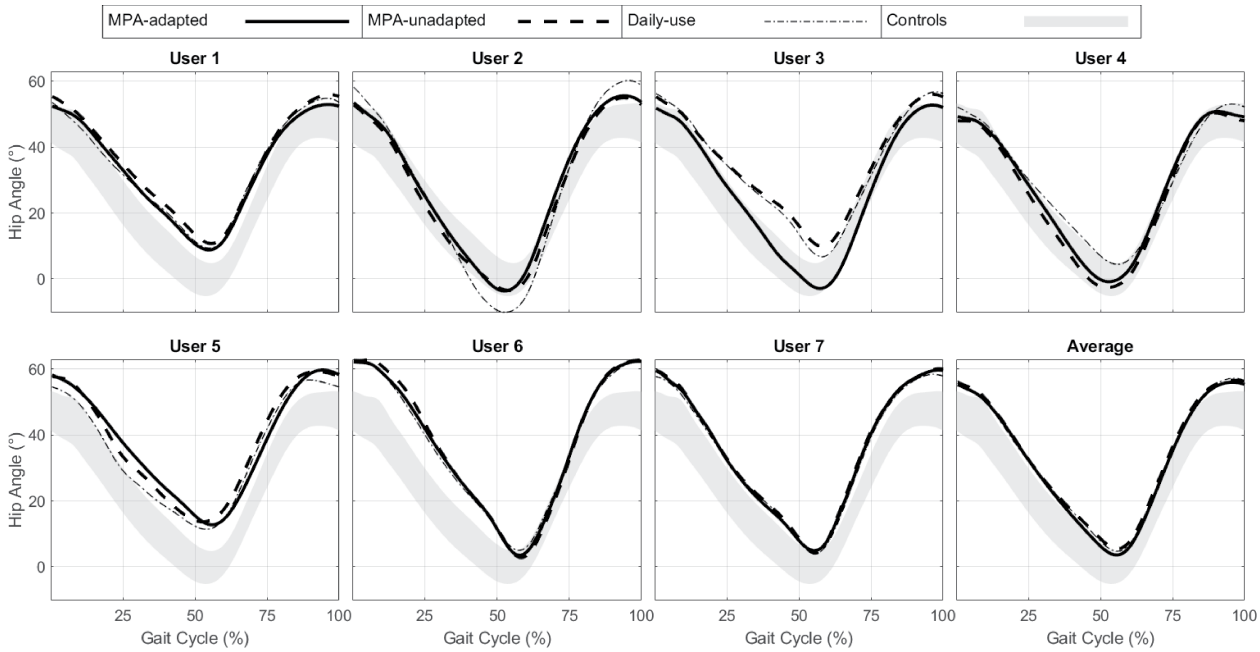

Figure B.8: Prosthetic-side sagittal hip angle for each prosthesis user, as well as the seven-subject average during incline walking. Positive values indicate hip flexion.

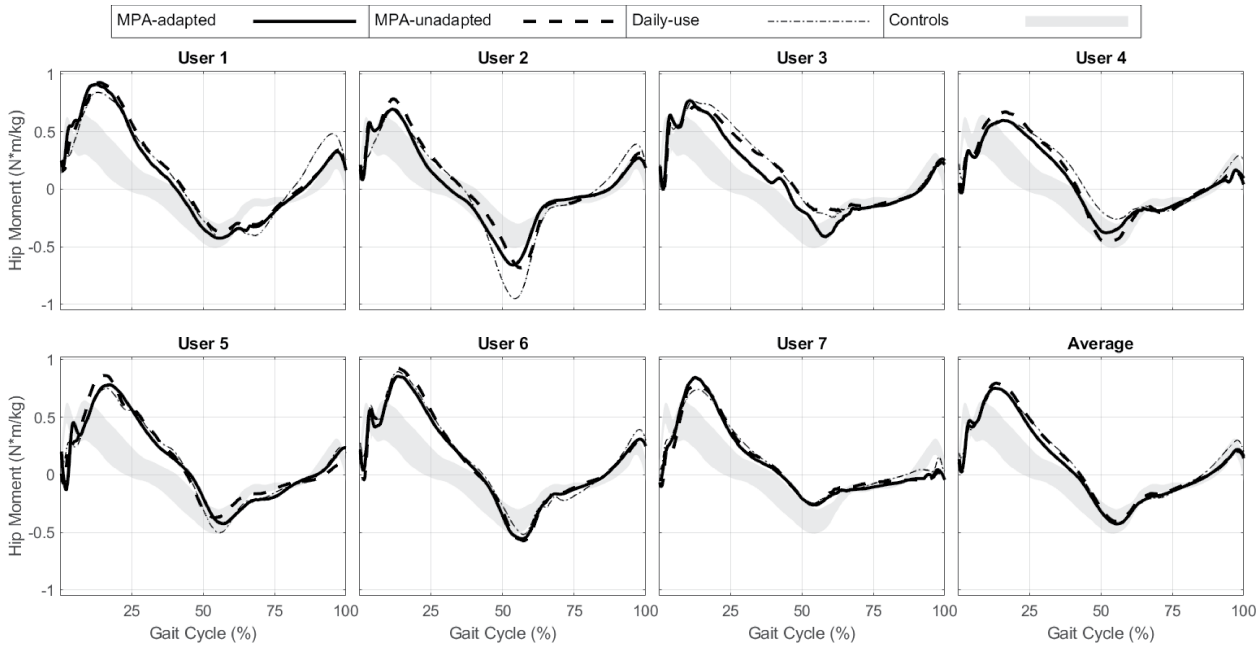

Figure B.9: Prosthetic-side sagittal hip moment for each prosthesis user, as well as the seven-subject average during incline walking. Positive values indicate hip flexion moments.

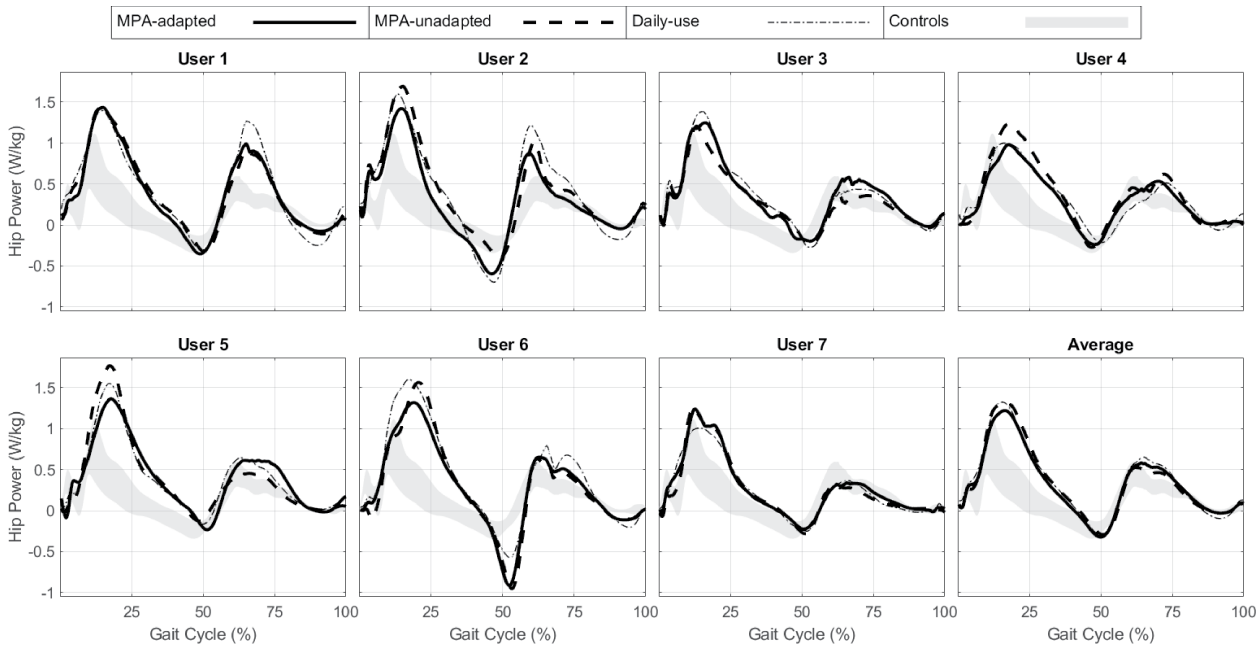

Figure B.10: Prosthetic-side sagittal hip power for each prosthesis user, as well as the seven-subject average during incline walking. Positive values indicate power generation.

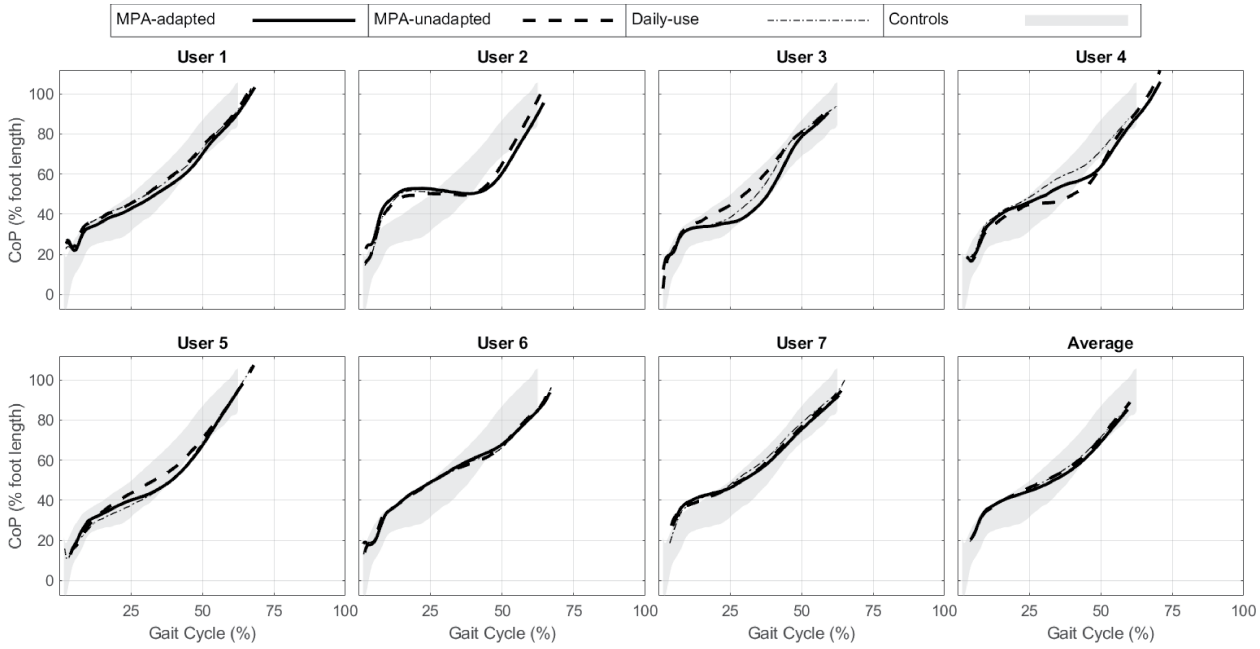

Figure B.11: Intact-side sagittal center of pressure (CoP) for each prosthesis user, as well as the seven-subject average during incline walking, where 0% and 100% correspond to the heel and toe, respectively.

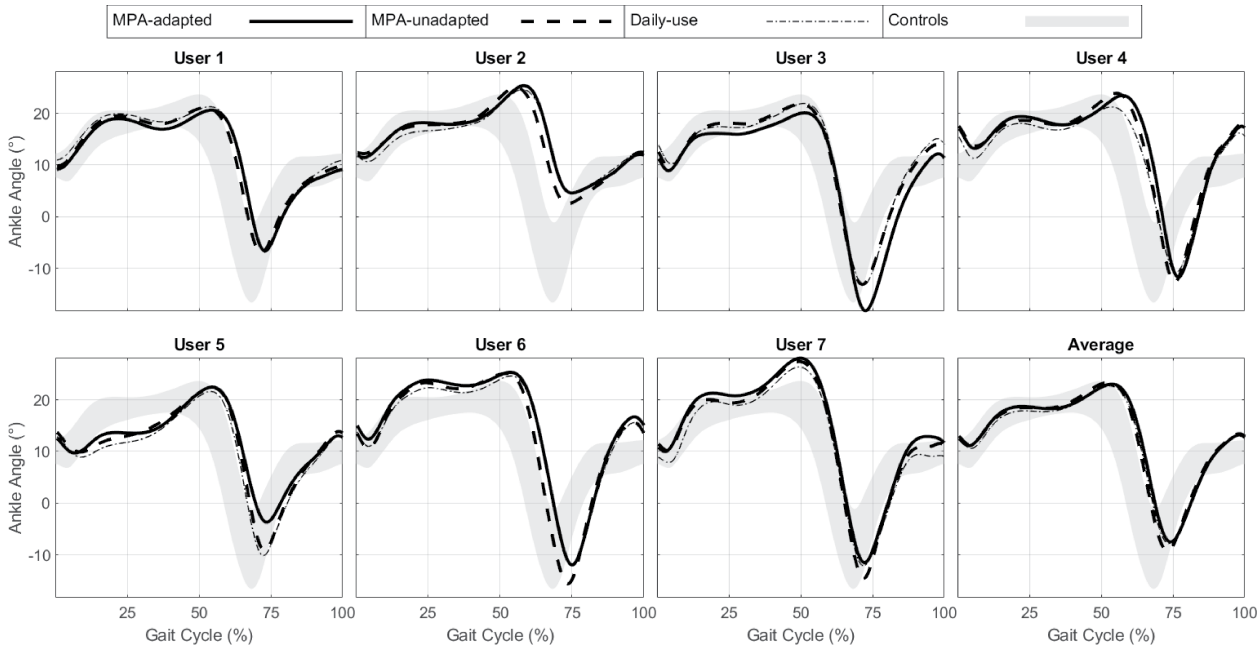

Figure B.12: Intact-side sagittal ankle angle for each prosthesis user, as well as the seven-subject average during incline walking. Positive values indicate ankle dorsiflexion.

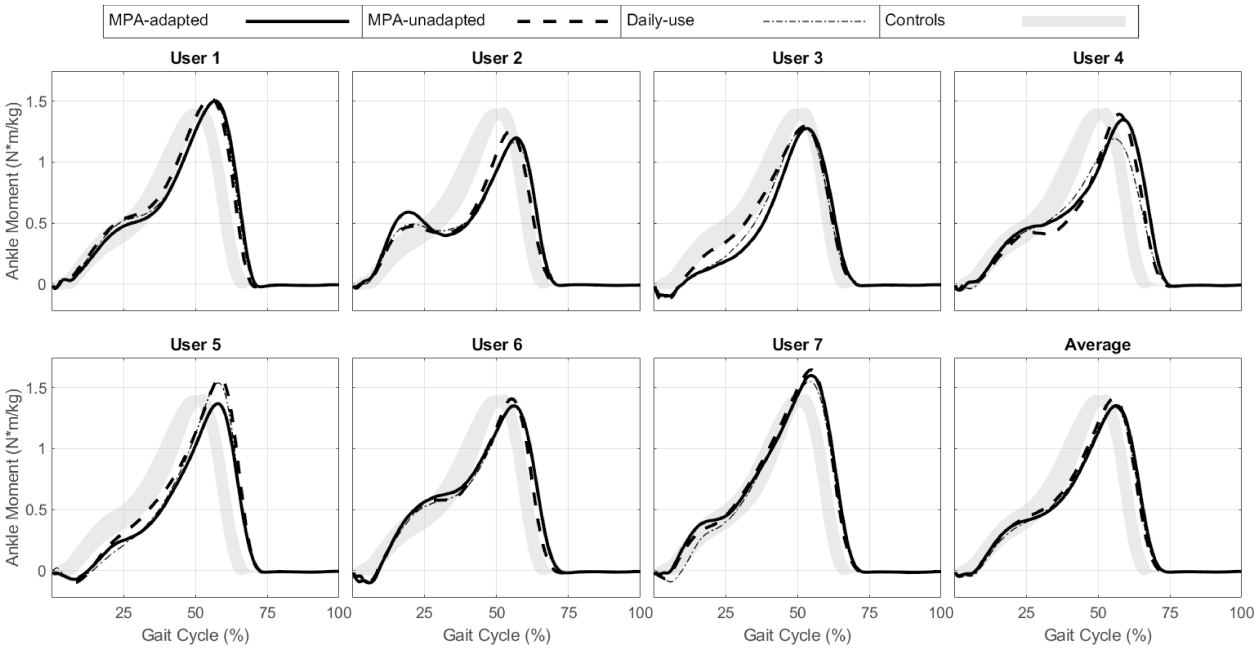

Figure B.13: Intact-side sagittal ankle moment for each prosthesis user, as well as the seven-subject average during incline walking. Negative values indicate ankle plantarflexion moments.

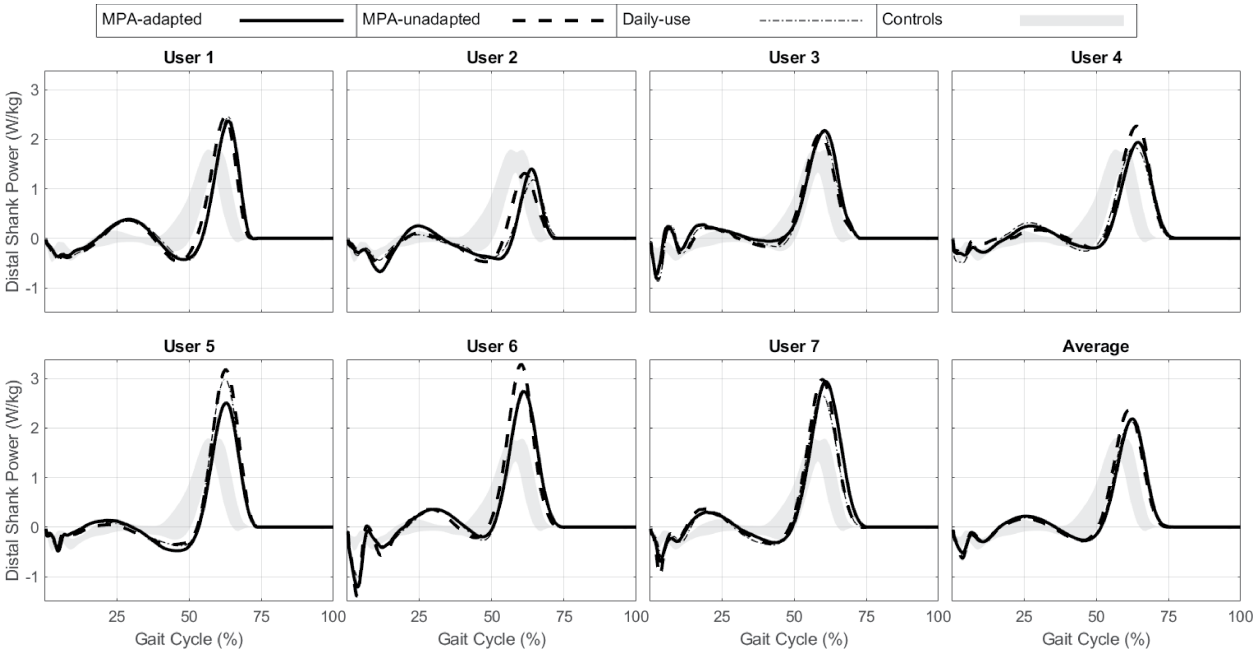

Figure B.14: Intact-side distal shank power for each prosthesis user, as well as the seven-subject average during incline walking. Positive values indicate power generation.

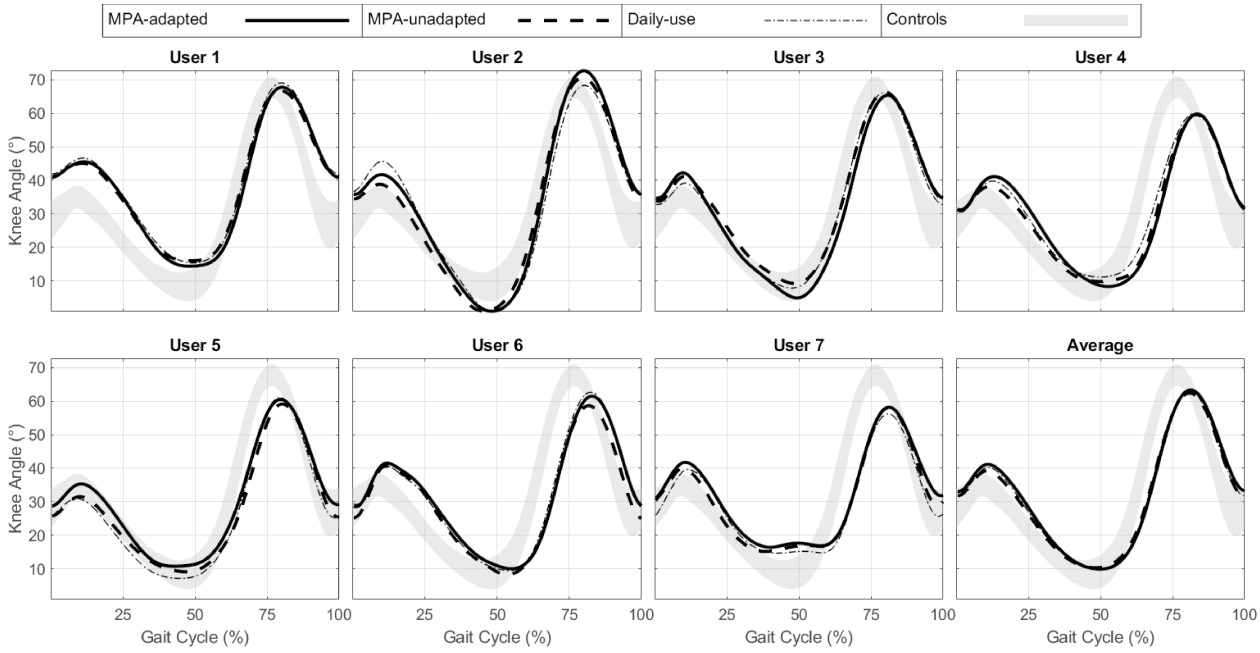

Figure B.15: Intact-side sagittal knee angle for each prosthesis user, as well as the seven-subject average during incline walking. Positive values indicate knee flexion.

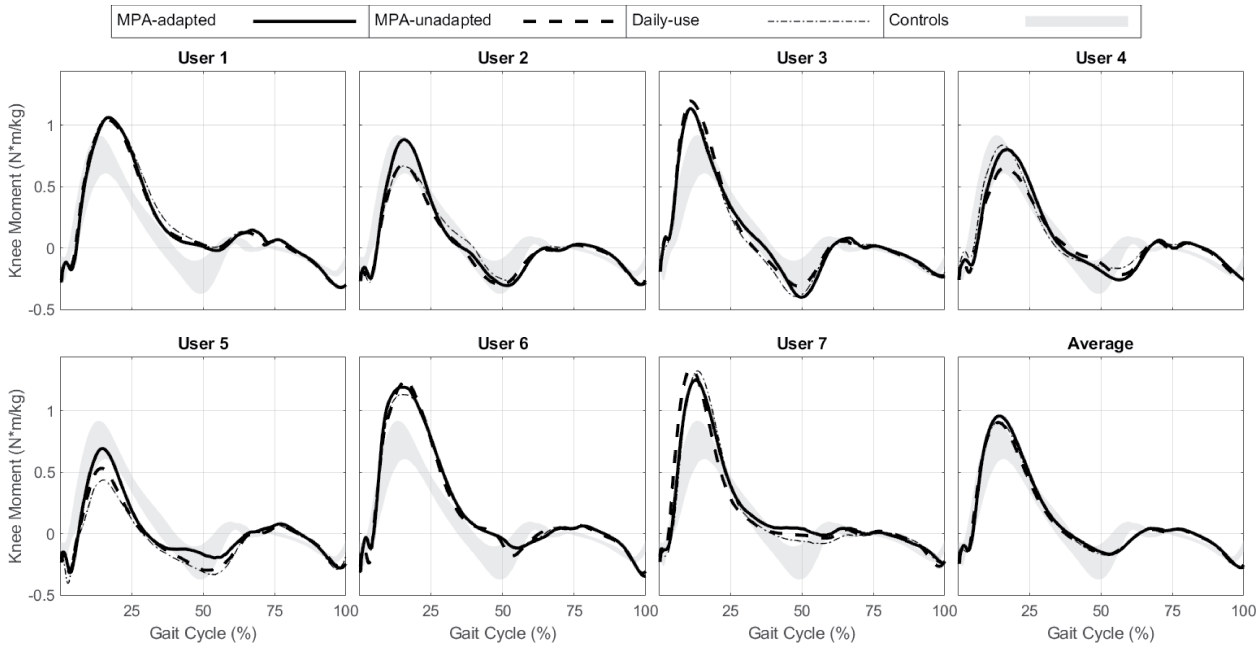

Figure B.16: Intact-side sagittal knee moment for each prosthesis user, as well as the seven-subject average during incline walking. Positive values indicate knee extension moments.

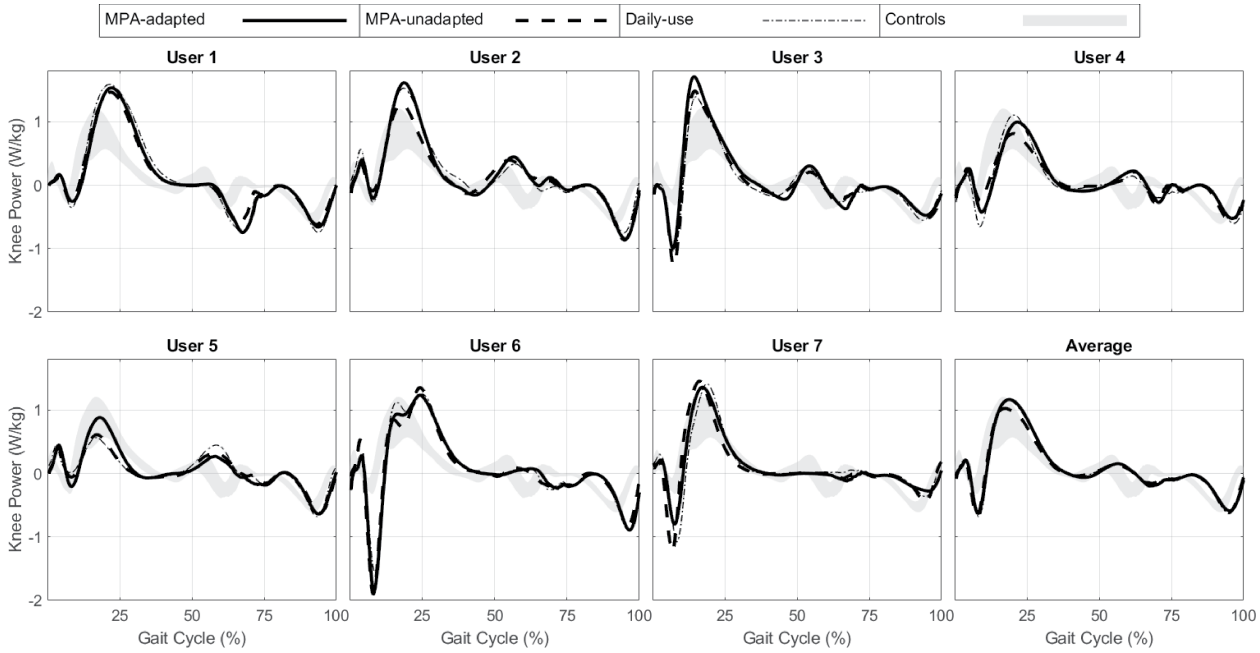

Figure B.17: Intact-side sagittal knee power for each prosthesis user, as well as the seven-subject average during incline walking. Positive values indicate power generation.

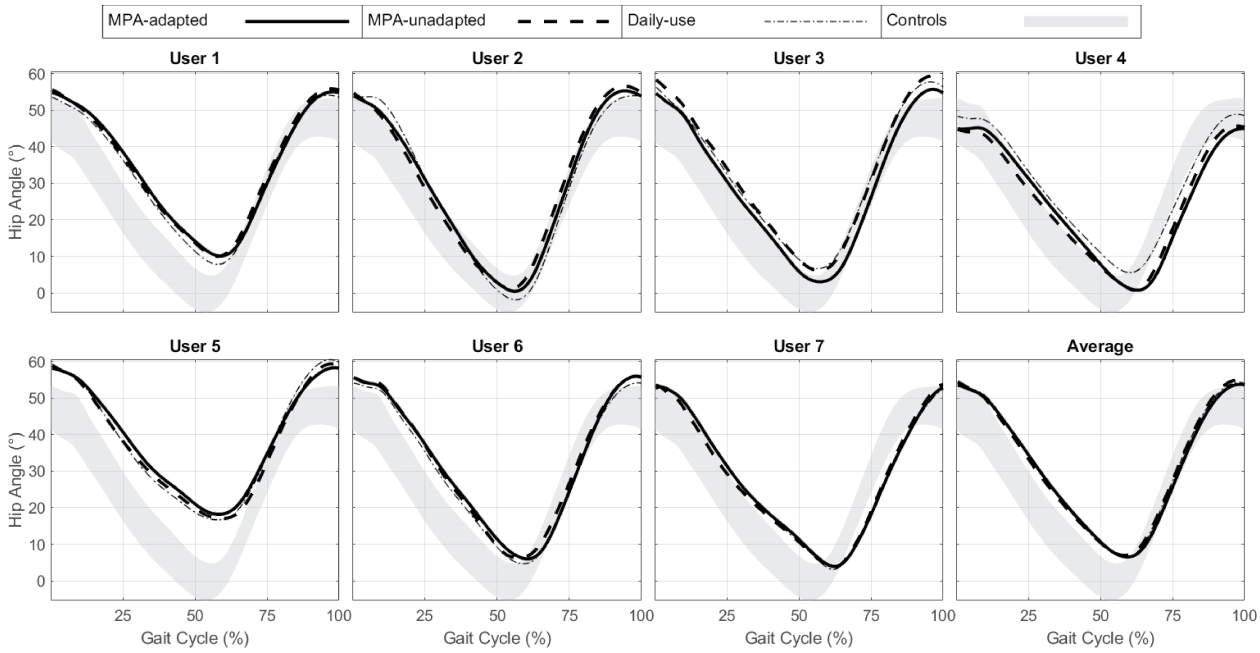

Figure B.18: Intact-side sagittal hip angle for each prosthesis user, as well as the seven-subject average during incline walking. Positive values indicate hip flexion.

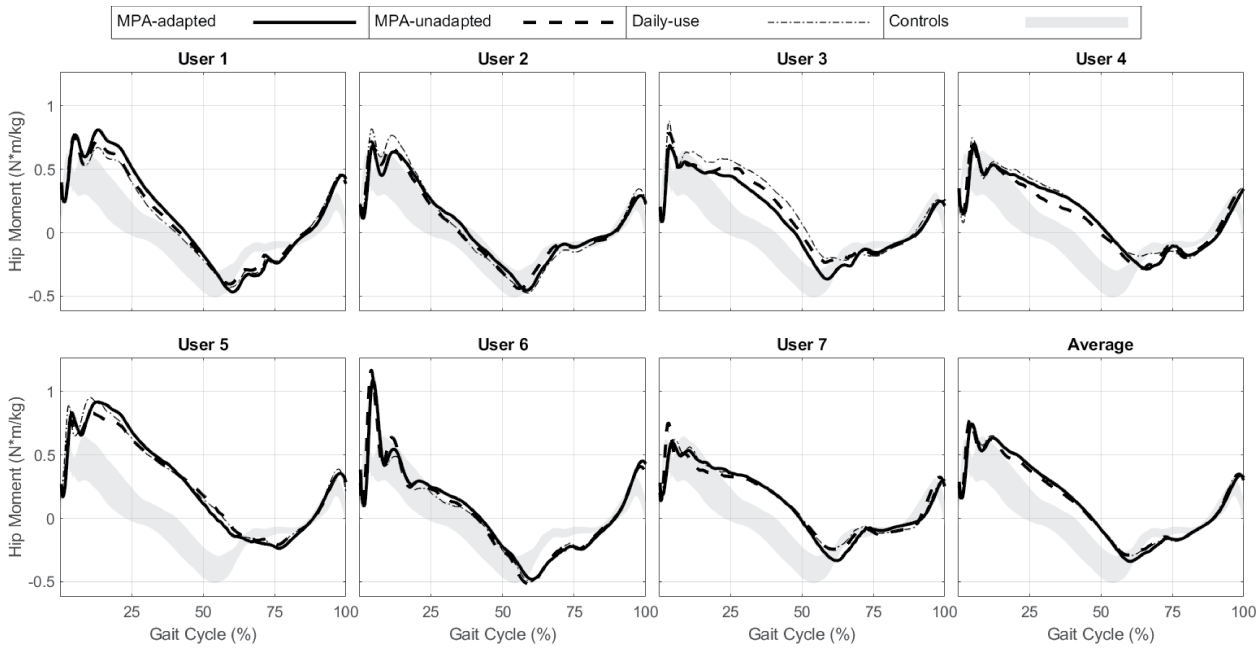

Figure B.19: Intact-side sagittal hip moment for each prosthesis user, as well as the seven-subject average during incline walking. Positive values indicate hip flexion moments.

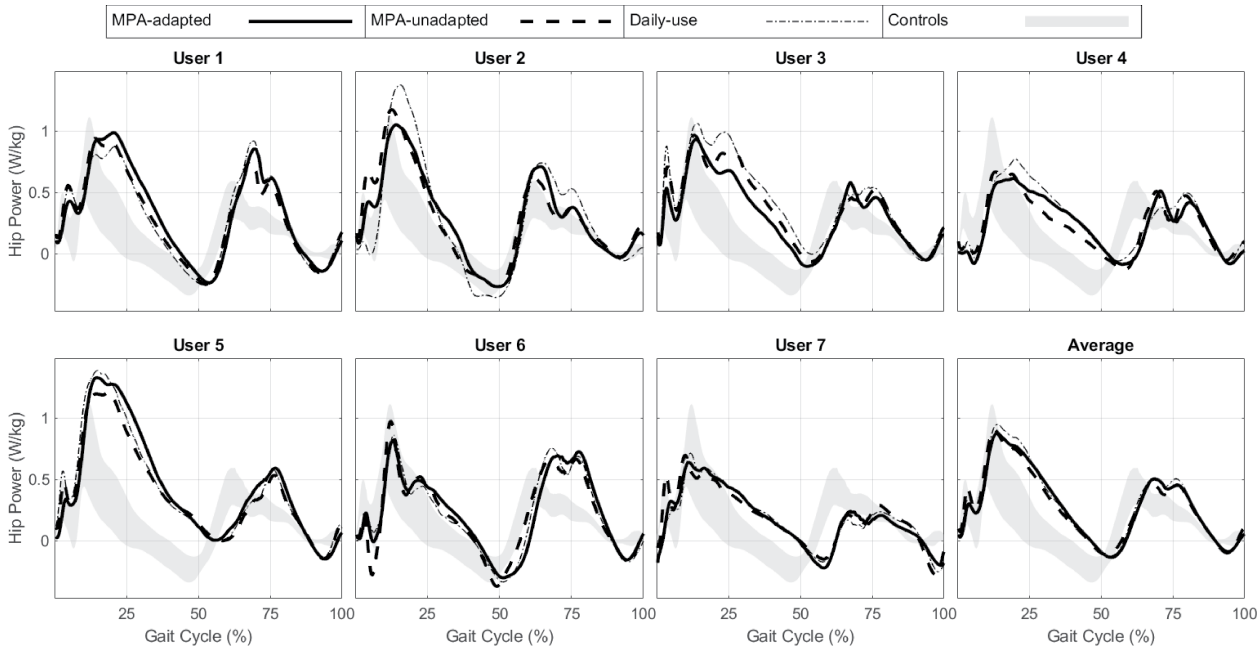

Figure B.20: Intact-side sagittal hip power for each prosthesis user, as well as the seven-subject average during incline walking. Positive values indicate power generation.

Appendix C

Chapter 5 Appendix

Table C.1: **Subject survey responses after performing a series of common movement tasks with the extensible exosuit in disengaged mode**. Subject responses are **bold and underlined**.

Sit in chair for $\geq$ 1 minute: **The exosuit interfered while sitting in the chair**	Strongly Agree	Agree	Neutral	Disagree	**Strongly Disagree**
Sit-to-stand transitions for $\geq$ 10 cycles: **The exosuit interfered while transitioning between sitting and standing**	Strongly Agree	Agree	Neutral	**Disagree**	Strongly Disagree
Squatting for $\geq$ 10 cycles: **The exosuit interfered while squatting**	Strongly Agree	Agree	Neutral	Disagree	**Strongly Disagree**
Lifting for $\geq$ 10 cycles: **The exosuit interfered while lifting**	Strongly Agree	Agree	Neutral	Disagree	**Strongly Disagree**
Leaning forward & backward for $\geq$ 10 cycles: **The exosuit interfered while leaning forward or backward**	Strongly Agree	Agree	Neutral	Disagree	**Strongly Disagree**
Leaning left & right for $\geq$ 10 cycles: **The exosuit interfered while leaning to the left or right**	Strongly Agree	Agree	Neutral	Disagree	**Strongly Disagree**
Twisting left & right $\geq$ 10 cycles: **The exosuit interfered while twisting left or right**	Strongly Agree	Agree	Neutral	Disagree	**Strongly Disagree**
Level walking for $\geq$ 1 minute: **The exosuit interfered while walking**	Strongly Agree	Agree	Neutral	**Disagree**	Strongly Disagree
Walking & carrying a box for $\geq$ 1 minute: **The exosuit interfered while walking and carrying a box**	Strongly Agree	Agree	Neutral	Disagree	**Strongly Disagree**
Walking up & down stairs for $\geq$ 1 minute: **The exosuit interfered while walking up or down stairs**	Strongly Agree	Agree	Neutral	Disagree	**Strongly Disagree**

C.0.1 Extended Results from Model Parameter Sweep Exploration

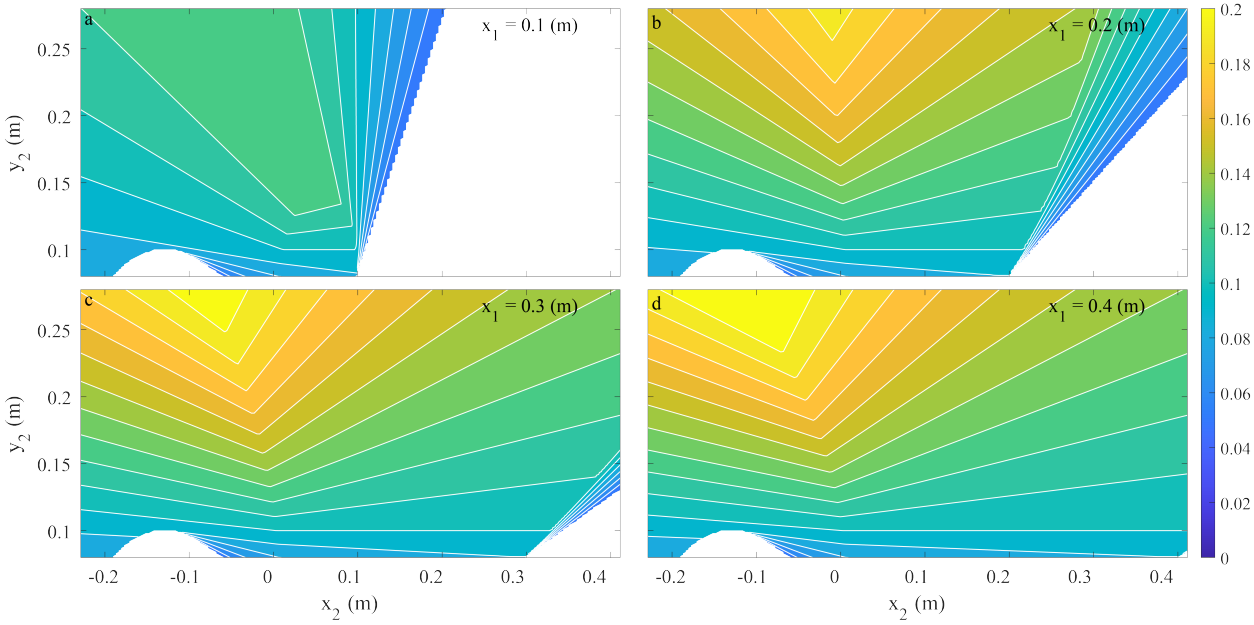

Figure C.1: **Extensible exosuit moment arm (r_T) calculated from Equation (5.4) across the x_2 and y_2 parameter domain specified in Table 5.1**. Each subplot includes a contour plot for a different constant x_1 value (**a**: x_1 = 0.1 m, **b**: x_1 = 0.2 m, **c**: x_1 = 0.3 m, **d**: x_1 = 0.4 m). All points along a contour line denote parameter combinations with a constant r_T in meters. As a reminder, in this model higher values of r_T signify lower device-to-body forces on the shoulders and legs. The x- and y-locations of the routing point p_2 are the axes of the plot (x_2 along the x-axis and y_2 along the y-axis). White regions in the contour plots indicate invalid parameter combinations.

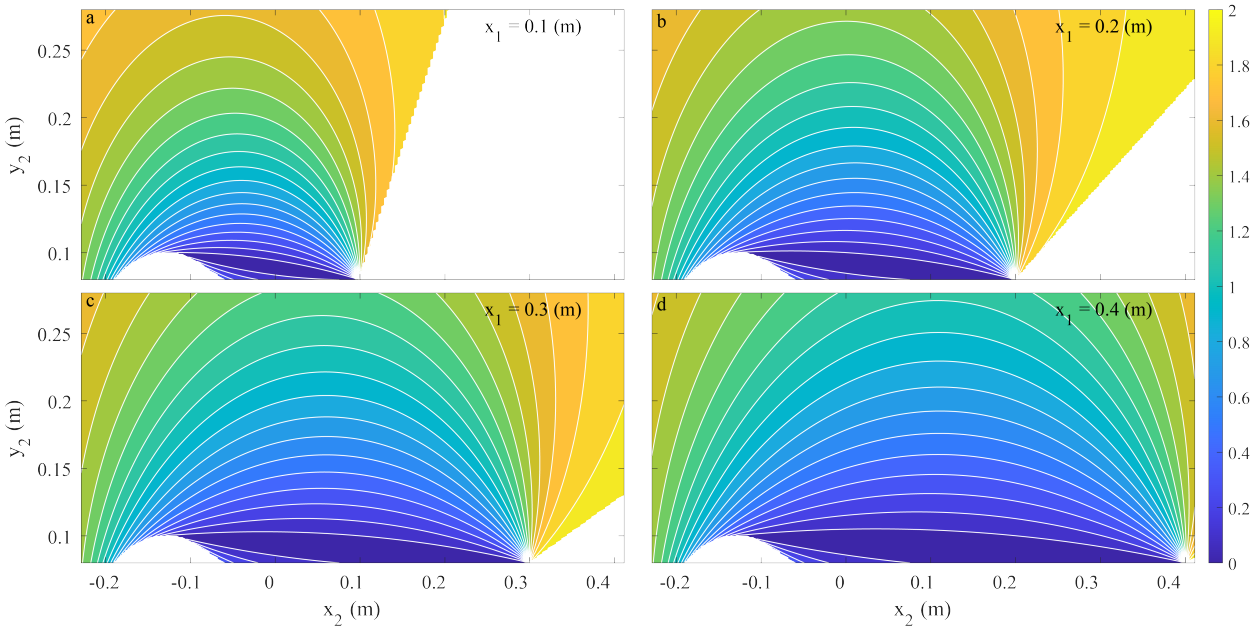

Figure C.2: **Extensible exosuit k_R calculated from Equation (5.5) across the x_2 and y_2 parameter domain specified in Table 5.1**. Each subplot includes a contour plot for a different constant x_1 value (**a**: x_1 = 0.1 m, **b**: x_1 = 0.2 m, **c**: x_1 = 0.3 m, **d**: x_1 = 0.4 m). All points along a contour line denote parameter combinations with a constant k_R. As a reminder, in this model lower values of k_R signify lower device-to-body forces from the extension mechanism onto the back or waist. The x- and y-locations of the routing point p_2 are the axes of the plot (x_2 along the x-axis and y_2 along the y-axis). White regions in the contour plots indicate invalid parameter combinations.

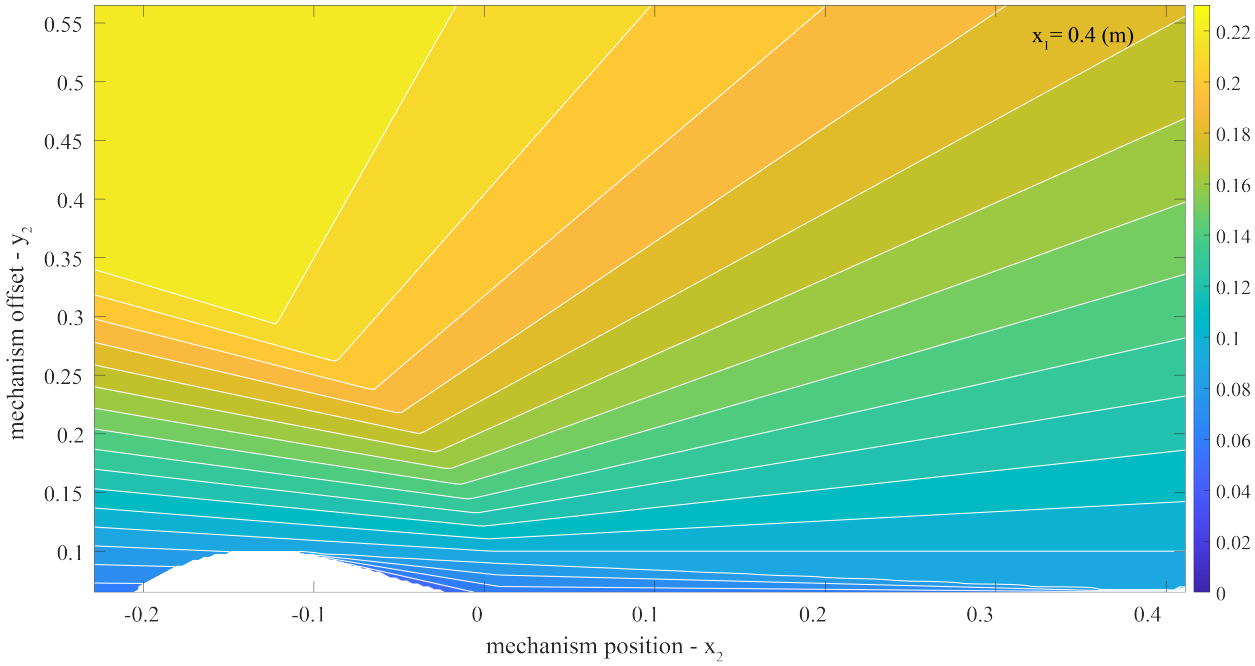

Figure C.3: **Extensible exosuit moment arm (r_T) with y_2 ranging from 0.1 m to 0.58 m** calculated from **Equation** (5.4) across the x_2 parameter domain specified in Table 5.1 and for a constant x_1 = 0.4 m. We note here that although the mechanism offset (y_2) continues to increase, the moment arm plateaus around 0.22 m (large yellow area in the top left of the plot). This suggests that for the specific proof-of-concept prototype explored here, the maximum moment arm is about 0.22 m. See **Section 5.6.4** for extended discussion of this topic.

C.0.2 Model Parameter Selection

For our proof-of-concept prototype we initially aimed to design an extensible exosuit that would reduce $\|\overrightarrow{F_T}\|$ by about 50% and minimize the exosuit footprint (i.e. minimum extension mechanism offset y_2) for the average male user (e.g. 50^{th} percentile). Reducing $\|\overrightarrow{F_T}\|$ by 50% is analytically equivalent to doubling r_T. We followed this process below to establish target design parameters for the prototype:

- We first scaled the model to a 50^{th} percentile male based on anthropometric data (**Table 5.1**, bottom, [75, 58]).

- Next, using the scaled model, we defined our exosuit design parameter ranges (i.e. minimum and maximum values, **Table 5.1**, top), generated 3D parameter grids

(e.g. meshgrid function in MATLAB), and fed these grids into **Equations** (5.4) and (5.5).

- Next we assumed a baseline r_T (0.08 m) based on our previous work [84]. Therefore our desired/target r_T was 0.16 m.
- Next we chose a trunk interface anchoring point (x_1 = 0.2 m) that worked best for our design constraints.
- With r_T and x_1 defined we are constrained to a single contour line (e.g. **Figure 5.3**). Along that contour line, we chose the point with the smallest y_2 in order to minimize the footprint of the exosuit. We found these to be x_2 = 0.0 m, y_2 = 0.18 m (**Figure 5.3**, black dot).
- The target parameters chosen were x_2 = 0.0 m, y_2 = 0.18 m, x_1 = 0.2 m.

C.0.3 Examples of Alternative Extensible Exosuit Designs

In the main text we describe numerous ways to alter the design of the extensible exosuit, for instance, by altering the location and number of extension mechanisms. Ultimately, these choices are driven by the specified goal of the exosuit, based on its intended end-user and use case. The breadth of design possibilities highlights the power of this extension mechanism concept. To make these possibilities less abstract, we provide a few tangible examples. These may provide a better sense of the versatility of this extensible exosuit concept, and elucidate how it can be applied to customize designs that, for instance, create non-linear assistive torque profiles or simultaneously increase the moment arm about multiple joints. For the models shown in **Figures C.4** to **C.6**, the magnitude of the extension mechanism offset (d) is the same, as are the model scaling parameters (e.g. r_{butt}, trunk and leg anchoring points). The parameters that changed between the models were the location and/or the number of extension mechanisms.

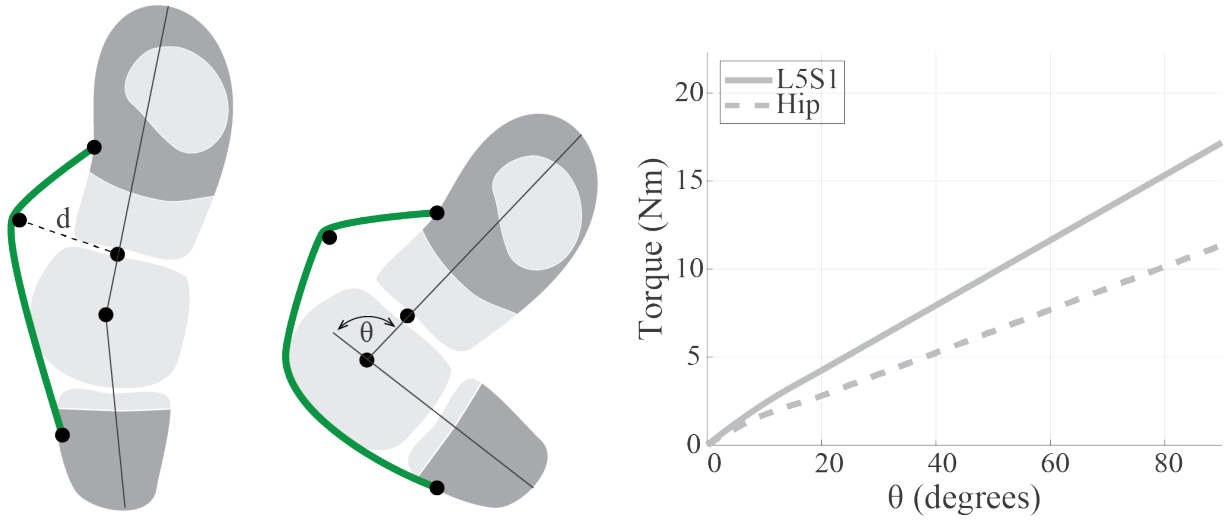

Figure C.4: **The proof-of-concept extensible exosuit with an extension mechanism on the back/waist (i.e. the design detailed in the main text). This configuration has an increased moment arm about the L5-S1 joint and a linear torque vs. angle profile, with a greater torque about the L5-S1 than the hip**. The L5-S1 and hip torque for the extensible exosuit prototype explored in this work are shown here (note we use the same model as discussed in **Section 5.3**, but expanded the model to estimate the change in torque across a lifting movement). We note that the torque curves for both the L5-S1 and hip are largely linear, and that the torque at the hip is lower than the L5-S1 (because the moment arm is increased at the L5-S1 but not the hip). We include this model as a comparison for the alternative design approaches shown in **Figures C.5** and **C.6**, which use one or more extension mechanism on different locations along the backside.

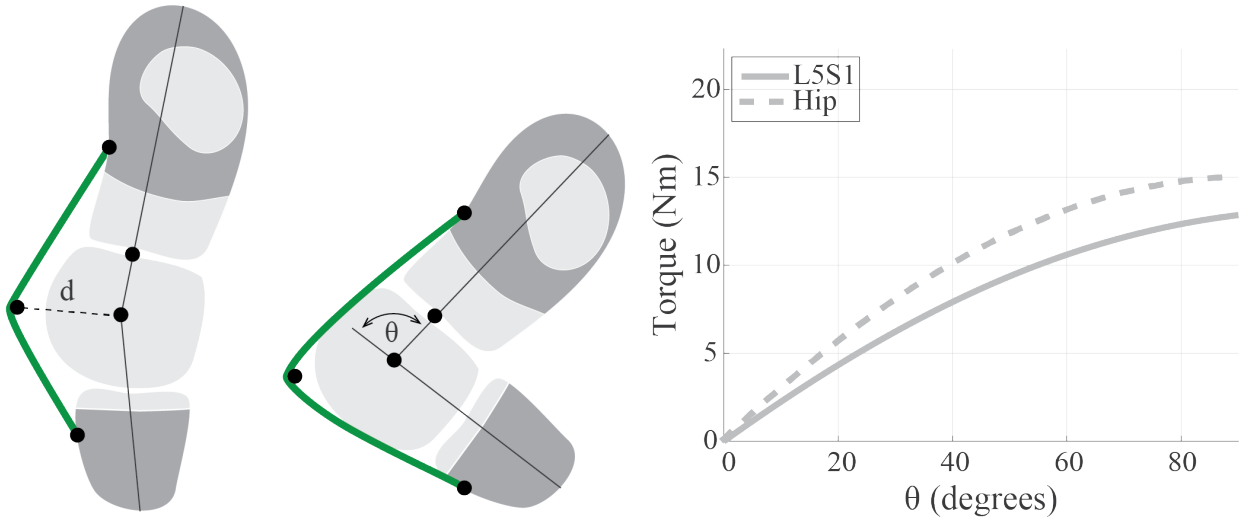

Figure C.5: **One alternative extensible exosuit design with an extension mechanism on the buttocks creates an increased moment arm and nonlinear torque profiles at both the hip and L5-S1**. The geometry of this exosuit changes as the user flexes forward (θ), which changes the moment arm of the exosuit with respect to the L5-S1 and hip joints. This also causes a nonlinear displacement of the elastic bands, with a greater torque about the hip than the L5-S1 joint. The result is a nonlinear (softening spring) assistive torque profile for both the hip and the L5-S1 joints.

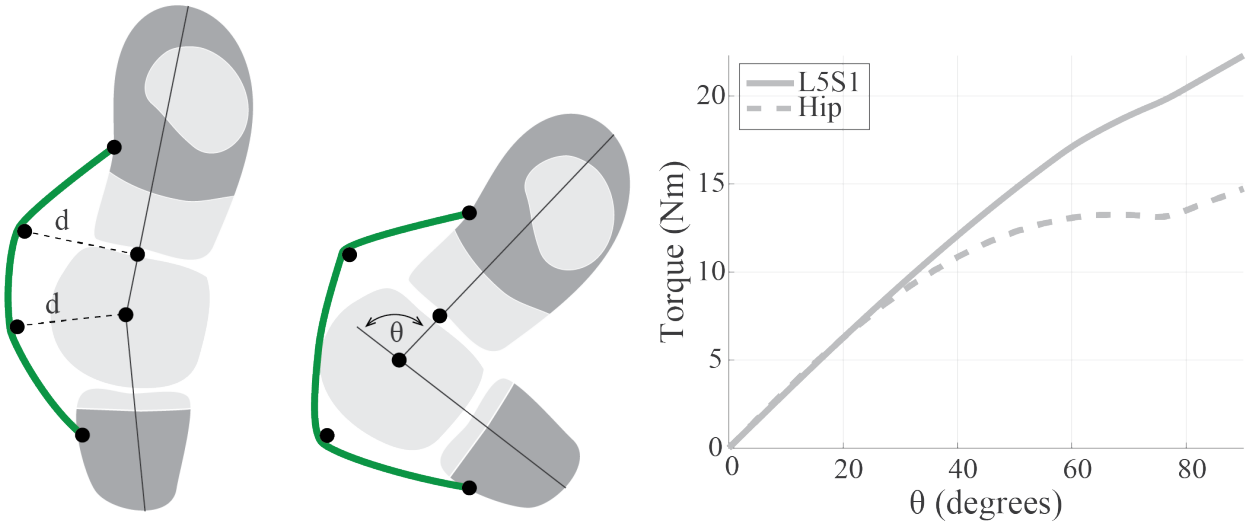

Figure C.6: **A second alternative extensible exosuit design uses two extension mechanisms.** This design includes two offsets, one near the low back and another near the bottom of the buttocks. Compared to the extensible exosuit design tested in the main text of this work, this alternative design increases moment arms relative to both the L5-S1 and hip joints. Additionally, due to the altered geometry, the rate of elastic element displacement is accelerated (relative to **Figure C.4**) and the hip torque becomes nonlinear. The net effect is that the exosuit torque magnitudes about the hip and L5-S1 are increased relative to **Figure C.4**.

C.0.4 Butt Friction and Dissipative Butt Work

In this section we expound upon model insights related to how the placement of the elastic element within the band affects butt friction and dissipative butt work. For the purposes of this summary section, the term band refers to the entire physical connection between the trunk and leg interfaces. The band is comprised of both elastic (stretch) and non-stretch (non-stretch) elements in series with each other.

We begin with a brief summary of how friction between the buttocks and band is expected to affect exosuit dynamics: The buttocks (and other body segments such as the lower back [73]) deform in a way that changes it's surface length (i.e. arc length) during movement (e.g. hip flexion). If the elastic element is positioned over the buttocks (as with the extensible exosuit prototype, **Figure 5.6**), then the elastic element will experience the

same (or similar) displacement as the buttocks surface, with minimal sliding relative to the buttocks (**Figure C.7**). However, if instead, the non-stretch element is placed over the buttocks, then this non-stretch material will need to slide relative to the buttocks during movement **Figures C.8** and **C.9**). As a result, placing the non-stretch element over the buttocks introduces friction forces which changes the tension along the length of the band, performs dissipative work and is a potential source of chafing over time. Energy dissipated due to friction would otherwise have gone into assisting a user as they are lifting, or returning from a crouched/stooped posture to a standing posture.

Next we provide a more technical summary of the model predictions, which elucidate how tension in different portions of the band, butt friction and dissipative work are related and expected to change during movement, for instance, during a squat lift:

First let us consider an exosuit design with an non-stretch element over the buttocks and an elastic element positioned over the back. As the user squats down (i.e. hips flexing), the non-stretch element and the buttocks slide relative to each other, causing the band to experience a shearing friction force. This increases the band tension such that $\|\vec{F_L}\| > \|\vec{F_T}\|$ (**Figure C.8**). Next as the user stands back up (i.e. hips extending), the non-stretch element experiences friction which reduces the band tension such that $\|\vec{F_L}\| < \|\vec{F_T}\|$ (**Figure C.8**).

Using a simple model based on the Euler-Eytelwein formula ([44]) for capstan friction, we estimate the expected relationship between the force magnitudes at the trunk and the leg: in the **Equation** (C.1) below, r_{butt} is the radius of the buttocks (considered here as the distance from the hip joint center to the buttocks skin surface), μ_{butt} is the kinetic coefficient of friction between the band and the buttocks (here assumed to be the kinetic coefficient of friction between the exosuit and a clothed user, i.e. fabric-on-fabric), $k_{elastic}$ is the spring constant of the elastic element, and θ is the angle of the leg with respect to the trunk as shown in **Figure C.7**.

$$\|\overrightarrow{F_L}\| = \|\overrightarrow{F_T}\| e^{\theta \mu_{butt} sgn(\dot{\theta})} = r_{butt} k_{elastic} \theta e^{\theta \mu_{butt} sgn(\dot{\theta})} \quad \text{(C.1)}$$

In **Equation** (C.1) $\|\overrightarrow{F_L}\| > \|\overrightarrow{F_T}\|$ when the hip is flexing (i.e. $\dot{\theta} > 0$), and conversely $\|\overrightarrow{F_L}\| < \|\overrightarrow{F_T}\|$ when the hip is extending (i.e. $\dot{\theta} < 0$) for the case shown in **Figure C.8**. Functionally this means that when the non-stretch element is positioned over the buttocks (as shown in **Figure C.8**), a higher exosuit torque is created about the hip when it is flexing (bending down), but a lower exosuit torque is created about the hip when extending (standing up), and the L5-S1 exosuit torque remains unchanged relative to the configuration in (**Figure C.7**) where the elastic element is over the buttocks.

Second, consider an exosuit design where the non-stretch element is still positioned over the buttocks but the elastic element is over the leg (as shown in **Figure C.9**). For this configuration, **Equation** (C.1) is adjusted by swapping $\|\overrightarrow{F_L}\|$ and $\|\overrightarrow{F_T}\|$. In this new configuration (as shown in **Figure C.9**), a higher exosuit torque is created about the L5-S1 joint when the hips are flexing (bending down), because $\|\overrightarrow{F_T}\| > \|\overrightarrow{F_L}\|$. But a lower exosuit torque is created about the L5-S1 joint when the hips are extending (standing up), because $\|\overrightarrow{F_T}\| < \|\overrightarrow{F_L}\|$. Meanwhile the exosuit hip torque remains unchanged relative to the configuration in **Figure C.7** where the elastic element is over the buttocks.

Third, consider an exosuit design where the elastic element is positioned over the buttocks, and the non-stretch elements are only located below the trunk interface and above the leg interface (**Figure C.7**). Since the elastic element deforms and stretches with the buttocks throughout the bending and lifting cycle the frictional effects are negligible in the model, and therefore the exosuit torque generated about the L5-S1 and hip joints during bending and lifting follow similar profiles.

In the configurations in which the non-stretch element is positioned over the buttocks, the butt friction forces are expected to dissipate energy as the user moves (due to the relative motion between the band and buttocks). This dissipated energy, or butt friction work ($W_{buttfriction}$) can be estimated by the model (**Equation** (C.2)) over a full

flexion/extension movement cycle ($\theta_{initial} \rightarrow \theta_{final} \rightarrow \theta_{initial}$):

$$W_{buttfriction} = -r_{butt}^2 k_{elastic} \left(\int_{\theta_{initial}}^{\theta_{final}} \theta(e^{\theta \mu_{butt}} - 1) d\theta + \int_{\theta_{final}}^{\theta_{initial}} \theta(e^{-\theta \mu_{butt}} - 1) d\theta \right) \quad \text{(C.2)}$$

From **Equation** (C.2) we can see that for a given cycle ($\theta_{initial} \rightarrow \theta_{final} \rightarrow \theta_{initial}$) the magnitude of dissipative butt friction work increases exponentially with θ (the angle of the leg relative to the trunk). This means the dissipative work due to butt friction is expected to increase significantly as a person bends or crouches more deeply. Another insight from this equation is that dissipative butt friction work is proportional to butt radius squared (i.e. r_{butt}^2). This suggests an interesting potential trade-off when using an exosuit with an non-stretch element over the buttocks: On one hand, a larger butt radius provides a benefit because it increases the moment arm by which the tension in the exosuit band can provide torque assistance about the hips and back. On the other hand, the biomechanical drawback to a larger butt radius is that it introduces more dissipative energy losses due to friction, per **Equation** (C.2). The solution suggested by this model is simply to place the elastic element over the buttocks (instead of the non-stretch element), which enables the exosuit to retain it's moment arm benefit due to butt radius, but without incurring the proportional increase in dissipative butt friction work.

This modeling is presented to provide general insight and physics-based expectations that help inform exosuit design. There are various model limitations, similar to those discussed in the main text. Although the model takeaways seem to make sense and match our intuition and prior experiences, these takeaways should be treated as predictions/expectations, which still require empirical confirmation in the future.

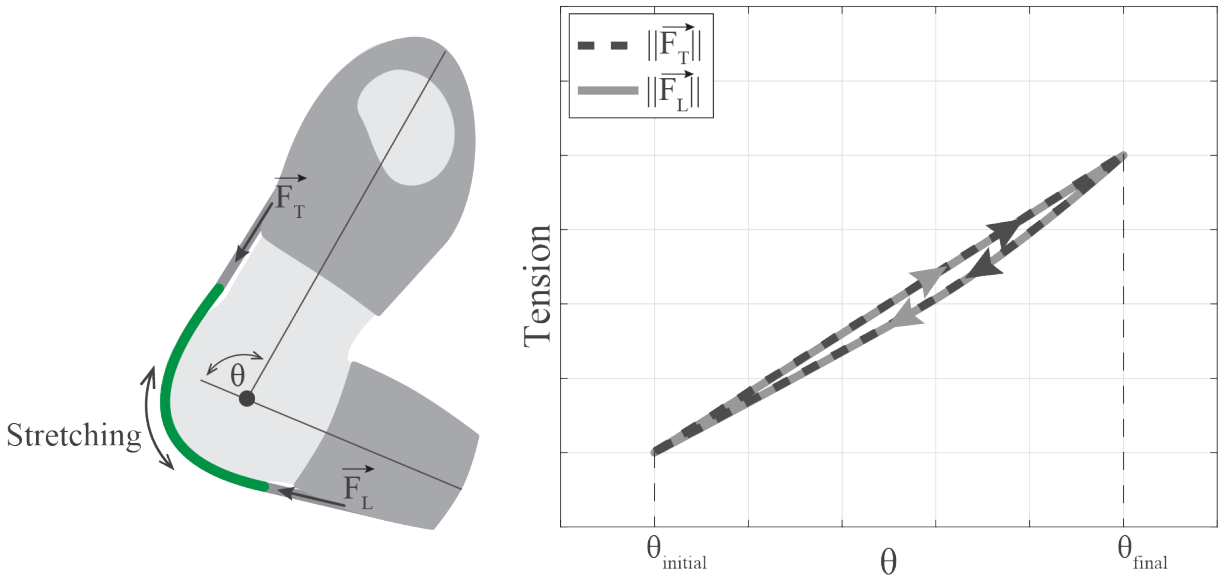

Figure C.7: **Exosuit with elastic element over the buttocks (green) and non-stretch elements (gray) spanning the back and leg**. The elastic element is expected to deform with the buttocks' change in arc length during squatting or bending, such that there is minimal relative movement between the band and buttocks. As a result, the model suggests that the tension magnitude at the leg ($\|\vec{F_L}\|$) and the trunk ($\|\vec{F_T}\|$) will be approximately equal. The plot on the right is a qualitative representation to provide intuition on the expected dynamics of the exosuit. In this exosuit configuration energy losses due to butt friction are expected to be minimal.

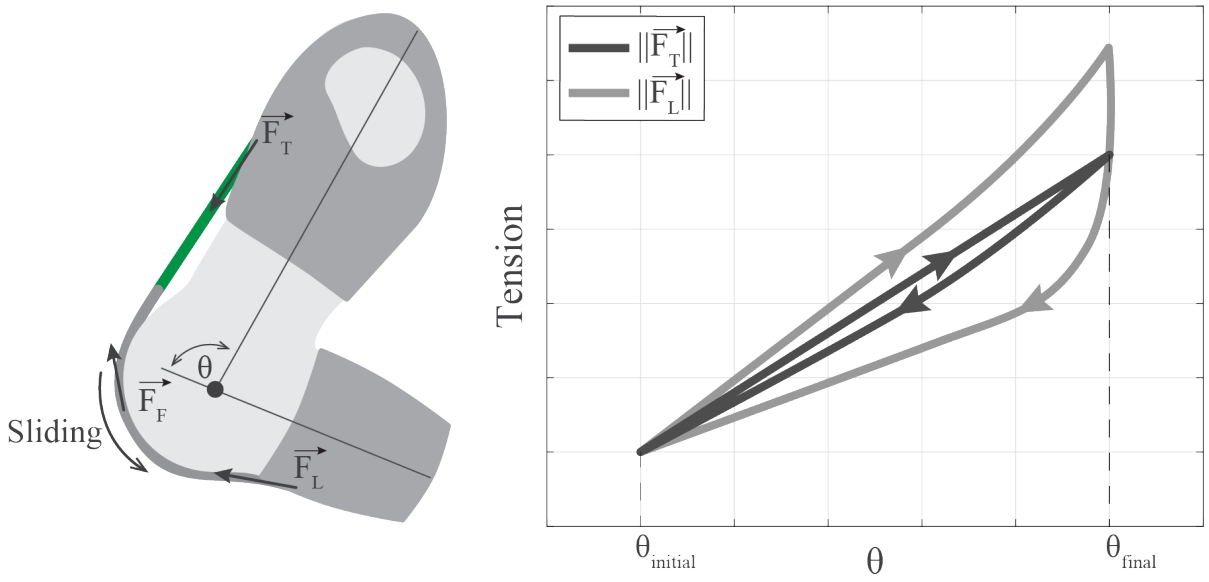

Figure C.8: **Exosuit with non-stretch element (gray) over the buttocks, and elastic element (green) above it**. The model suggests that $\|\overrightarrow{F_L}\|$ will be increased during hip flexion ($\theta_{initial} \rightarrow \theta_{final}$), but decreased during hip extension ($\theta_{final} \rightarrow \theta_{initial}$), relative to $\|\overrightarrow{F_T}\|$ due to the presence of the frictional force at the butt ($\|\overrightarrow{F_T}\|$). This difference in tension forces is illustrated by the plot of the light gray curve in the plot on the right. This plot is a qualitative representation to provide intuition on the expected dynamics of the exosuit. In this exosuit configuration energy losses due to butt friction are expected to be non-negligible.

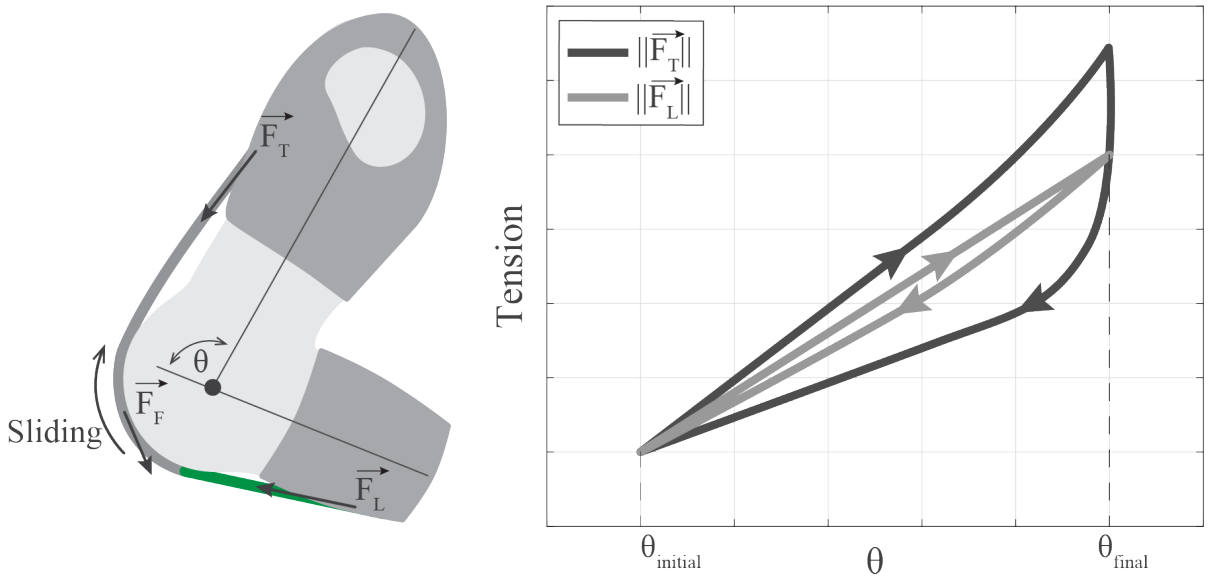

Figure C.9: **Exosuit with non-stretch element (gray) over the buttocks, and elastic element (green) below it**. The model suggests that $\|\overrightarrow{F_T}\|$ will be increased during bending ($\theta_{initial} \rightarrow \theta_{final}$), but decreased during lifting ($\theta_{final} \rightarrow \theta_{initial}$), relative to $\|\overrightarrow{F_L}\|$ due to the presence of the frictional force at the butt $\|\overrightarrow{F_T}\|$. This difference in tension forces is illustrated by the plot of the dark gray curve in the plot on the right. This plot is a qualitative representation to provide intuition on the expected dynamics of the exosuit. In this exosuit configuration energy losses due to butt friction are expected to be non-negligible.

C.0.5 Table of Evidence for Low-Back Exosuits

Year	Source	Peer Reviewed	Findings
2005	Abdoli-Eramaki et al. (Clinical Biomechanics)	Yes	Exosuit reduced integrated EMG of lumbar and thoracic erector spinae by 14 to 28% respectively during stoop, squat and free lifting techniques (5, 15 and 25 kg). N=9 (all male)
2007	Abdoli-Eramaki et al. (J Biomechanics)	Yes	Exosuit provided 23-36 Nm of torque and reduced spine compression and shear forces by an estimated 23-29% and 8-9% respectively during lifting tasks. Mathematical proof (using simplified free body diagrams and two-dimensional moment balance equations) explains how and why this type of passive exosuit reduces loading on back extensor muscles and spine. N=9 (all male)
2008	Graham MS Thesis (Queen's University)	No	Subjects reported feeling positive assistance from exosuit in automotive assembly task, 8/10 would wear device every day.
2009	Lotz et al. (J Electromyography & Kinesiology)	Yes	Exosuit reduced rate of back muscle and cardiovascular fatigue (EMG RMS, median frequency, perceived exertion ratings, endurance time) during cyclic lifting. N=10 (all male)
2009	Abdoli-Eramaki (US Patent, 7,553,266B2)	No	Exosuit reduced hamstring and low back muscle activity.
2009	Frost et al. (J Electromyography & Kinesiology)	Yes	Increasing stiffness in exosuit elastic bands resulted in greater assistive magnitude, and greater reductions in erector spinae activity (up to 38%). The relationship between elastic band stiffness and EMG reduction appeared to be linear and comparable between different lifting styles (stoop, squat, freestyle). N=13 (all male)
2009	Godwin et al (IJIE)	Yes	Exosuit significantly reduced fatigue for all subjects during 45-min lifting session. N=12 (all female)
2011	Fick MS Thesis (Queen's University)	No	Overwhelmingly positive feedback on perceived assistance from exosuit during field tests.
2011	Sadler et al. (Ergonomics)	Yes	Exosuit significantly reduced lumbar & thoracic flexion and significantly increase hip and ankle flexion (for both males & females). Results suggests exosuit encouraged safe lifting practices without adversely affecting lifting technique (N=30).
2014	Whitfield et al. (IJIE)	Yes	Exosuit reduced thoracic erector spinae and biceps femoris muscle activity by 8 and 14 % respectively during box lifting. Exosuit had no significant effect on metabolic rate. N=15 (all males).
2018	Zelik, Yandell, Howser and Lamers (PCT Patent App, WO2018136722A1)	No	Form-fitting exosuit reduced low back muscle activity during leaning and lifting.
2018	Lamers, Yang & Zelik (IEEE TBME)	Yes	Exosuit reduced average erector spinae activity 23-43% during leaning, and 14-16% during lifting. Peak EMG reduced by 19-23% during lifting (N=8). Physics model (using a simple moment balance) indicated that offloading the low back muscles with this type of exosuit is also expected to reduce intervertebral disc compression forces. Model indicates the reduction in loading of back muscles and discs is expected to increase with both increasing elastic band force and increasing moment arm. N=8, (7 male, 1 female)
2019	Galiana et al. (PCT Patent App WO2019161232A1)	No	Exosuit reductions in EMG: 20-40% for biceps femoris, 20-30% for gluteus maximus, 15-30% for lumbar erector spinae, 40-60% for thoracic erector spinae during leaning (N=1).
2019	Swissport & Auxivo (IATA Presentation Slides)	No	Exosuit reduced erector spinae by 15%, multifidus by 30%, gluteus maximus by 50%, and biceps femoris by 10% (N=unknown).
2020	Yandell et al. (WeRob Conference Abstract)	No	Exosuit reduced average and peak back muscle activity in this field test by ∼10% during lifting/lowering tasks. Two thirds of workers exhibited reductions 15%. 90% of workers reported feeling assisted and that the exosuit made lifting easier.
2020	Lamers et al. (Nature Scientific Reports)	Yes	Five of 6 subjects show reductions in back muscle fatigue rate (26-87 % for individual muscles) during sustained leaning. Average reduction in back muscle fatigue was 30-40 across all muscles and study participants. N=6 (4 male, 2 female)

Table C.2: Summary of prior modeling, laboratory and field-based evidence from the last 15 years showing that these types of exosuits reduce back muscle activity, muscle strain, muscle fatigue, spine compression and perceived exertion during lifting, bending, leaning and stooping tasks. Each of the studies summarized below tested a device/prototype that is functionally similar to the extensible or form-fitting exosuit in the engaged mode.